# Light Driven Catalytic $CO_2$ Reduction: Lessons Learnt when Low is Actually No Activity

Varinder Singh[1]‡, Kieran DeMonte[1]‡, Olivier Schott,[2] Folaranmi S. Akogun,[1,2] Garry S. Hanan[2]* and Sally Brooker[1]*

[1]*Department of Chemistry and MacDiarmid Institute for Advanced Materials and Nanotechnology, University of Otago, PO Box 56, Dunedin 9054, New Zealand.*
*E-mail: sbrooker@chemistry.otago.ac.nz*

[2]*Département de Chimie, Université de Montréal, Quebec, Canada.*

‡ *these two authors contributed equally*

# *Electronic Supporting Information*

# Contents

# 1. Synthetic protocols and NMR spectra

## 1.1. Synthesis of 1,3-dimethyl-2-phenyl-2,3-dihydro-1H-benzo[d]imidazole (BIH)

The synthesis of BIH was carried in four steps as reported in the literature (Figure S1).[1-3] NMR spectra for each of the intermediates, and the product BIH, are provided below.

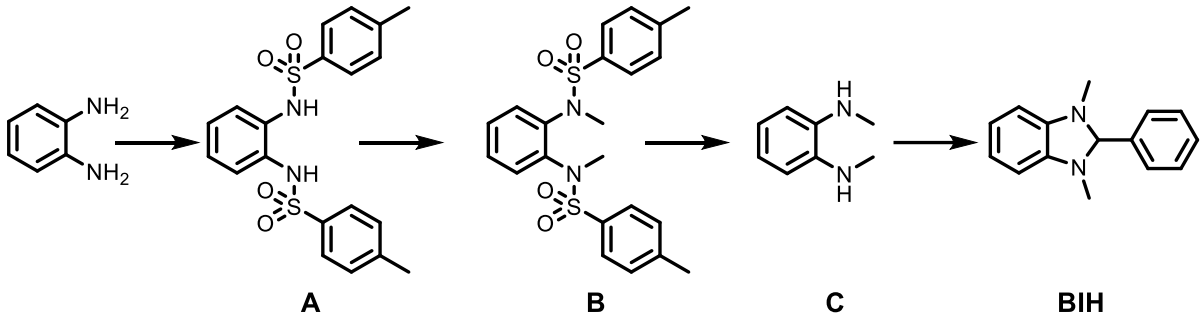


***Figure S1:*** *Literature synthesis of BIH in 4 steps from commercially available o-phenylenediamine, p-toluenesulfonyl chloride and benzaldehyde.[1, 2]*

***N,N'*-Di(p-toluenesulfonyl)-o-phenylenediamine (A).**

A mixture of *o*-phenylenediamine (20 g, 0.19 mol) and *p*-toluenesulfonyl chloride (71.5 g, 0.38 mol) in pyridine (450 mL) was stirred overnight at room temperature. Then, with cooling of the stirring mixture with an ice bath, 700 mL of 15% aq. HCl (280 mL conc. HCl in 420 mL water) was slowly added to the resulting dark red solution, resulting in a white precipitate in an orange solution. The white precipitate collected, then re-suspended in EtOH (600 mL) and refluxed overnight. The resulting orange solution was allowed to cool and then transferred to a refrigerator overnight. The resulting white precipitate of A was collected, washed with cold EtOH (60 mL) and dried in vacuo to obtain A (66 g, 86%). $^1$H NMR (400 MHz, DMSO): δ/ppm = 9.30 (s, 2H), 7.61 (d, 4H), 7.35 (dd, 4H), 7.00 (m, 4H), 2.34 (s, 6H).

***N,N'*-Dimethyl-*N,N'*-di(p-toluenesulfonyl)-o-phenylenediamine (B).**

A white suspension of **A** (66 g, 0.16 mol) and $K_2CO_3$ (78 g, 0.56 mol) in MeCN (900 mL) was stirred at room temperature for an hour. 24 mL of methyl iodide (54 g, 0.38 mol) was added slowly and the resulting creamy suspension refluxed overnight. The resulting white suspension was taken to dryness and the white solid residue was taken up in $H_2O$ (400 mL) and extracted with $CH_2Cl_2$ (3x200 mL). The combined $CH_2Cl_2$ layers were collected, taken to dryness and the obtained off-white solid recrystallized from approximately 550 mL EtOH, giving B as white crystals, which were collected, washed with cold EtOH (60 mL) and dried in vacuo (62.6 g, 89%). $^1$H NMR (400 MHz, $CDCl_3$): δ/ppm = 7.74 (d, 4H), 7.36 (d, 4H), 7.26 (m, 2H), 6.91 (m, 2H), 3.24 (s, 6H), 2.47 (s, 6H).

***N,N*'-Dimethyl-o-phenylenediamine (C)**

B (62.5 g, 0.14 mol) was dissolved in 340 mL of aq. $H_2SO_4$ (90% v/v of conc. $H_2SO_4$ to water) and the colourless solution was heated to 90 °C. The resulting red solution was allowed to cool to room temperature, then it was transferred into about 2 cups of ice and the pH of the mixture was adjusted by addition of NaOH pellets (about 450 gm) until a pH of ~11 was attained. The resulting red aqueous phase was extracted with diethyl ether (3x300 mL). The resulting brown organic phase was washed with water (400 mL), dried over $MgSO_4$, and taken to dryness, giving **C** as a sticky brown oil (17.24 g, 90%). $^1$H NMR (400 MHz, $CDCl_3$): δ/ppm = 6.85 (dd, 2H), 6.70 (dd, 2H), 3.28(s, 2H), 2.87 (s, 6H).

**1,3-Dimethyl-2-phenyl-2,3-dihydro-1H-benzo[d]imidazole (BIH)**

The sticky brown oil **C** (17.24 g, 0.125 mol) was dissolved in MeOH (300 mL) followed by the addition of benzaldehyde (14.3 g, 0.135 mol) and ~8 drops of acetic acid. The green solution was sonicated for half an hour. The white precipitate that formed was filtered off, rinsed with minimum cold MeOH (about 5 mL), then dried *in vacuo* for a week, giving BIH as a white powder (17 g, 60%). Anal. Calcd. for $C_{15}H_{16}N_2$: C 80.32, H 7.19, N 12.49%; found: C 80.66, H 7.14, N 12.34. $^1$H NMR (400 MHz, $CD_3CN$): δ/ppm = 7.61 (dd, 2H), 7.48 (m, 3H), 6.71 (dd, 2H), 6.48 (dd, 2H), 4.88 (s, 1H), 2.55 (s, 6H).

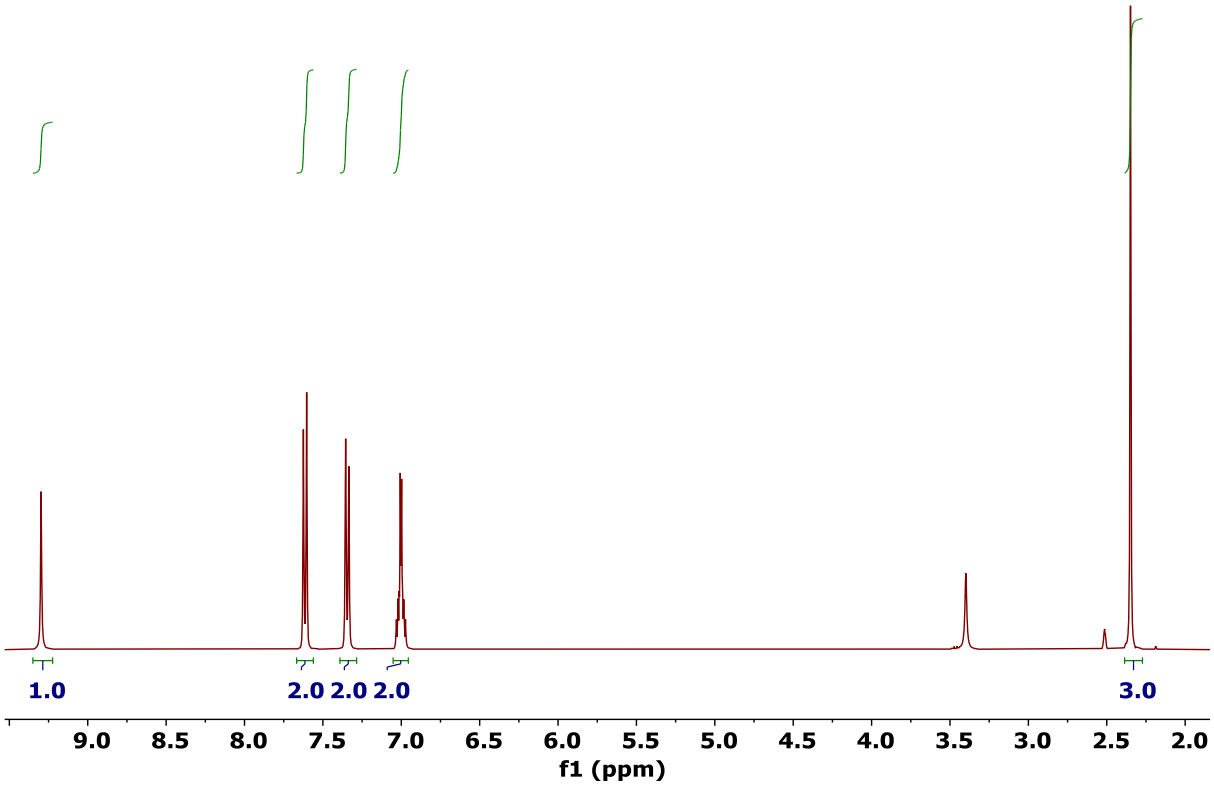


*Figure S2: $^{1}H$ NMR spectrum of **A** (N,N'-di(p-toluenesulfonyl)-o-phenylenediamine) in DMSO*

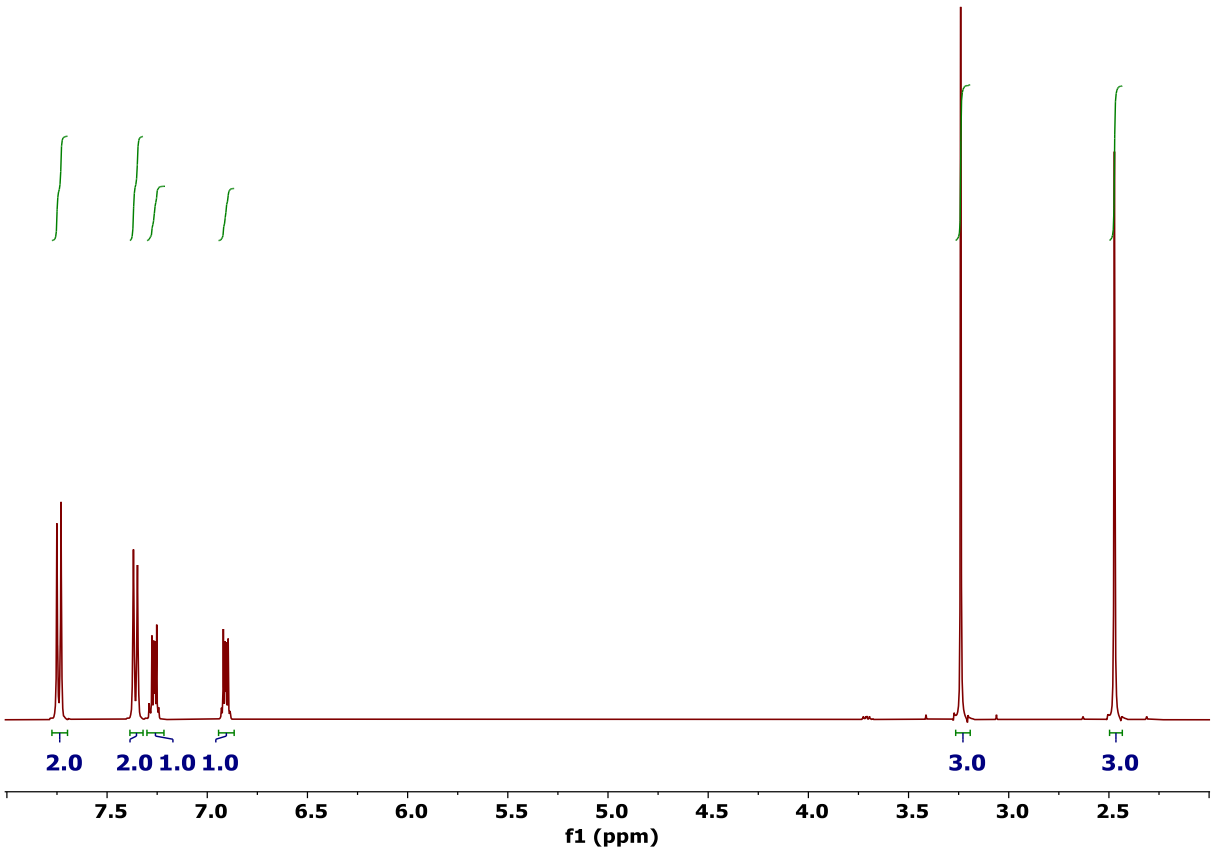


***Figure S3:** $^{1}H$ NMR spectrum of **B** (N,N'-dimethyl-N,N'-di(p-toluenesulfonyl)-o-phenylenediamine) in $CDCl_3$*

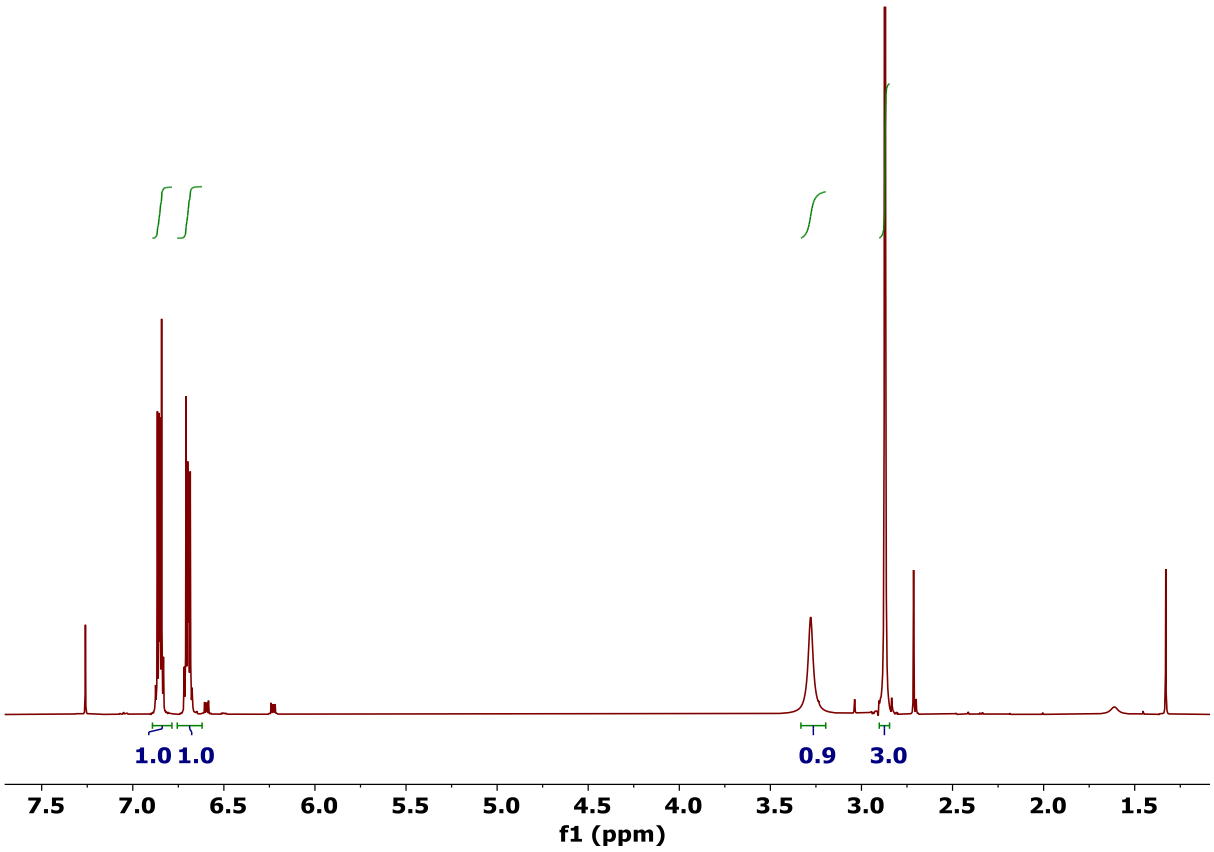


***Figure S4:*** *$^1$H NMR spectrum of **C** (N,N'-dimethyl-o-phenylenediamine) in $CDCl_3$.*

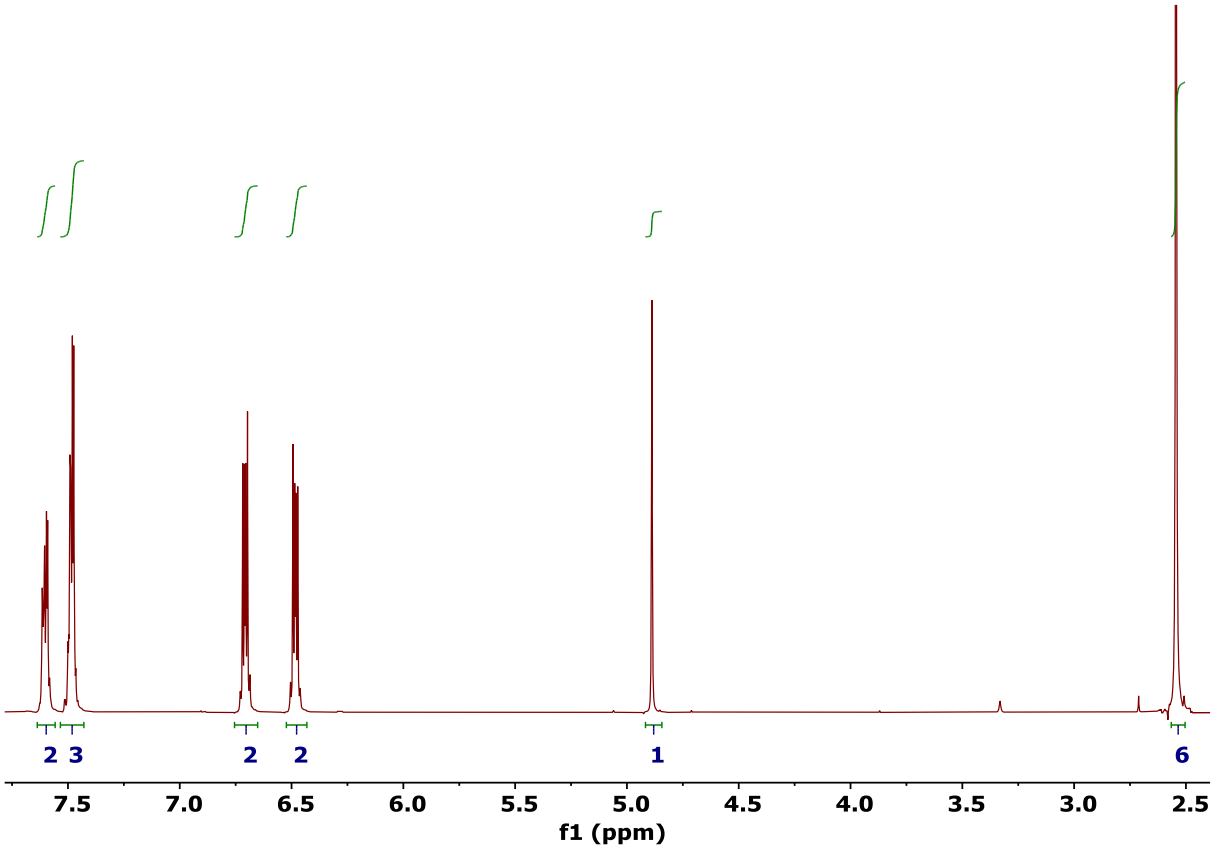


***Figure S5:*** *$^1$H NMR spectrum of **BIH** (1,3-dimethyl-2-phenyl-2,3-dihydro-1H-benzo[d]imidazole) in $CD_3CN$.*

## 1.2. Synthesis of $[Ru(bpy)_3](PF_6)_2$

Preparation of the complex is adapted from the literature procedure.[4] Solid bipyridine (187 mg, 1.2 mmol) and $RuCl_3 \cdot 3H_2O$ (100 mg, 0.38 mmol) were added to ethylene glycol (50 ml) and the mixture was refluxed for 5 h. The resulting red solution was cooled to room temperature and a saturated aqueous solution of potassium hexafluorophosphate (about 9 mL) was added dropwise, until all of the red complex had precipitated. The red precipitate was collected on a pad of 3 cm of celite (the celite was pre-treated by washing with 30 mL acetonitrile, then 100 mL water) in a 9 cm diameter frit, then washed with water (100 ml). The red product was extracted from the celite by washing it through with acetonitrile (30 ml), and then re-precipitated by adding diethyl ether (40 ml). The red powder was collected, then redissolved in acetonitrile (20 ml), then water (about 20 mL) was added slowly with stirring until a weak cloud of precipitate was formed and dissolved again. If necessary, few drops of acetonitrile were added to obtain a clear red solution. Slow evaporation of this clear red solution gave, after a few days, red rod crystals which were filtered, ground and dried at 45 °C under vaccum for 4 days (0.228 g, 70%). $^1$H NMR (400 MHz, $CD_3CN$-$d_6$): δ(ppm): 8.36 (ddd, *J* = 8, 1.4, 0.8 Hz, 2 H), 8,17 (ddd, *J* = 8.8, 8, 1.5 Hz, 2H), 7,74 (ddd, *J* = 6.0, 2, 0.8 Hz, 2H), 7,533 (ddd, *J* =8, 5.6, 1.28 Hz). Anal. Calc. for $C_{30}H_{24}N_6RuP_2F_{12}$: C, 41.92; H, 2.81; N, 9.78. Found : C, 41.75; H, 2.43; N, 9.74.

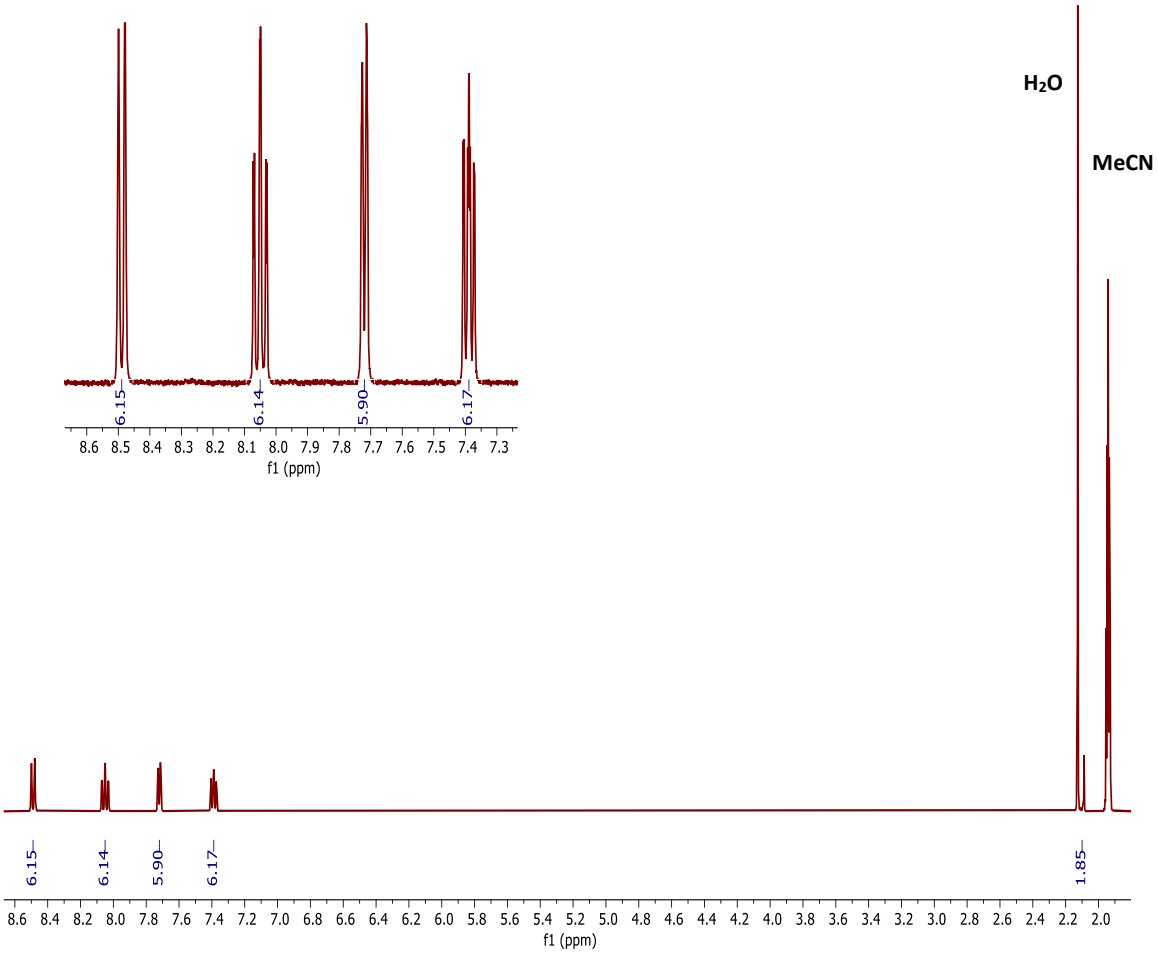


***Figure S6:*** *$^1$H NMR spectrum of* $[Ru(bpy)_3](PF_6)_2$ *in* $CD_3CN$.

# 2. Photocatalytic $CO_2$RR

## 2.1. Chemicals, solvents and light source

$[Ru(bpy)_3](PF_6)_2$ (bpy = 2,2′-bipyridine), see above for synthesis, has been used as photosensitizer (PS). The solvent used for testing **1-3** was acetonitrile (99.9 % ACS grade, MeCN) that had been dried over activated 4 Å sieves, then distilled over calcium hydride under nitrogen, and stored in the glovebox, whilst for testing **4-5** dimethylformamide (99.9 % ACS grade, DMF) that had been dried over activated 4 Å sieves, then distilled under vacuum, and stored in the glovebox was used. Triethanolamine (TEOA, Sigma-Aldrich, >99%, product 33729; stored and used, as received, in the glovebox) was employed as proton acceptor, and 1,3-dimethyl-2-(o-hydroxyphenyl)-2,3-dihydro-1H-benzo[d]imidazole (BIH, see above for synthesis) as sacrificial electron donor (SD). Details of the blue 10 W LED irradiation source (445 nm) employed are provided below (Section 2.3).

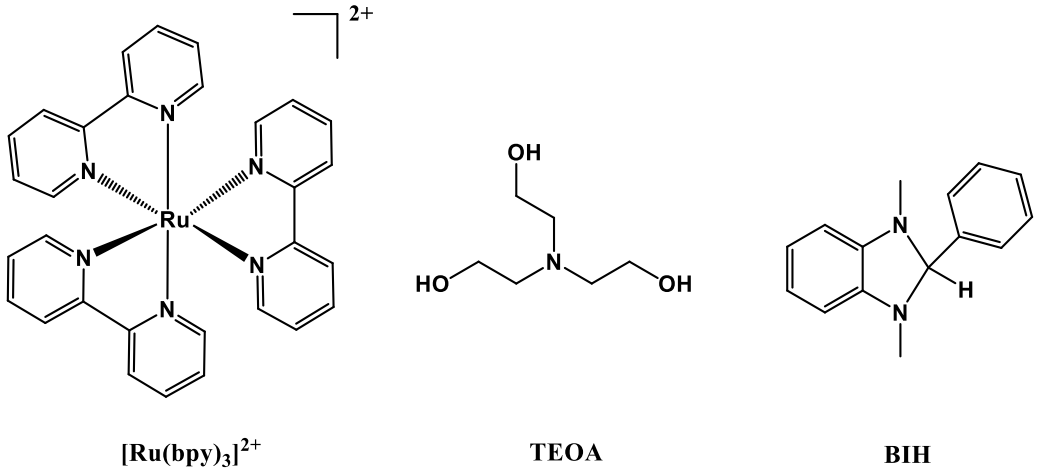


$[Ru(bpy)_3]^{2+}$ TEOA BIH

***Figure S7:*** Photosensitizer ($[Ru(bpy)_3]^{2+}$), proton acceptor (TEOA) and sacrificial electron donor (BIH) used herein.

## 2.2. Preparation of reaction solutions for photocatalysis

All of the MeCN/DMF reaction mixtures used in the photoreactions were prepared in the glovebox under a nitrogen atmosphere, in 20 mL vials that are closed with a septum, and protected from air and light until brought out to the photoreactor.

**For experiments in MeCN**, three distinct standard solutions were freshly prepared:

1) PS stock solution of $[Ru(bpy)_3](PF_6)_2$ (18 mg, 0.021 mmol) in 25 mL dry MeCN,
2) 10 mL TEOA stock solution comprised of:
   Either (a) (i) 1 mL TEOA plus 9 mL dry MeCN to obtain 0.38 M [TEOA] (5 % TEOA in photocat. solution), or
   (ii) 4 mL TEOA plus 6 mL dry MeCN to obtain 1.5 M [TEOA] (20 % TEOA in photocat. solution)
   Or (b) when water used as additional proton source; 1 mL TEOA plus 1 mL water plus 8 mL dry MeCN,
3) Catalyst stock solutions of 2 mg of either **1**, **2**, or **3** in 20 mL dry MeCN.

Next, the following were mixed and topped up with dry MeCN to give a total of 20 mL:
5 mL of PS stock solution,
10 mL of the chosen TEOA stock solution, and
0.45 mL (**1**), 0.53 mL (**2**), or 0.59 mL (**3**) of the selected catalyst stock solution (each containing $1 \times 10^{-4}$ mmol catalyst) – note: for blank runs the same volume of pure dry solvent was used instead.

Finally, this 20 mL solution was divided into 4 separate 20 mL vials, each already containing solid BIH (57 mg, 0.25 mmol). The resulting 5 mL of *standard reaction solution* in each 20 mL vial was ready for photocatalysis testing, and contained the following molar concentrations of each of the photocatalytic components: 0.2 mM $[Ru(bpy)_3](PF_6)_2$, 0.05 M BIH, either 0.38 M (5 %) or 1.5 M (20 %) TEOA, 2.8 M (5%) water (when water present), and $C_{cat}$ = 5 μM.

**For experiments in DMF,** three distinct solutions were freshly prepared:

1) PS stock solution of $[Ru(bpy)_3](PF_6)_2$ (18 mg, 0.021 mmol) in 25 mL dry DMF,
2) 10 mL TEOA stock solution comprised of:
   Either (a) 4 mL TEOA plus 6 mL dry DMF
   Or (b) when water was used as additional proton source; 1 mL water plus 4 mL TEOA plus 5 mL dry DMF,
3) catalyst stock solutions comprising:
   Either (a) $8\times10^{-5}$ M catalyst, comprising 2 mg of either **4** or **5** in 20 mL dry DMF
   Or (b) $32 \times10^{-5}$ M catalyst, comprising 8 mg of either **4** or **5** in 20 mL dry DMF

Next, the following were mixed to give a total of 20 mL:
5 mL of PS stock solution,
10 mL of the chosen TEOA stock solution, and
5 mL of the selected catalyst standard solution (**4** or **5**) – note: for blank runs the same volume of pure dry solvent was used instead

Finally, this 20 mL solution was divided into 4 separate 20 mL vials, each already containing solid BIH (57 mg, 0.25 mmol). The resulting 5 mL of *standard reaction solution* in each 20 mL vial was ready for photocatalysis testing, and contained the following molar concentrations of each of the photocatalytic components: 0.2 mM $[Ru(bpy)_3](PF_6)_2$, 0.05 M BIH, 1.5 M TEOA (20%), 2.8 M (5%) water (when water present) and $C_{cat}$ either 5 μM or 20 μM (for increased concentration experiments).

## 2.3. Photocatalytic experimental setup

A mass flow controller (Alicat 0-20 SCCM) is configured to deliver a constant $CO_2$ flow rate of 5 mL/min, through a series of stainless steel cannulae. The first cannula pierces the septum of a pre-loaded 20 mL vial containing 5 mL of acetonitrile or DMF, which saturates the $CO_2$ gas with the appropriate solvent, before a second cannula carries it into the 20 mL reaction vial containing the 5 mL reaction solution. A third stainless steel cannula, inserted into the reaction vial's septum, directs the gas flow to a 2 mL empty vial, acting as a trap to prevent

any accidental MeCN/DMF droplets from reaching the gas chromatograph (GC). This vial is connected to an 8-port stream select valve (VICCI), which directs the gas stream to the sample loop of the GC (see next section for more details).

A digital flowmeter (Perkin Elmer FlowMark) is used to verify the flow rate. The solutions are degassed under a $CO_2$ flow for 45 minutes before switching on the light. The flexible stainless-steel tubing allows the reaction vial to be placed in a thermostated photoreactor at 20°C.

The photoreactor is illuminated by a 10 W blue LED set (λ = 445 nm) with an irradiation power of 88 mW·cm$^{-2}$. The bottom surface of the vial, with an area of 3.8 cm², is fully irradiated. An analog power meter (PM100A, THORLABS), coupled with a compact photodiode power head equipped with a silicon detector (S120C), is used to measure the photon flux. The photodiode detector is placed at the same distance from the LED as the reaction vial to ensure accurate power measurement. The light intensity was kept between (17 to 20 mW.cm$^{-2}$) at top of the photoreactor to get 88 mW·cm$^{-2}$ at the bottom surface of the vial.

## 2.4. Gaseous products quantification by GC

CO and $H_2$ were monitored using a PerkinElmer Clarus-480 and PerkinElmer Clarus-580 gas chromatograph (GC) equipped with a 7-inch HayeSep N 60/80 pre-column, a 9-inch molecular sieve 13×45/60 column, and a 2 mL injection loop. A flame ionisation detector (FID) quantified the CO, and thermal conductivity detector (TCD) the $H_2$. Argon is used as carrier gas and $CO_2$ as eluent gas.

First a calibration curve is established to determine the relationship (equation 1) between the integration of the $H_2$ or CO signals in the TCD or FID trace (y) and the concentration of $H_2$ or CO in the gas sample (x). This is achieved by flowing various accurately known concentrations (x) of standard $H_2$ and CO gas mixtures (with argon as the balance) into the sample loop and integrating the observed area (y) under the $H_2$ peak in the TCD trace or the CO peak in the FID signal.

$$y = ax + b \qquad \textbf{eq. 1}$$

$$\mathbf{GC_{ProductArea} = \mathit{a}[product\ in\ carrier\ gas] + \mathit{b}}$$

x = concentration of $H_2$ or CO, in µL.L$^{-1}$ (known for calibration, but to be determined for the reaction products later)
y = $H_2$ TCD area or CO FID area, in µV.s
*a* = slope
*b* = noise seen in $H_2$ TCD area or CO FID area without hydrogen or CO present, in µV.s

Calibration establishes the values of *a* (the constant of proportionality, or slope) and *b* (noise correction) in equation **1**. This enables $\mathbf{GC_{ProductArea}}$, the observed area in the $H_2$ peak or CO peak in the TCD or FID trace obtained as these gaseous products of photocatalysis are

monitored by GC, to be converted, using equation **1**, into [product in carrier gas], the concentration of $H_2$ in $\mu L.L^{-1}$ ($\mu L_{H2}.L^{-1}$ ) or CO in $\mu L.L^{-1}$ ($\mu L_{CO}.L^{-1}$ ).

Next, as the flow rate of the argon vector gas is known, the rate of $H_2$ ($\mu L_{H2}.min^{-1}$) or CO ($\mu L_{CO}.min^{-1}$) generation can be readily calculated using equation 2 (and similarly for CO):

Rate of production of $H_2$ ($\mu L_{H2}.min^{-1}$ ) = [$H_2$ in carrier gas] ($\mu L_{H2}.L^{-1}$ ) x Ar flow rate ($L.min^{-1}$) **eq. 2**

$$\text{Volume of } H_2 \text{ or CO (L)} = \frac{\text{Rate of production of } H_2 \text{ or CO } (\mu L.\, min^{-1}) \times \text{Time (min)}}{1 \times 10^6} \quad \textbf{eq. 3}$$

The ideal gas law (eq. 4) then permits the conversion of the volume of $H_2$ (or CO) in L to the amount of $H_2$ (or CO) in mol, $n_{H2}$ (or $n_{CO}$):

$$PV = nRT \leftrightarrow n_{product} = PV/RT \quad \textbf{eq.4}$$

P = pressure = 1 atm
T = temperature = 298 K
R = ideal gas constant = 0.082 $L.atm.K^{-1}.mol^{-1}$
V = volume of hydrogen (or CO) in L
n = amount of hydrogen (or CO) in mol

**Turnover number (TON):**

This "specifies the maximum use that can be made of a catalyst for a special reaction under defined reaction conditions by the number of molecular reactions or reaction cycles occurring at the reactive centre up to the decay of activity".[5] The TON achieved by the catalyst, $TON_{CAT}$, is calculated using **Eq. 5**, and reflects the lifetime, and hence robustness, of the active catalyst.

$$TON_{CAT} = \frac{n_{product}}{n_{CAT}} \quad \textbf{eq. 5}$$

$$TON_{PS} = \frac{n_{product}}{n_{PS}} \quad \textbf{eq.6}$$

$TON_{CAT}$ is sometimes underestimated, as it is common to assume that all molecules of the catalyst are active, also, the reactions are not always run till the activity drops to zero, so both $TON_{CAT}$ and $TON_{PS}$ can be underestimates.

**Turnover frequency (TOF):**

"This measures the instantaneous efficiency of the catalyst, it can be derived from the number of the turnovers of the catalytic cycle with respect of the time per active site" **Eq. 7** is commonly used to estimate the TOF of molecular catalyst." [5]

$$TOF_{CAT} = \frac{n_{product}}{n_{CAT} \times time} = \frac{TON_{CAT}}{time} \quad \textbf{eq.7}$$

$$TOF_{PS} = \frac{n_{product}}{n_{PS} \times time} = \frac{TON_{PS}}{time} \quad \textbf{eq.8}$$

The errors associated with the TON and TOF are estimated to be 10%.

## 2.5. Liquid product quantification by $^1$H NMR procedure

### 2.5.1 Materials and solvents

NMR deuterated solvents were purchased from Sigma Aldrich. All measurements are taken with a Bruker Ultrashield 500 spectrometer at room temperature. First, a classical instrumental method is used to screen a wide spectral width SW = 15 ppm and a D1=30 s. A second instrumental method is designed to have optimal quantitative sensitivity on formate singlet peak, (SW=5.48 ppm and D1 is 60 s). The range of irradiation is selected in chemical shift range of formate to avoid the intense signal of triethanolamine and acetonitrile. All the experiments are run in automatic mode within a few hours of preparation of the sample.

### 2.5.2 $^1$H NMR spectra of the calibrant compounds

**Note:** To obtain a calibration curve for formate in MeCN, two internal chemical references, benzyl benzoate and dimethyl 5-methoxyisophthalate, were added. In contrast, to obtain calibration curve for formate in DMF, only benzyl benzoate was used as the internal chemical reference.

Commercial chemical references with distinct proton NMR signals that do not overlap the signals of protons of the photocatalytic mixture were chosen. The NMR shift of **$CH_2$ singlet of benzyl benzoate appears around 5.4 ppm** in the NMR spectrum (Figure S8), the area integration of this singlet is used as internal quantitative reference. To check the integrity of the benzyl benzoate signal, the **singlet proton NMR signal around 8.1 ppm of dimethyl 5-methoxyisophthalate** (Figure S9) was used as another reference in the NMR tube. In the NMR spectrum, the phase is adjusted so that the baseline appears flat around the peaks of the reference and formate. The integration is carefully done manually, between both extremities of the base of the peak.

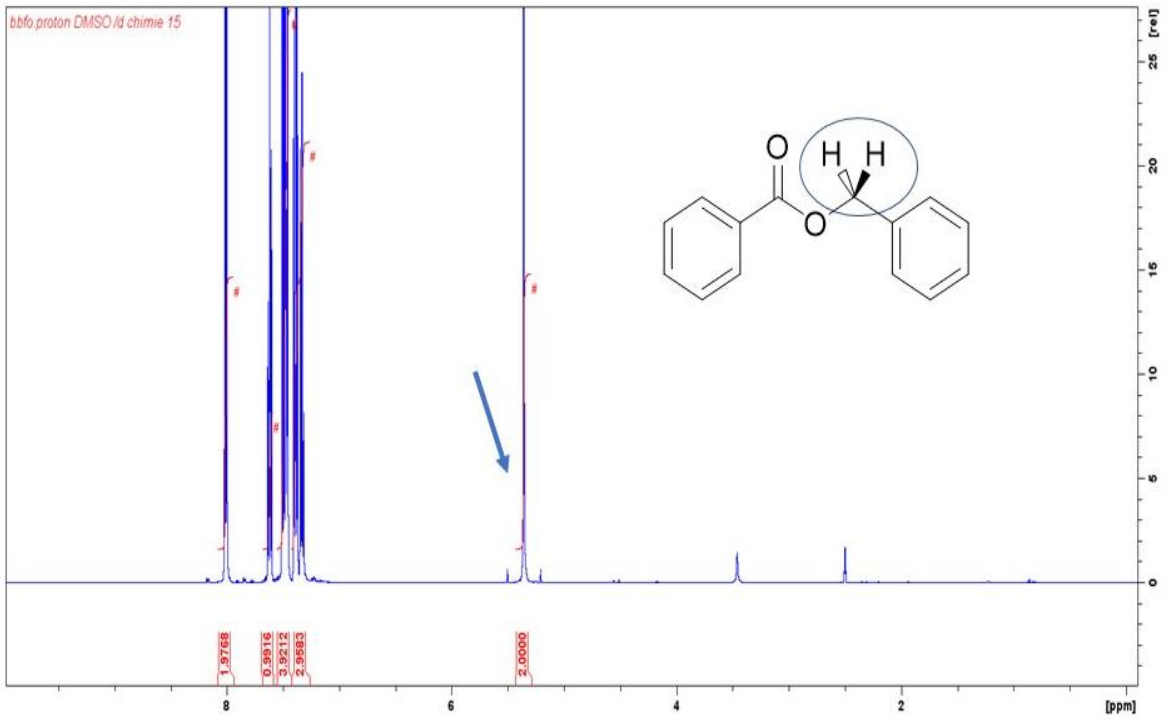


***Figure S8:*** *$^1$H NMR spectrum of benzyl benzoate (one of the two chemical references used herein to obtain calibration curve and quantify formate in both MeCN and DMF) in $d_6$-DMSO. Routine NMR method in automatic mode, 500 MHz.*

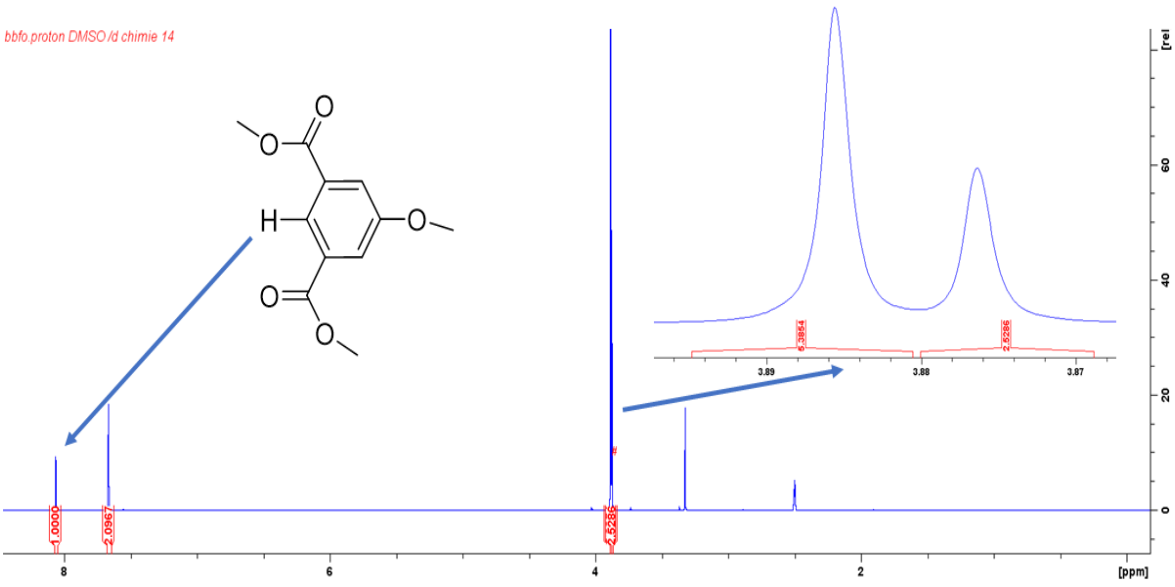


***Figure S9:*** *$^1$H NMR spectrum of dimethyl 5-methoxyisophthalate (one of the two chemical references used to obtain calibration curve for formate in MeCN only) in $d_6$-DMSO. Routine NMR method in automatic mode, 500 MHz.*

### 2.5.3 Generating formate calibration curve for MeCN solution

Two calibration datasets, **series 1** and **series 2**, were run in MeCN, both with the **two different internal references** (benzyl benzoate and dimethyl 5-methoxyisophthalate, see above section) **present**, to enable analysis of the relative ease and consistency of formate quantification, across a range of formate concentrations (0-6mM), which established benzyl benzoate as the preferred internal reference for formate quantification, not least as the peak is more readily integrated than that of the dimethyl 5-methoxyisophthalate.

NMR tubes were then filled to 4.5 cm from the bottom of the tube with the calibration or test solution (see below for how these were prepared), and the NMR spectrum obtained. The integration of the $CH_2$ singlet of benzylbenzoate at 5.4 ppm was always set to 2H, and the relative integration of the formate signal (1H) at 8.5 ppm, and of the second internal reference signal, the CH (1H) aromatic singlet signal of the dimethyl 5-methoxyisophthalate at 8.1 ppm determined (see Tables S1a and S2a, for **series 1 and 2** respectively).

In order to try and ensure consistency between the relative integrations of the key peaks in the NMR spectra for the calibration solutions and those for the post-reaction solutions, all of the calibration solutions contained an aliquot (detailed below) of post-catalysis blank reaction solution (in which all components except catalyst are present, made up as detailed in the above section). It should be noted that small amounts of formate are formed in these solutions, despite the lack of catalyst (see below, including Tables S1 and S2).

Hence photocatalysis on the blank reaction solution was conducted for either 2 hours (**series 1**) or 48 hours (**series 2**), resulting in the generation of small amounts of formate, before aliquots of it were used as follows:

In both calibration datasets (**series 1 and 2**), the first NMR solution prepared contained no added formate (Figure S10 and S15), but instead comprised a total of 1 mL made up of:

- 0.7 mL of post-photocatalysis blank solution (photocatalysis run for either 2 or 48 hrs, for series 1 and 2, respectively) made up as described in section 2.2, without the catalyst,
- 0.1 mL of dry MeCN containing 10 mM benzyl benzoate and 10 mM dimethyl 5-methoxyisophthalate,
- 0.2 mL of $d_6$-DMSO.

The resulting concentration of benzylbenzoate in the NMR tube is 1 mM and the integration of its $CH_2$ singlet at 5.4 ppm is set to 2H, then the relative integration of the 1H signal for formate at 8.5 ppm and the 1H signal at 8.1 ppm for the second internal reference is determined. This comparison enabled the quantity of formate (small) formed after 2 or 48 hours of photocatalysis in the absence of the catalyst to be determined.

Next, a series of NMR solutions containing known amounts of added formate (0.5, 1 and 5 mM; Figures S11-S13, first calibration dataset; Figures S16-S18, second calibration dataset) were prepared as follows.

Firstly, a series of standard dry MeCN solutions containing 5 mM, 10 mM and 50 mM formate were prepared.

Then a series of 1 mL NMR solutions containing 3 different concentrations of added formate was made up as follows:

- 0.6 mL of post-photocatalysis blank solution (photocatalysis run for either 2 or 48 hrs, for series 1 and 2, respectively) made up as described in section 2.2, without the catalyst
- 0.1 mL of either the 5, 10 or 50 mM formate dry MeCN solution,
- 0.1 mL of dry MeCN containing 10 mM benzyl benzoate and 10 mM dimethyl 5-methoxyisophthalate,
- 0.2 mL of $d_6$-DMSO.

As above, the resulting concentration of benzylbenzoate in the NMR tube is 1 mM and the integration of its $CH_2$ singlet at 5.4 ppm is set to 2H. Then the relative integration of the $^1H$ signal for formate at 8.5 ppm and the $^1H$ signal at 8.1 ppm for the second internal reference are determined (see the last 3 rows in Tables S1a and S2a). The resulting concentration of the deliberately added formate is 0.5 mM, 1 mM or 5 mM, but in both **series 1 and 2** some formate is also produced after photocatalysis in the absence of the catalyst for 2 or 48 hr, respectively.

**First series of calibration data (using post-2h photocatalysis blank solution)**

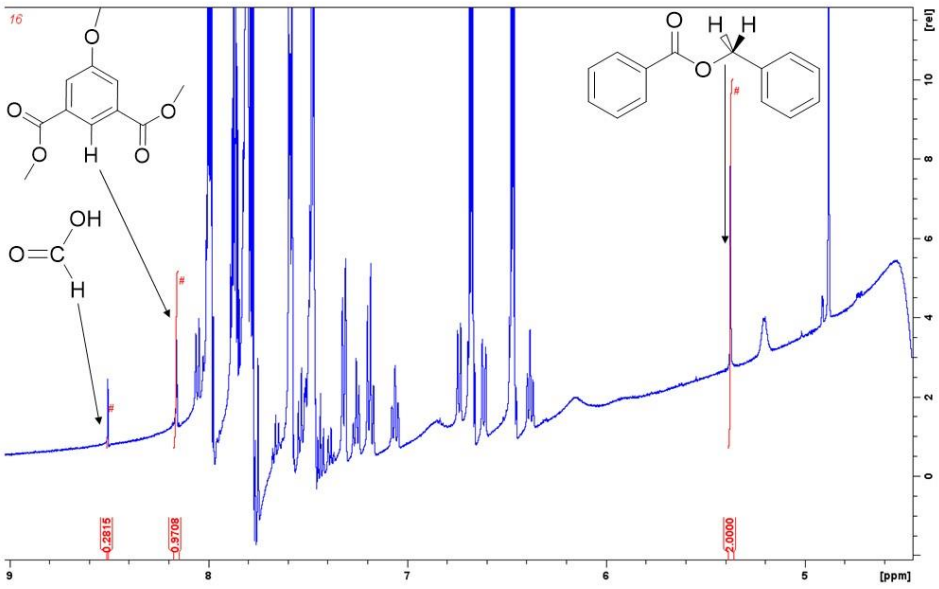


***Figure S10:*** *$^1H$ NMR spectrum showing peaks of the chemical references and formate in the photocatalytic solution. The solution is made up of: 70% blank post-2h-photocatalytic solution, 20% $d_6$-DMSO, 10% 10 mmol/L of both dimethyl 5-methoxyisophthalate and benzylbenzoate in acetonitrile solution. The integration of $CH_2$ benzylbenzoate is set at 2H to be used as internal reference, 500 MHz. The Ru(trisbipyridine) system without the catalyst generates formate.*

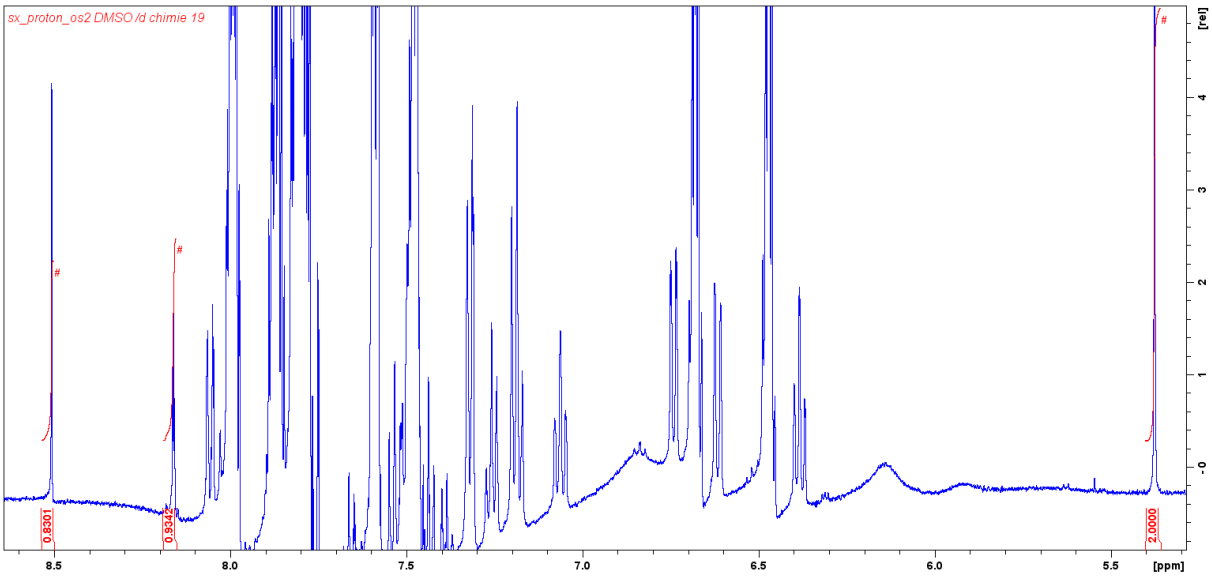


***Figure S11:*** *$^1$H NMR spectrum of 0.6 mL of blank post-2h-photocatalytic MeCN solution, spiked by 0.1 mL of* ***5 mM*** *formate MeCN solution, 0.1 mL of reference solution and 0.2 mL of $d_6$-DMSO, 500 MHz.*

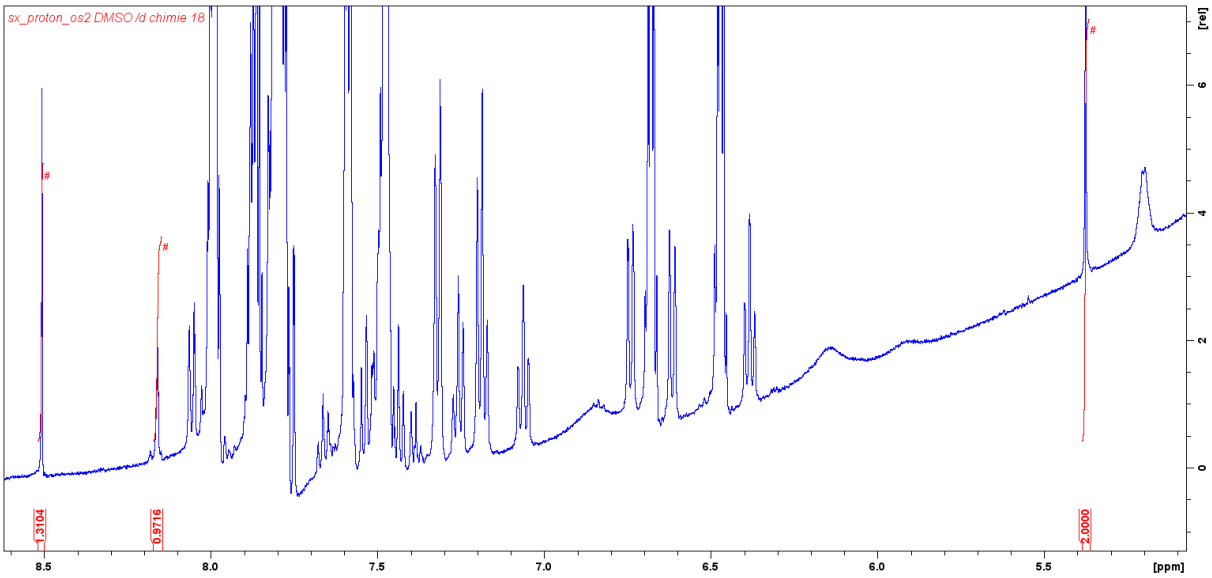


***Figure S12:*** *$^1$H NMR spectrum of 0.6 mL of blank post-2h-photocatalytic MeCN solution, spiked by 0.1 mL of* ***10 mM*** *formate MeCN solution, 0.1 mL of reference solution and 0.2 mL of $d_6$-DMSO, 500 MHz.*

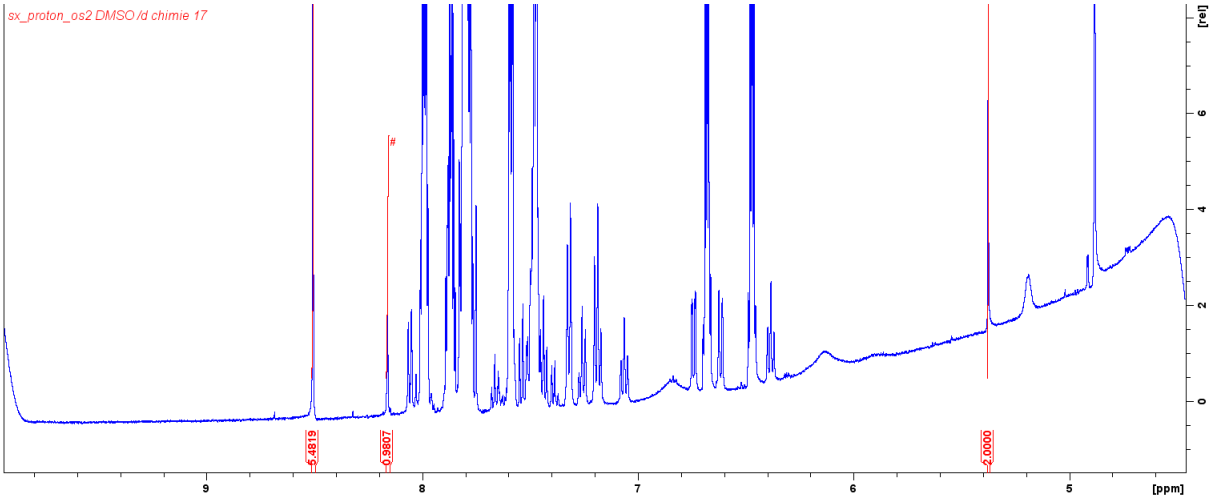


***Figure S13:*** *$^1$H NMR spectrum of 0.6 mL of blank post-2h-photocatalytic MeCN solution, spiked by 0.1 mL of **50 mM** formate MeCN solution, 0.1 mL of reference solution and 0.2 mL of $d_6$-DMSO, 500 MHz.*

**Protocol for working up the relative integrations of the key peaks in the $^1$H NMR spectra:**
Integration of $CH_2$ signal of benzyl benzoate (always present at 1mM in the NMR tube; used as internal reference) is set to 2H, and the relative integration of the 1H signal of formate and of the 1H signal of the other internal reference (dimethyl 5-methoxyisophthalate, always present at 1mM, included for completeness here but it was not employed as a reference herein) determined (Table S1a).

As the relative integration of the baseline at 8.5 ppm (formate signal location) determined for a 80:20 D-acetonitrile : D-dmso solution was 0.01, all of the 'raw' values obtained for the formate peak relative integration, $RI(formate)_{raw}$ were corrected for this by subtracting 0.01, giving RI(formate).

We note that given the benzyl benzoate concentration is always 1 mM and the 2H signal in it is always set to 2H, a relative integration of 1 for the 1H of formate would normally correspond to a 1mM concentration of formate in the NMR solution, i.e. normally RI(formate) would correspond to [formate] in mM - but it is clear from the zero added formate row of data that a small amount of formate is made during photocatalysis on the blank solution, causing these values to be higher than the added formate values - so this is allowed for as follows.

***Table S1a**: Series 1 (using a post-2h-photocatalysis blank MeCN solution): $^1$H NMR spectra relative integrations of key peaks in the four calibration solutions used for formate quantification in MeCN, plus in the far right column the RI(formate) values obtained after a baseline correction was applied, as described in the text. See table S1b for determination of [formate]$_{NMRtube}$.*

| **[formate]$_{added}$** Concentration in mM of formate in NMR calibration solution that is due to **deliberate addition** | **Observed relative NMR integrations of key peaks** | | | **Baseline corrected to give RI(formate) = [formate]$_{obs}$** in mM |
|---|---|---|---|---|
| | benzyl benzoate $CH_2$ (2H) integration **set to 2H** | dimethyl 5-methoxyisophthalate 1H signal relative integration | formate 1H signal relative integration **RI(formate)$_{raw}$** | **RI(formate)** = **RI(formate)$_{raw}$** – 0.01 (see text) |
| **0** | 2 | 0.93 | 0.28 | **0.27** |
| **0.50** | 2 | 0.97 | 0.83 | **0.82** |
| **1.00** | 2 | 0.98 | 1.31 | **1.30** |
| **5.00** | 2 | 0.97 | 5.48 | **5.47** |

i.e. for the 0 added formate calibration NMR solution, [formate]$_{added}$ = 0, the RI(formate) = 0.27 obtained corresponds to [formate]$_{nmr\ tube}$ = 0.27 mM being present, all of which arises from the 2h photocatalysis run, so [formate]$_{2h\text{-}photocat}$ = 0.27 mM. This value was then used to determine the total formate concentration in the NMR tube, [formate]$_{nmr\ tube}$, for all of the other calibration solutions, as these were all made up using aliquots of the same post-2h photocatalysis blank solution, so [formate]$_{nmr\ tube}$ = [formate]$_{added}$ + 0.27 (Table S1b).

Finally, the correlation graph (Figure S14) was prepared for this series 1 data in MeCN, by plotting **RI(formate)** (Table S1a, which equals [formate]$_{obs}$ in mM) vs **[formate]$_{nmr\ tube}$** (Table S1b).

***Table S1b**: Series 1 (using a post-2h-photocatalysis blank MeCN solution) formate calibration data in MeCN (concentrations in mM), detailing the correction to the deliberately added formate by the concentration present due to 2h photocatalysis, determined from the $^1$H NMR calibration data (Table S1a), as described in the text.*

| **[formate]$_{added}$** Concentration (mM) of formate in calibration solution that is due to **deliberate addition** | **[formate]$_{2h\text{-}photocat}$** Concentration (mM) of formate in calibration solution that is due to **2 h photocat** | **[formate]$_{nmr\ tube}$** Total concentration (mM) of formate in calibration solution is [formate]$_{added}$ + [formate]$_{2h\text{-}photocat}$ |
|---|---|---|
| 0 | 0.27 | **0.27** |
| 0.50 | 0.27 | **0.77** |
| 1.00 | 0.27 | **1.27** |
| 5.00 | 0.27 | **5.27** |

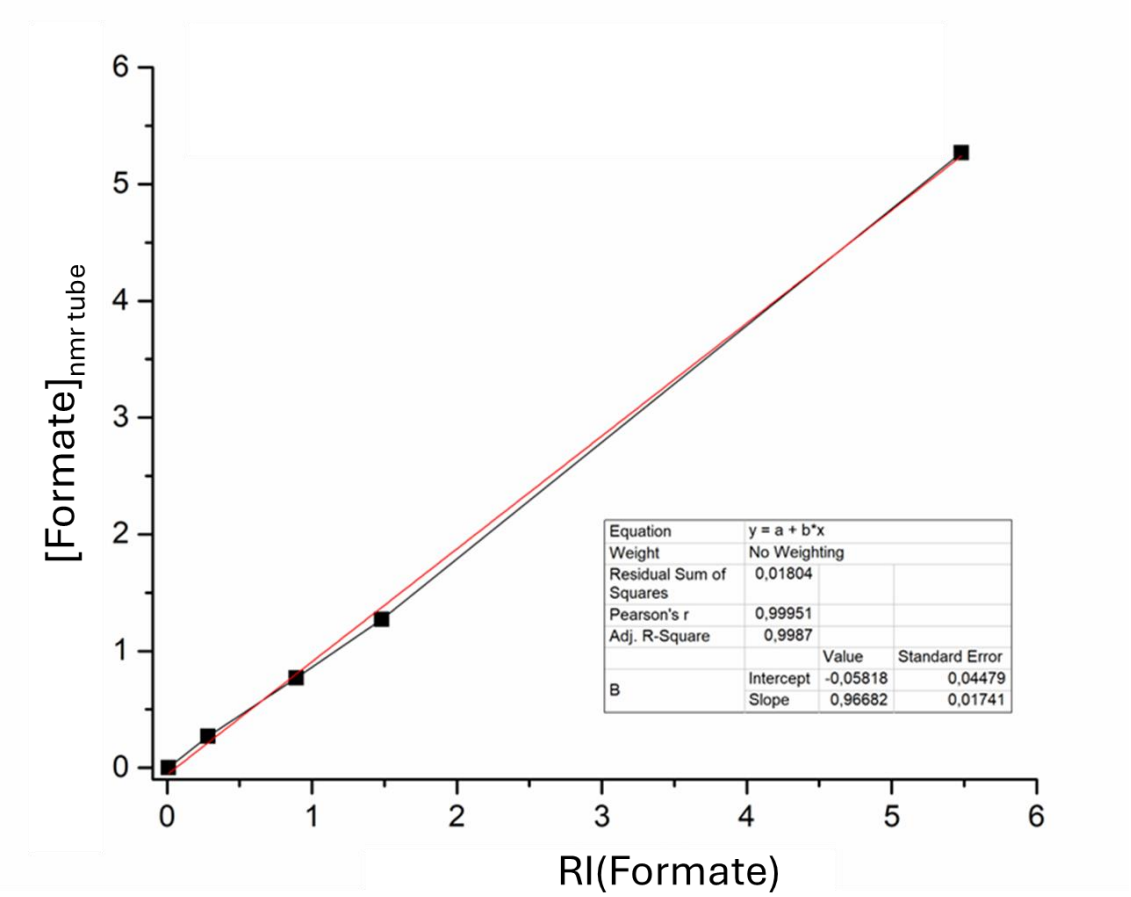


***Figure S14:*** *Series 1 correlation between the known concentration of formate in the NMR tube, [formate]$_{nmr\ tube}$ (mM) vs the relative integration of the formate peak, RI(formate) (relative to the $CH_2$ of the internal standard benzyl benzoate, set to 2H) in acetonitrile/dmso (see Tables S1a and S1b for the data plotted here). Linear fit of data points shown in red, whereas the black line simply joins the dots.*

## Second series of calibration data (using post-48h photocatalysis blank solution)

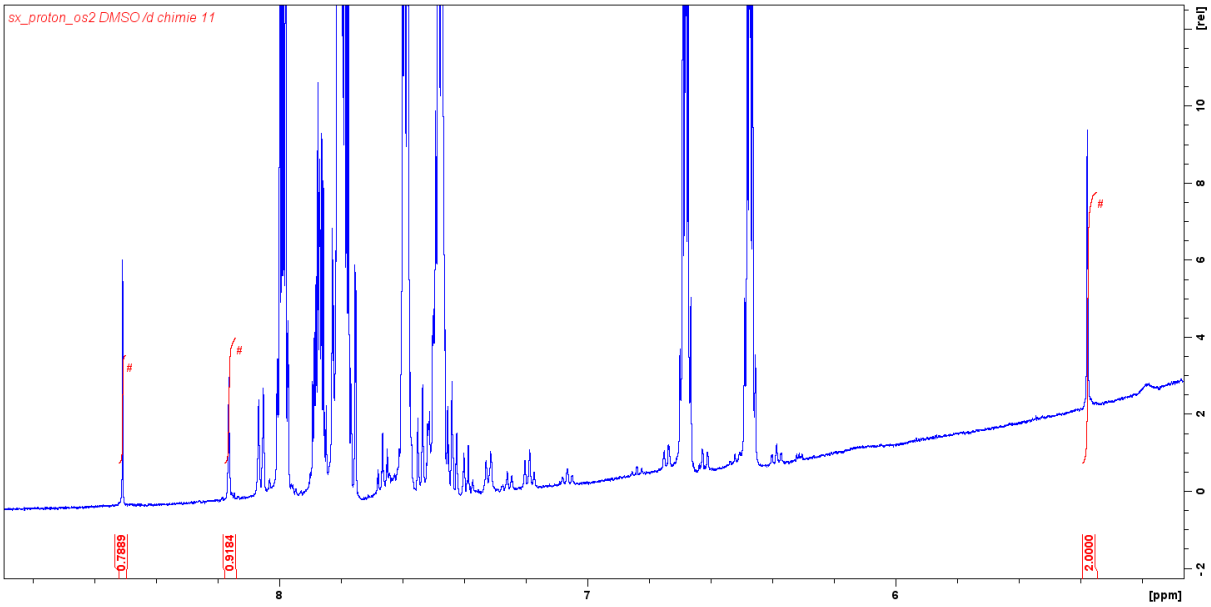


***Figure S15:*** *$^1$H NMR spectrum showing peaks of the chemical references and formate in the photocatalytic solution. The solution is made up of: 70% post-photocatalytic blank solution, 20% $d_6$-DMSO, 10% 10 mmol/L of both dimethyl 5-methoxyisophthalate and benzylbenzoate in acetonitrile solution. The integration of $CH_2$ benzylbenzoate is calibrated at 2 to be used as internal reference, 500 MHz. The Ru(trisbipyridine) system without the catalyst generates formate.*

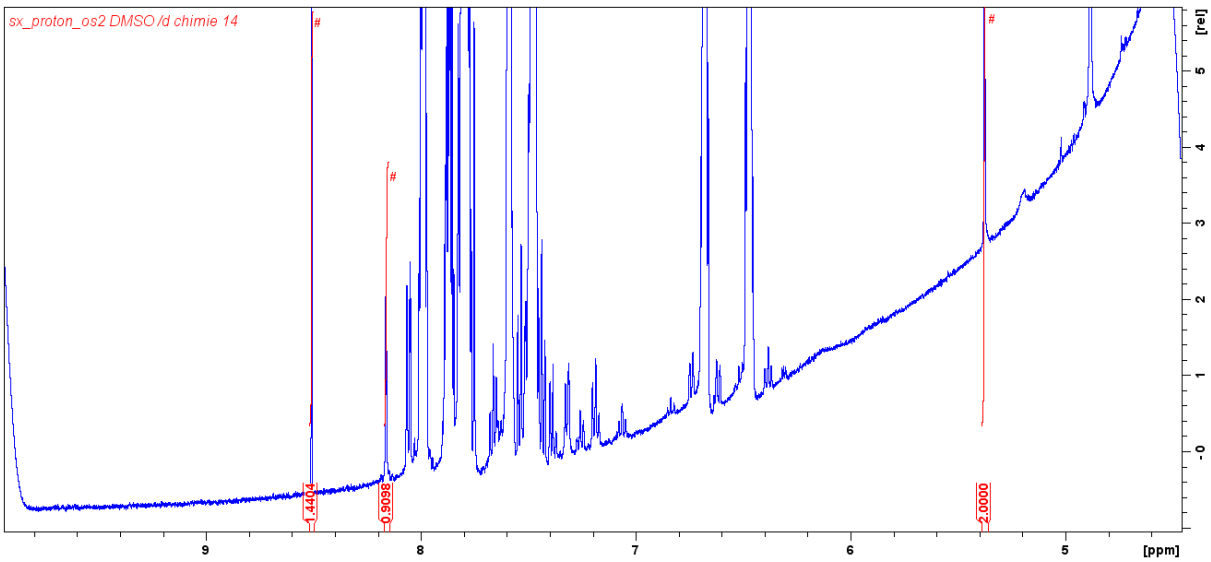


***Figure S16:*** *$^1$H NMR spectrum of 0.6 mL of blank post-48h-photocatalytic MeCN solution, 0.1 mL of **5 mM** formate acetonitrile solution, 0.1 mL of reference solution and 0.2 mL of $d_6$-DMSO, 500 MHz.*

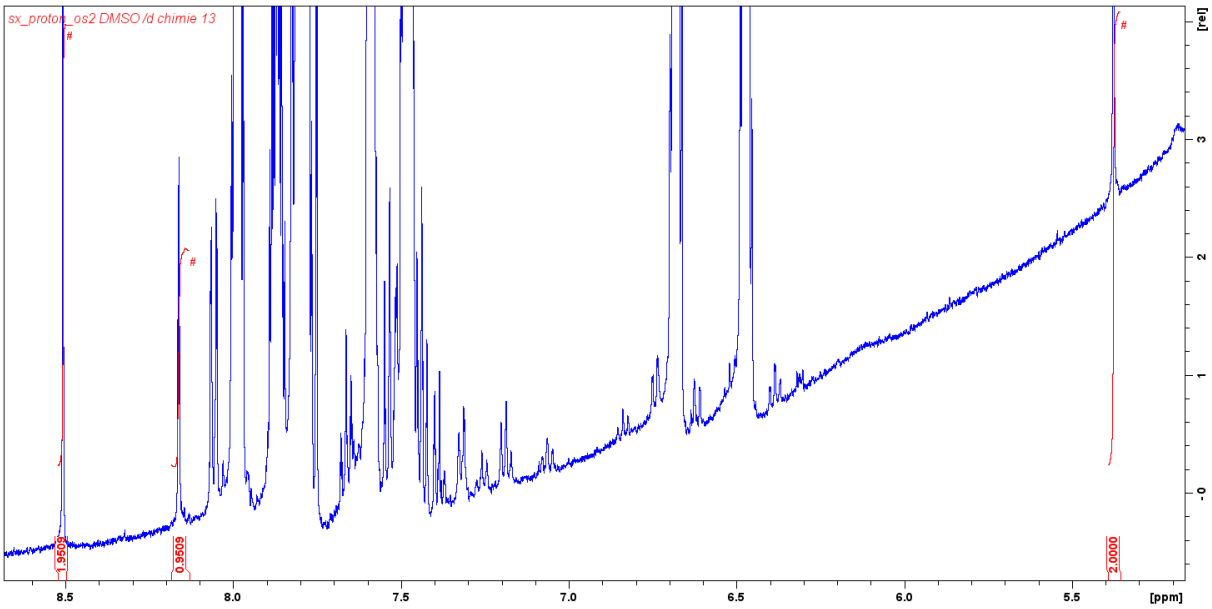


***Figure S17:*** *$^1$H NMR spectrum of 0.6 mL of blank post-48h-photocatalytic MeCN solution, 0.1 mL of* ***10 mM*** *formate acetonitrile solution, 0.1 mL of reference solution and 0.2 mL of $d_6$-DMSO, 500 MHz.*

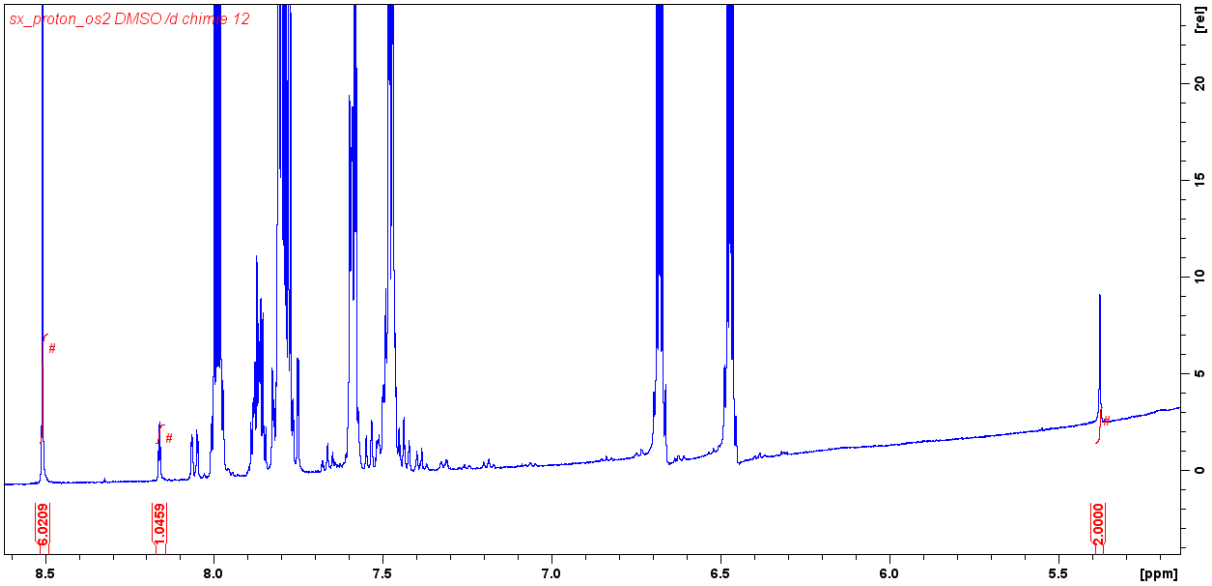


***Figure S18:*** *$^1$H NMR spectrum of 0.6 mL of blank post-48h-photocatalytic MeCN solution, 0.1 mL of* ***50 mM*** *formate acetonitrile solution, 0.1 mL of reference solution and 0.2 mL of $d^6$-DMSO, 500 MHz.*

The same style of analysis as detailed above for the **series 1** calibration dataset in MeCN (using post-2h photocatalytic solution) was carried out for this **series 2** calibration dataset in MeCN (using post-48h photocatalytic solution), with the results shown in Tables S2a and S2b and the resulting calibration graph in Figure S19.

***Table S2a**: Series 2 (using a post-48h-photocatalytic blank MeCN solution) relative $^1$H NMR spectra integrations of key peaks in the calibration solutions used for formate quantification in MeCN, plus in the far right column the RI(formate) values obtained after a baseline correction was applied, as described in the text. See table S2b for determination of [formate]$_{NMRtube}$.*

| **[formate]$_{added}$** Concentration in mM of formate in NMR calibration solution that is due to **deliberate addition** | **Observed relative NMR integrations of key peaks** | | | **Baseline corrected to give RI(formate) = [formate]$_{obs}$** in mM |
|---|---|---|---|---|
| | benzyl benzoate $CH_2$ (2H) integration **set to 2H** | dimethyl 5-methoxyisophthalate 1H signal relative integration | formate 1H signal relative integration **RI(formate)$_{raw}$** | **RI(formate)** = **RI(formate)$_{raw}$** – 0.01 (see text) |
| **0** | 2 | 0.92 | 0.79 | **0.78** |
| **0.50** | 2 | 0.91 | 1.44 | **1.43** |
| **1.00** | 2 | 0.95 | 1.95 | **1.94** |
| **5.00** | 2 | 1.05 | 6.02 | **6.01** |

For the 0 added formate calibration NMR solution, [formate]$_{added}$ = 0, the RI(formate) = 0.78 obtained corresponds to [formate]$_{nmr\ tube}$ = 0.78 mM being present, all of which arises from the 48h photocatalysis run, so [formate]$_{48h\text{-}photocat}$ = 0.78 mM. This value was then used to determine the total formate concentration in the NMR tube, [formate]$_{nmr\ tube}$, for all of the other calibration solutions, as these were all made up using aliquots of the same post-48h photocatalysis blank solution, so [formate]$_{nmr\ tube}$ = [formate]$_{added}$ + 0.78 (Table S2b).

Finally, the correlation graph (Figure S19) was prepared for this series 2 data in MeCN, by plotting **RI(formate)** (Table S2a, which equals [formate]$_{obs}$ in mM) vs **[formate]$_{nmr\ tube}$** (Table S2b).

***Table S2b**: Series 2 (using a post-48h-photocatalysis blank MeCN solution) formate calibration in MeCN (concentrations in mM), detailing the correction to the deliberately added formate by the concentration present due to 48h photocatalysis, determined from the $^1$H NMR calibration data (Table S2a), as described in the text.*

| **[formate]$_{added}$** Concentration (mM) of formate in calibration solution that is due to **deliberate addition** | **[formate]$_{48h\text{-}photocat}$** Concentration (mM) of formate in calibration solution that is due to **48 h photocat** | **[formate]$_{nmr\ tube}$** Total concentration (mM) of formate in calibration solution is [formate]$_{added}$ + [formate]$_{48h\text{-}photocat}$ |
|---|---|---|
| 0 | 0.78 | **0.78** |
| 0.50 | 0.78 | **1.28** |
| 1.00 | 0.78 | **1.78** |
| 5.00 | 0.78 | **5.78** |

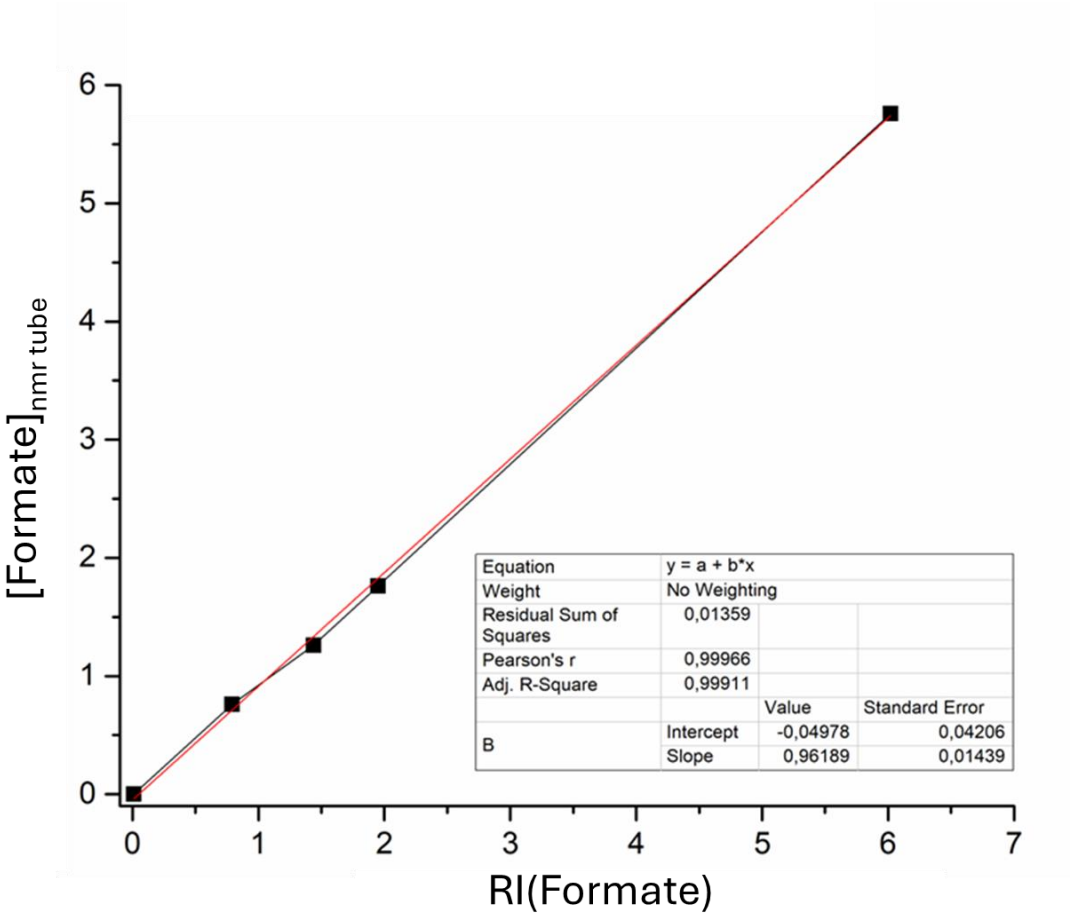


***Figure S19:*** *Series 2 correlation between the known concentration of formate in the NMR tube, [formate]$_{nmr\ tube}$ (mM) vs the relative integration of the formate peak, RI(formate) (relative to the $CH_2$ of the internal standard benzyl benzoate, set to 2H) in acetonitrile/dmso (see Table S2a and S2b for the data plotted here) with the linear fit shown in red, whereas the black line simply joins the dots.*

**Note regarding the second internal reference (not used any further herein)**

We note that the relative integration of the 1H signal at 9.1 ppm for the second internal reference, dimethyl 5-methoxyisophthalate, should be steady at 1H in the above tables (Tables S1a and S2a) but it varies from this by up to 9% in second series (Table S2a) vs by up to 7% in the first series (Table S1a). This signal was not as easy to integrate as that from the benzyl benzoate internal reference, so this compound was not used as a calibrant herein.

**Averaging the 2 calibration lines (using 2h or 48h photocatalysis blank solution) for MeCN**

The linear fit of **RI(formate)** (Table S2a, which equals [formate]$_{obs}$ in mM) vs **[formate]$_{nmr\ tube}$** (Table S2b, formate present in the NMR tube) for the second series of calibration data gave a slope of 0.9618 vs 0.9668 for the first series (average 0.96), and an intercept of -0.050 vs -0.058 for the first series (average -0.05). The linear fit parameters for both series are very similar, so were averaged, resulting in the values shown in equation (eq.9):

$$\textbf{[formate]}_{\textbf{NMR tube}} = 0.96 \times \textbf{RI(formate)} - 0.05 \qquad \textbf{eq. 9}$$

Equation 9 was then used to convert the **RI(formate)** values [the relative formate integrations vs the benzyl benzoate $CH_2$ peak set to 2H, into the $\textbf{[formate]}_{\textbf{NMR tube}}$ values, for the unknown formate post-photocatalysis test solutions, which is subsequently converted into the post catalysis solution concentration, $\textbf{[formate]}_{\textbf{postcat soln}}$, as detailed in the next section.

### 2.5.4 Quantification of unknown formate in post-photocatalysis MeCN solutions

The above correlation (eq. 9) was used to quantify the unknown [formate] in the post-photocatalysis MeCN test solutions, after an aliquot of this solution was used to prepare an NMR sample from which RI(formate) could be determined versus the benzyl benzoate internal reference. The NMR solutions used for this purpose comprised:

- 0.7 mL of the post-photocatalysis test MeCN solution,
- 0.1 mL of 10 mM benzyl benzoate dry MeCN solution and
- 0.2 mL of $d_6$-DMSO.

All NMR tubes were then filled to 4.5 cm from the bottom of the tube with this solution. An example of the resulting $^1$H NMR spectrum (for a run with complex **1** in MeCN) is illustrated in Figure S20. As above, the $CH_2$ singlet of the benzyl benzoate is set to 2H, then the relative integration of the formate signal at 8.5 ppm determined, then corrected by -0.01 for the baseline (as above) to give **RI(formate)**. From this RI(formate) value, equation **9** enables calculation of $\textbf{[formate]}_{\textbf{NMR tube}}$ (in mM).

Finally, the $[\text{formate}]_{\text{NMR tube}}$ value (in mM) is converted into $\textbf{[formate]}_{\textbf{postcat soln}}$ (in mM) using equation **10** to correct for the dilution involved in making up the NMR sample from the postcatalysis test solution:

$$\textbf{[formate]}_{\textbf{postcat soln}} = \textbf{[formate]}_{\textbf{NMR tube}} \times (0.3+0.7)/0.7 \qquad \textbf{eq. 10}$$

The resulting values of $[\text{formate}]_{\text{postcat soln}}$, for all of the photocatalysis runs carried out in MeCN, are tabulated in Table S4 (see Section 5 below).

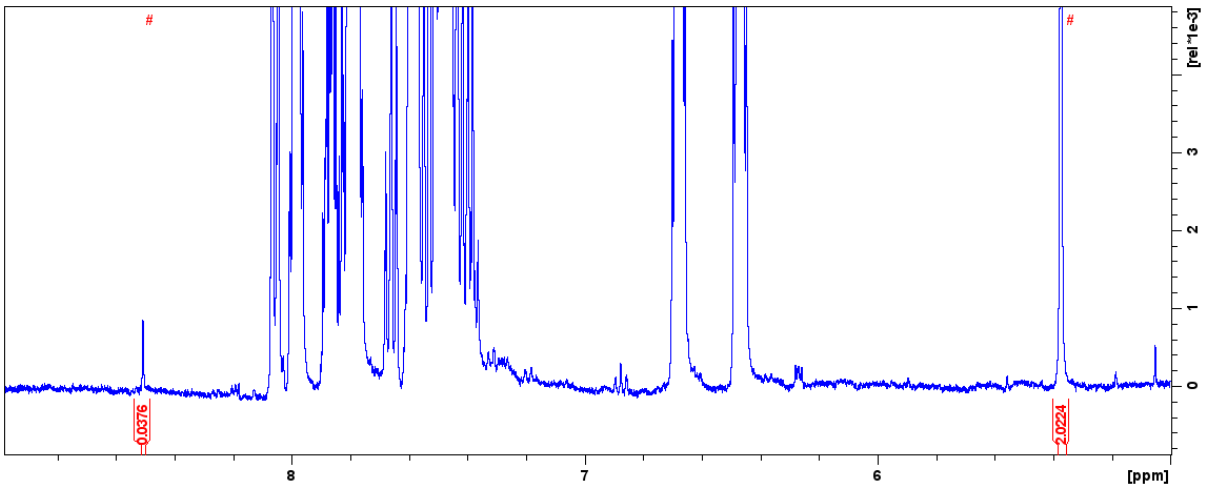


***Figure S20:*** *$^1$H-NMR spectrum (500 MHz, DMSO-d6). NMR solution: 70% post-photocatalytic test solution of complex **1**, 20% deuterated DMSO, and 10% benzylbenzoate 10 mmol/L solution. The spectrum is focused on the low ppm range.*

## 2.5.5 Generating formate calibration curve for DMF solution

In the above sections, benzyl benzoate was established as the preferred internal reference, so it was the only internal reference used in the DMF runs.

As above, the integration of the $CH_2$ singlet of benzylbenzoate at about 5.4 ppm is set to 2H and the relative integration of the 1H formate signal at about 8.5 ppm determined (Table S3a). In this case the concentration of benzylbenzoate present in the NMR tube is **5 mM** (not 1 mM as for MeCN above) so, for example, in this DMF system a relative integration of 1H for formate should correspond to a $[\text{formate}]_{\text{NMR tube}}$ = 5 mM.

For the calibration, it should be noted that in addition to the deliberately added formate, the post-5h-photocatalysis blank DMF solution (everything except catalyst) used had produced formate, which is accounted for in the same way as is detailed above for the above MeCN system, see Table S3b.

Hence, as in the MeCN case, first an NMR solution was prepared without adding any formate, in order to *evaluate the formate concentration of the post-photocatalysis blank solution itself* (Figure S21). The composition of this NMR solution is as follows:

- 0.7 mL of post-5 hr-photocatalytic DMF solution (made up as described in section 2.2 but without the catalyst),
- 0.1 mL of 50 mM benzyl benzoate (chemical internal reference) in dry DMF solution,
- 0.2 mL of $d_6$-DMSO.

Then, a series of four standard stock solutions with known concentrations of added formate (2.5, 5.0, 10, and 50 mM in the NMR tube) were prepared (Figures S22-S25) as follows:

- 0.6 mL of post-5h-photocatalysis test DMF solution (made up as described in section 2.2 but without the catalyst),
- 0.1 mL of 25, 50, 100, or 500 mM formate DMSO solution,
- 0.1 mL of 50 mM benzyl benzoate dry DMF solution,
- 0.2 mL of $d_6$-DMSO.

All NMR tubes are filled to 4.5 cm from the bottom of the tube and the $^{1}H$ NMR spectrum obtained. The integration of the $CH_2$ singlet of benzylbenzoate at 5.4 ppm was always set to 2H, and the relative integration of the formate signal (1H) at 8.5 ppm recorded (Table S3a).

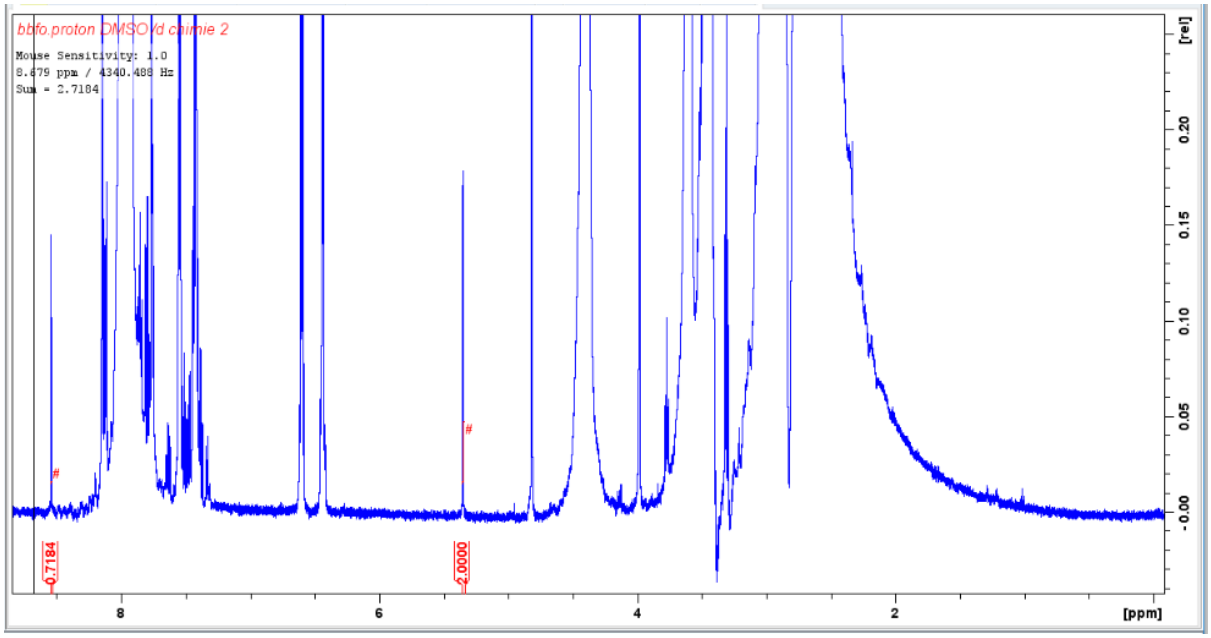


***Figure S21:*** *$^{1}H$ NMR spectrum of 0.7 mL of blank post-5h-photocatalytic DMF solution, 0.1 mL of 50 mM benzyl benzoate solution and 0.2 mL of $d_6$-DMSO, 500 MHz.*

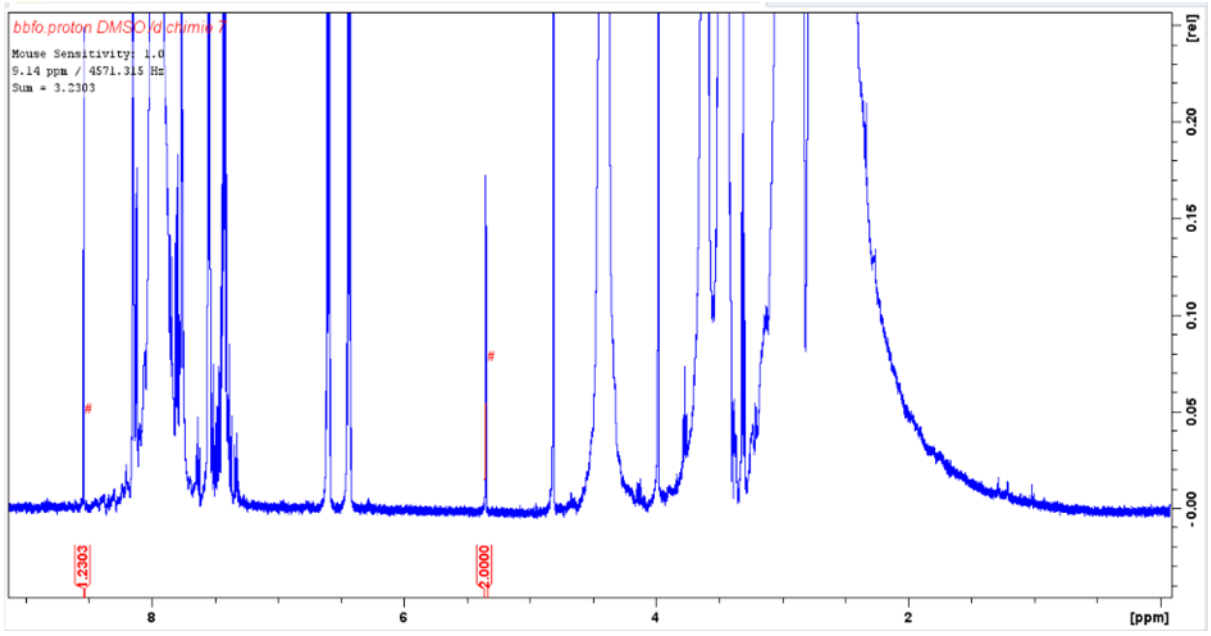


***Figure S22:*** *$^{1}H$ NMR spectrum with addition of 0.1 mL of **25 mM** formate in DMF, 0.6 mL of blank post-5h-photocatalytic DMF solution, 0.1 mL of 50 mM benzyl benzoate solution and 0.2 mL of $d_6$-DMSO, 500 MHz.*

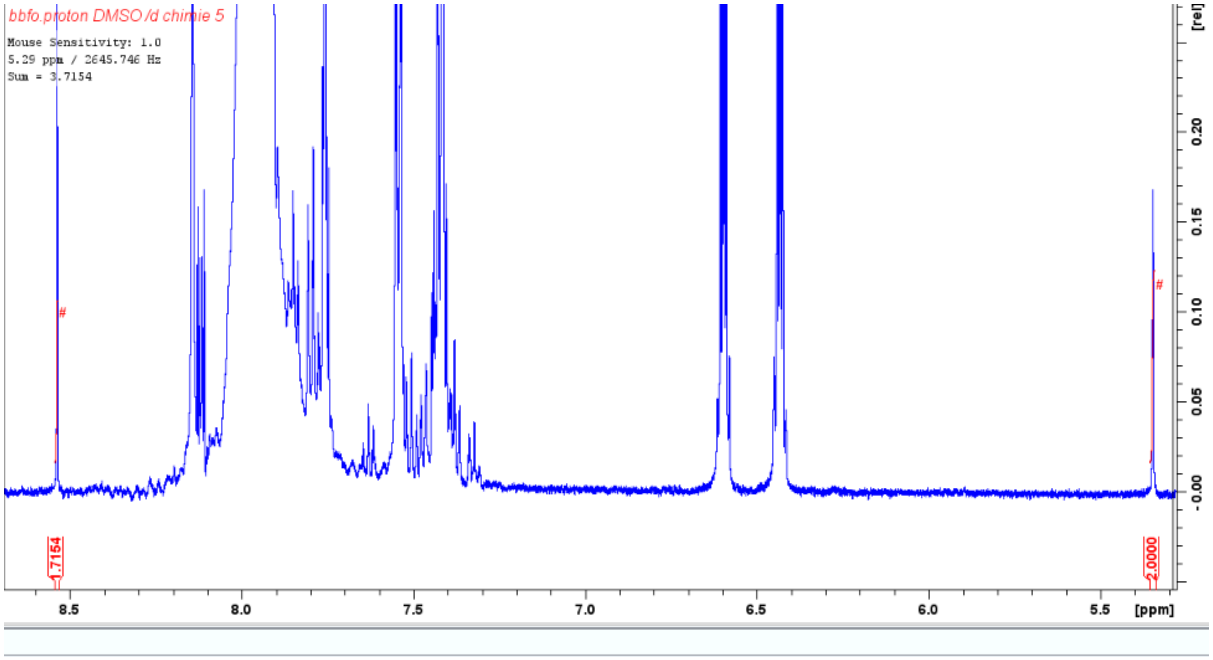


***Figure S23:*** *$^1$H NMR spectrum with addition of 0.1 mL of **50 mM** formate in DMF, 0.6 mL of blank post-5h-photocatalytic DMF solution, 0.1 mL of 50 mM benzyl benzoate solution and 0.2 mL of $d_6$-DMSO, 500 MHz.*

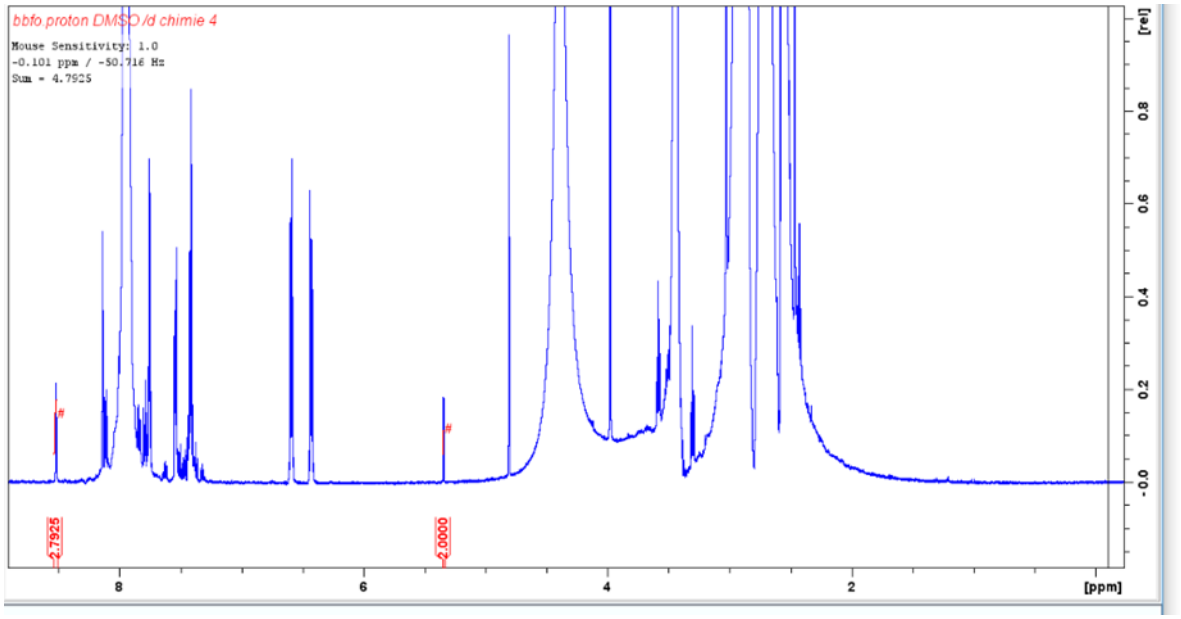


***Figure S24:*** *$^1$H NMR spectrum with addition of 0.1 mL of **100 mM** formate in DMF, 0.1 mL of blank post-5h-photocatalytic DMF solution, 0.1 mL of 50 mM benzyl benzoate solution and 0.2 mL of $d_6$-DMSO, 500 MHz.*

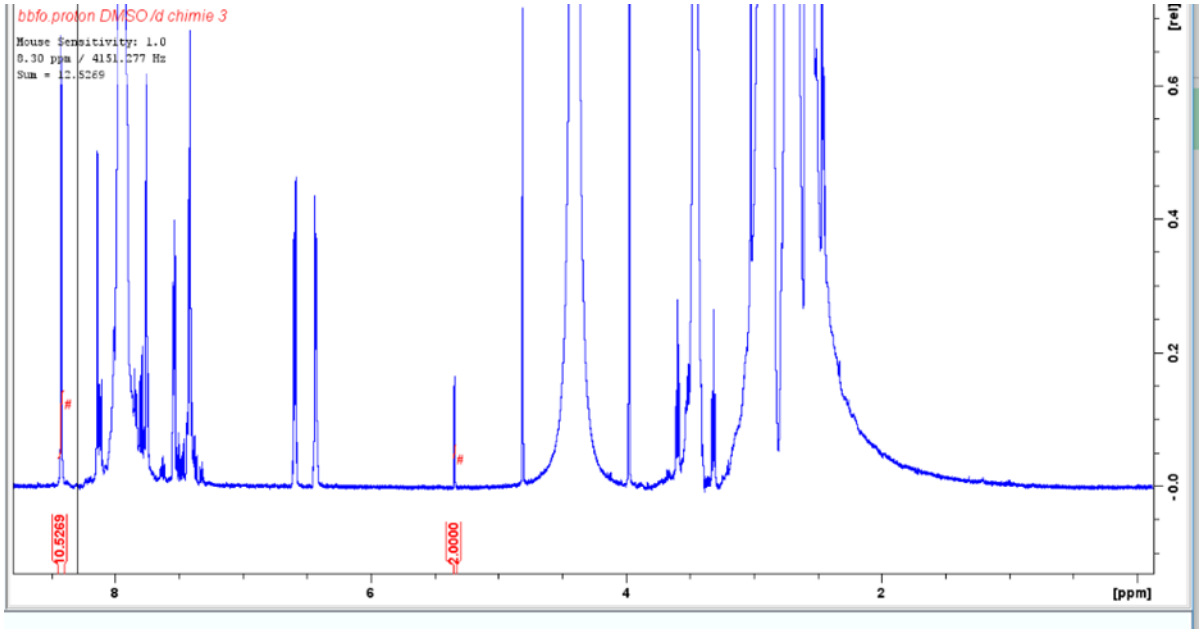


***Figure S25:*** *$^1$H NMR spectrum with addition of 0.1 mL of **500 mM** formate in DMF, 0.6 mL of blank post-5h-photocatalytic DMF solution, 0.1 mL of 50 mM benzyl benzoate solution and 0.2 mL of $d_6$-DMSO, 500 MHz.*

***Table S3a:*** *Formate in DMF calibration data (using a post-5h-photocatalysis blank DMF solution), showing relative $^1$H NMR spectra integrations of key peaks in the calibration solutions, used for formate quantification in DMF. No baseline correction applied. See table S3b for determination of [formate]$_{nmr\ tube}$.*

| **[Formate]$_{added}$** Concentration in mM of formate in NMR calibration solution that is due to **deliberate addition** | **Observed relative NMR integrations of key peaks** | |
|---|---|---|
| | Benzyl benzoate $CH_2$ (**2H**) integration set to 2H **(5 mM)** | Formate (**1H**) signal relative integration **RI(Formate)** |
| **0** | 2 | 0.72 |
| **2.5** | 2 | 1.23 |
| **5** | 2 | 1.72 |
| **10** | 2 | 2.79 |
| **50** | 2 | 10.53 |

As mentioned above, in this case the concentration of benzyl benzoate reference present in the NMR tube is **5 mM** (not 1mM as for MeCN above) so for example, in this DMF system a relative integration of 1 for the 1H signal at 8.5 ppm for formate, **RI(formate) = 1**, should correspond to a **[formate]$_{NMR\ tube}$ = 5 mM**. But herein the total amount of formate present is not as simple as being equal to the amount of formate added, as it is clear from the 'zero-added formate' row of data (Table S3a) that some formate was made during 5 h photocatalysis on the blank solution, causing the [**formate]$_{NMR\ tube}$** values to be higher than the [**formate]$_{added}$** values. This was allowed for in the same way as is detailed for MeCN above. Specifically, for zero added formate, **RI(formate) = 0.72** (actual value 0.7184 obtained was used herein) so, given the NMR solution is 5mM in benzyl benzoate, **[formate]$_{5h\text{-}photocat}$ = 5x 0.7184 = 3.59**. This correction was then applied to the other 'added formate' solutions as shown in Table S3b.

***Table S3b:*** *Formate calibration data, using a post-5h-photocatalysis blank DMF solution, detailing the correction to the deliberately added formate,* $[formate]_{added}$ *(mM), by adding the concentration present in the post-5h-catalysis solution (mM), determined from the above* $^1H$ *NMR calibration data (Table S3a), to yield* $[formate]_{nmr\ tube}$ *(mM).*

| **$[formate]_{added}$** Concentration (mM) of formate in calibration solution that is due to **deliberate addition** | **$[formate]_{5h\text{-}photocat}$** Concentration (mM) of formate in calibration solution that is due to **5 h photocat** | **$[formate]_{nmr\ tube}$** Total concentration (mM) of formate in calibration solution is $[formate]_{added}$ + $[formate]_{5h\text{-}photocat}$ |
|---|---|---|
| 0 | 3.59 | **3.59** |
| 2.50 | 3.59 | **6.09** |
| 5.00 | 3.59 | **8.59** |
| 10.00 | 3.59 | **13.59** |
| 50.00 | 3.59 | **53.59** |

The resulting correlation graph (Figure S26) was prepared for this data in DMF, by plotting **RI(formate)** (Table S3a) vs **$[formate]_{nmr\ tube}$** (Table S3b).

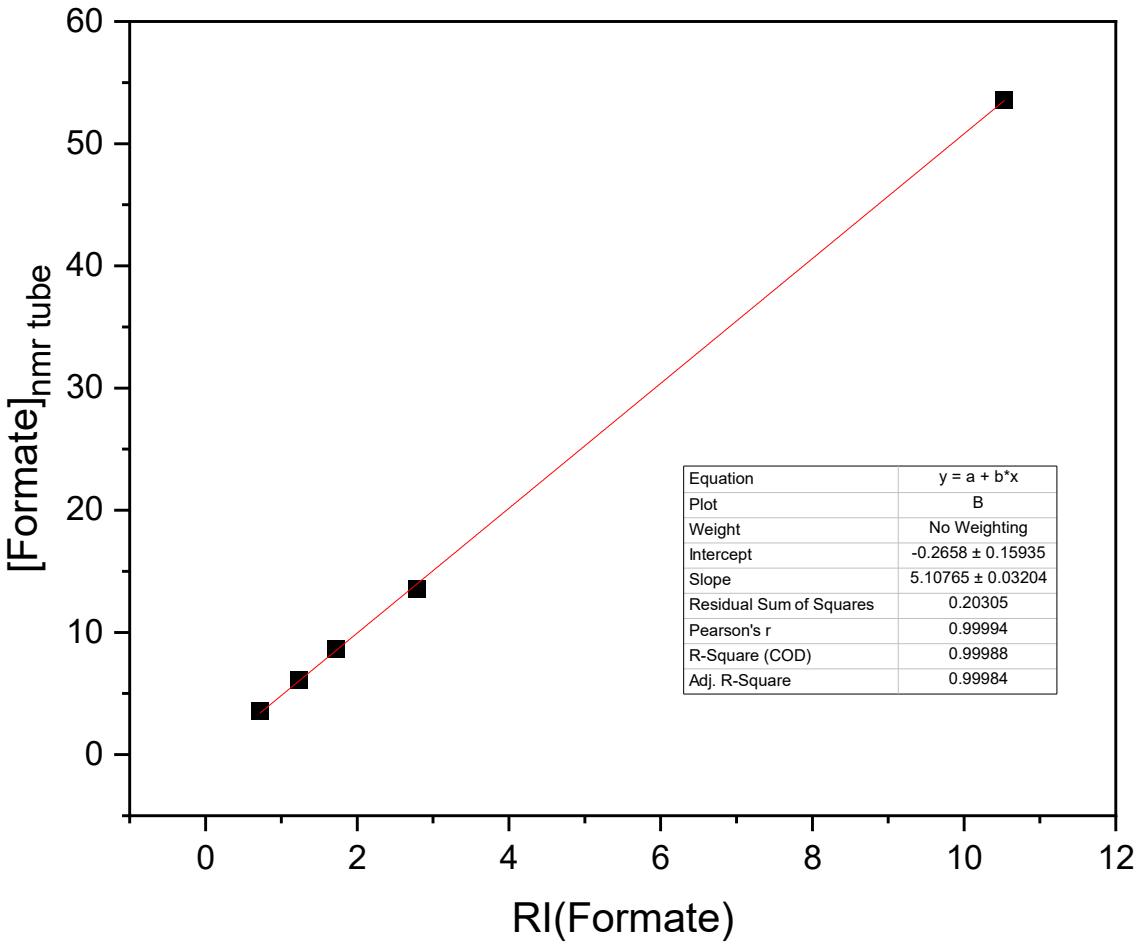


***Figure S26:*** *Correlation line between the known concentration of formate in the NMR tube (mM) vs the relative integration of the formate peak (versus internal standard 5mM benzyl benzoate 2H signal set to 2H) in DMF/DMSO (see Tables S3a and S3b for the data plotted here) with linear fit calculated and shown in red.*

The linear fit of **RI(formate)** (Table S3a) vs **[formate]$_{nmr\ tube}$** (Table S3b) calibration data gave a slope of 5.1 (not 1, because for the DMF studies the reference compound is 5mM, not 1mM, in the NMR tube) and an intercept of -0.27 (eq. 11):

$$\textbf{[formate]}_{\textbf{NMR tube}} = 5.1 \times \textbf{RI(formate)} - 0.27 \qquad \textbf{eq. 11}$$

Equation 8 was then used to convert the RI(formate) values (the relative formate integrations vs the benzyl benzoate $CH_2$ peak set to 2H), into the **[formate]$_{NMR\ tube}$** values, for the unknown formate post-photocatalysis test solutions, as is detailed in the next section.

## 2.5.6 Quantification of unknown formate in post-photocatalytic DMF solutions

The above correlation (**eq. 11**) was used to quantify the unknown [formate] as detailed above for MeCN.

The NMR solution used for formate quantification after completion of a photocatalysis run in DMF comprised:

- 0.7 mL of post-photocatalysis test DMF solution,
- 0.1 mL of 50 mmol/L benzyl benzoate DMSO solution and
- 0.2 mL of $d_6$-DMSO.

All NMR tubes were then filled to 4.5 cm from the bottom of the tube with this solution.

An example of an $^1$H NMR spectrum obtained for the complexes **4**-**5** tested herein in DMF is illustrated in Figure S27 (complex **4**). The $CH_2$ singlet of the benzyl benzoate is set to 2H, then the relative integration of the formate signal, **RI(formate)**, at 8.5 ppm was determined (Figure S8, S10 and S26), then using **equation 11** (the established calibration line) it is converted to **[formate]$_{nmr\ tube}$**, with the resulting values tabulated in Table S5 (see section 8 below).

Finally, in the same way as detailed for MeCN in section 2.5.4, the **[formate]$_{NMR\ tube}$** value (in mM) is converted into **[formate]$_{postcat\ soln}$** (in mM) using **equation 10** (which simply corrects for the dilution involved in preparing the NMR solution). The resulting values of **[formate]$_{postcat\ soln}$**, for all of the photocatalysis runs carried out in DMF, are tabulated in Table S5 (see Section 8 below).

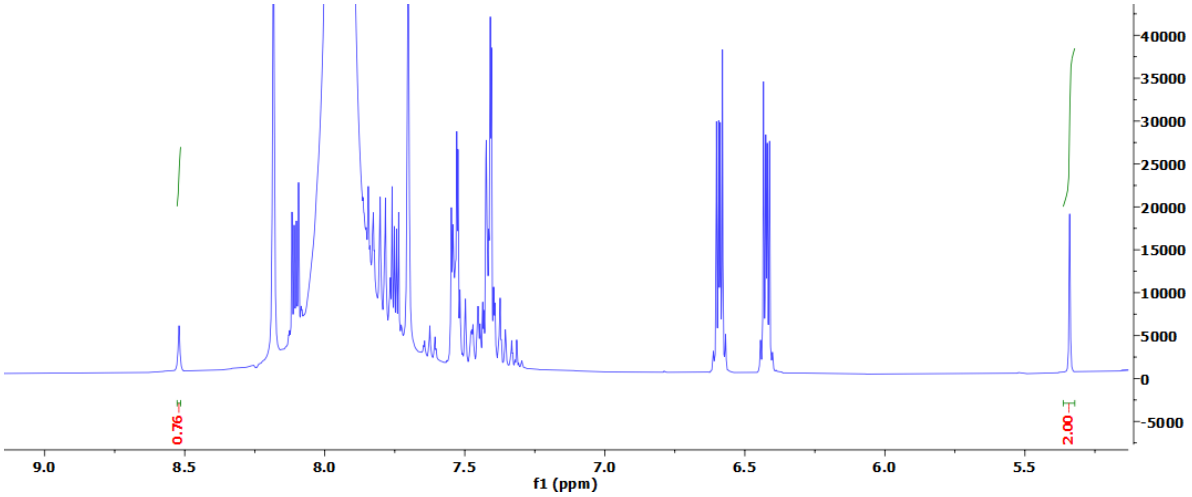


***Figure S27*:** *High ppm portion of the $^{1}$H-NMR spectrum (500 MHz, DMSO-$d_6$) of the following NMR solution: 70% post-photocatalytic test solution of complex **4**, 20% deuterated DMSO, and 10% benzyl benzoate 10 mM solution.*

# 3. Results of photocatalytic $CO_2$RR in MeCN

A large pure batch of BIH was synthesised by the literature procedure[1-3] (details provided above) and was used for all experiments in this section.

## 3.1. Blank experiments (no complex)

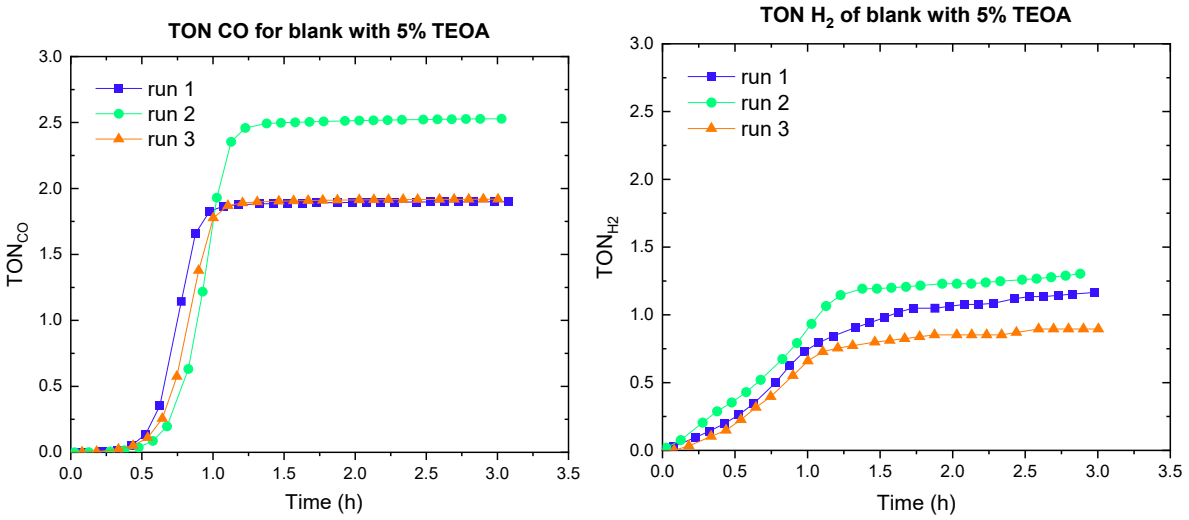


***Figure S28:*** Triplicate runs showing TON, $CO_2$ to CO (left) and $H_2$ (right) during $CO_2$RR for **blank** in MeCN, on irradiation with a blue LED (($\lambda$ = 445 nm), with 0.38 M (5%) TEOA, 0.2 mM $[Ru(bpy)_3](PF_6)_2$ and 0.05 M BIH under $CO_2$ saturated atmosphere.

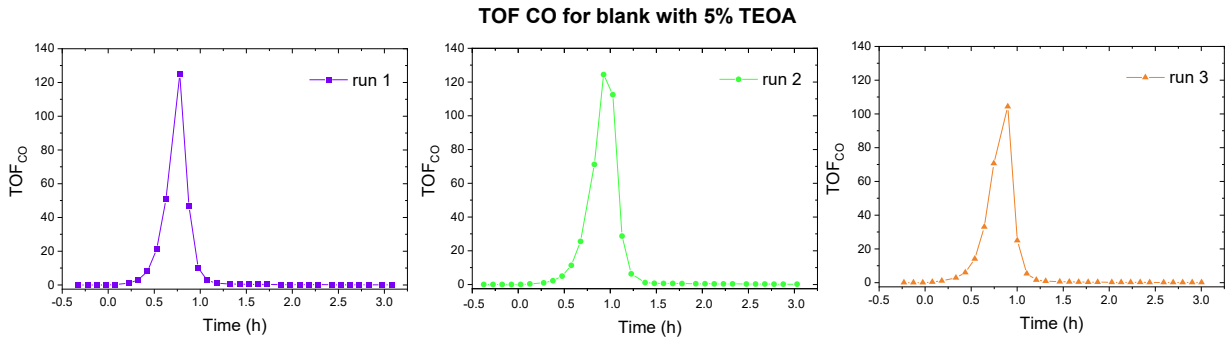


***Figure S29:*** Triplicate runs showing TOF, $CO_2$ to CO during $CO_2$RR for **blank** in MeCN, on irradiation with a blue LED (($\lambda$ = 445 nm), with 0.38 M (5%) TEOA, 0.2 mM $[Ru(bpy)_3](PF_6)_2$ and 0.05 M BIH under $CO_2$ saturated atmosphere.

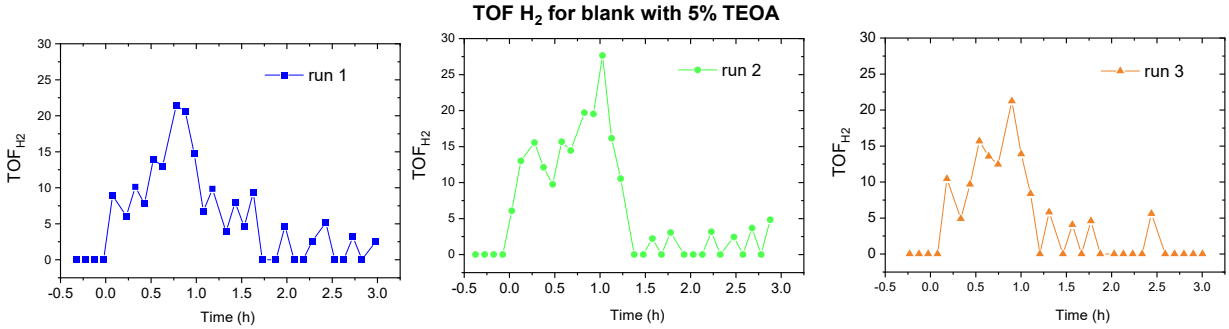


***Figure S30:*** Triplicate runs showing TOF, $CO_2$ to $H_2$ during $CO_2$RR for **blank** in MeCN, on irradiation with a blue LED (($\lambda$ = 445 nm), with 0.38 M (5%) TEOA, 0.2 mM $[Ru(bpy)_3](PF_6)_2$ and 0.05 M BIH under $CO_2$ saturated atmosphere.

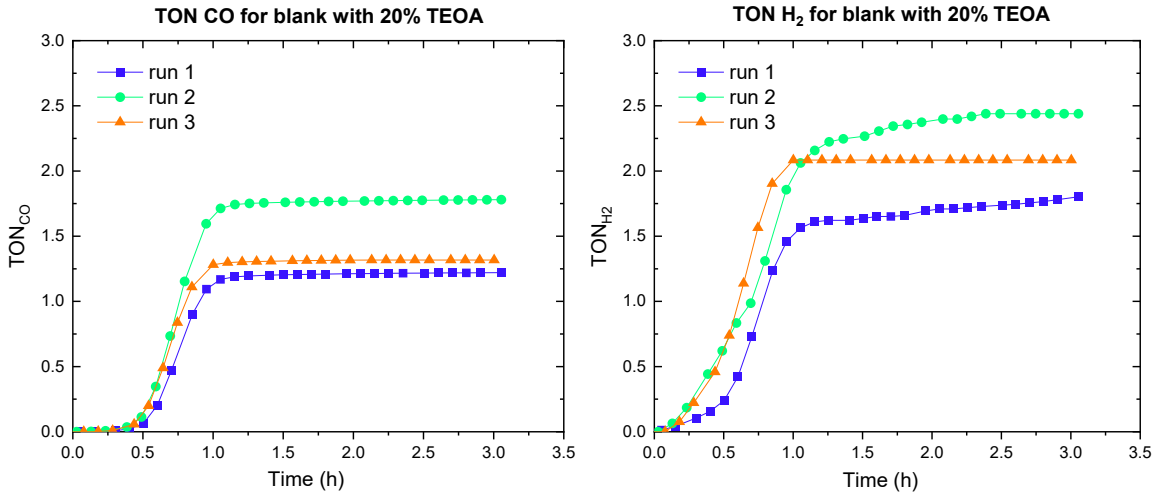


***Figure S31:*** Triplicate runs showing TON, $CO_2$ to CO (left) and $H_2$ (right) during $CO_2$RR for **blank** in MeCN, on irradiation with a blue LED ((λ = 445 nm), with 1.5 M (20%) TEOA, 0.2 mM $[Ru(bpy)_3](PF_6)_2$ and 0.05 M BIH under $CO_2$ saturated atmosphere.

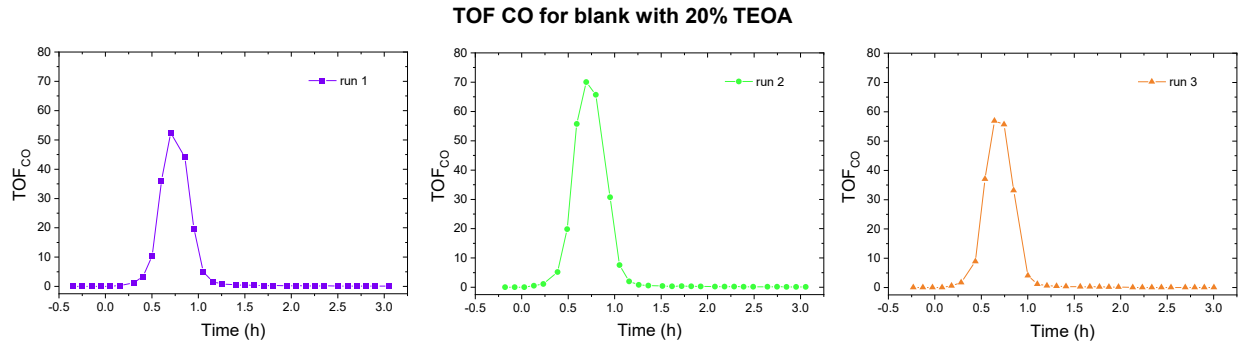


***Figure S32:*** Triplicate runs showing TOF, $CO_2$ to CO during $CO_2$RR for **blank** in MeCN, on irradiation with a blue LED ((λ = 445 nm), with 1.5 M (20%) TEOA, 0.2 mM $[Ru(bpy)_3](PF_6)_2$ and 0.05 M BIH under $CO_2$ saturated atmosphere.

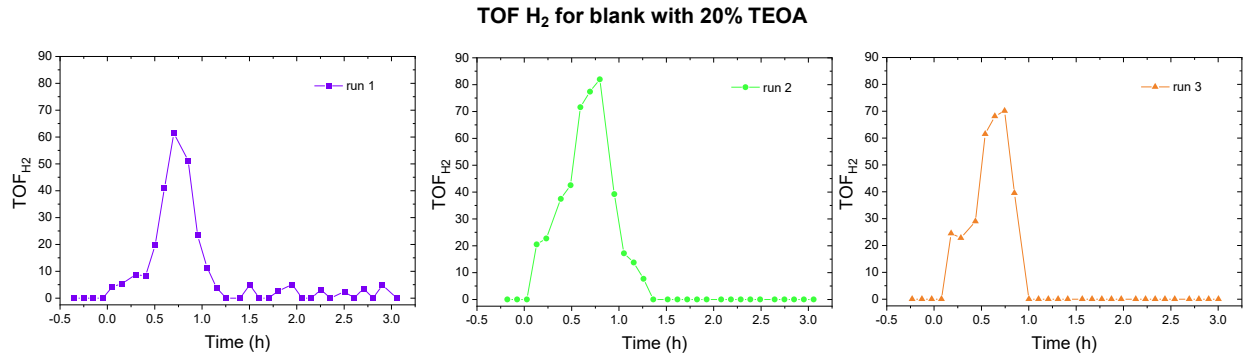


***Figure S33:*** Triplicate runs showing TOF, $CO_2$ to $H_2$ during $CO_2$RR for **blank** in MeCN, on irradiation with a blue LED ((λ = 445 nm), with 1.5 M (20%) TEOA, 0.2 mM $[Ru(bpy)_3](PF_6)_2$ and 0.05 M BIH under $CO_2$ saturated atmosphere.

## 3.2. Control with simple copper salt as catalyst

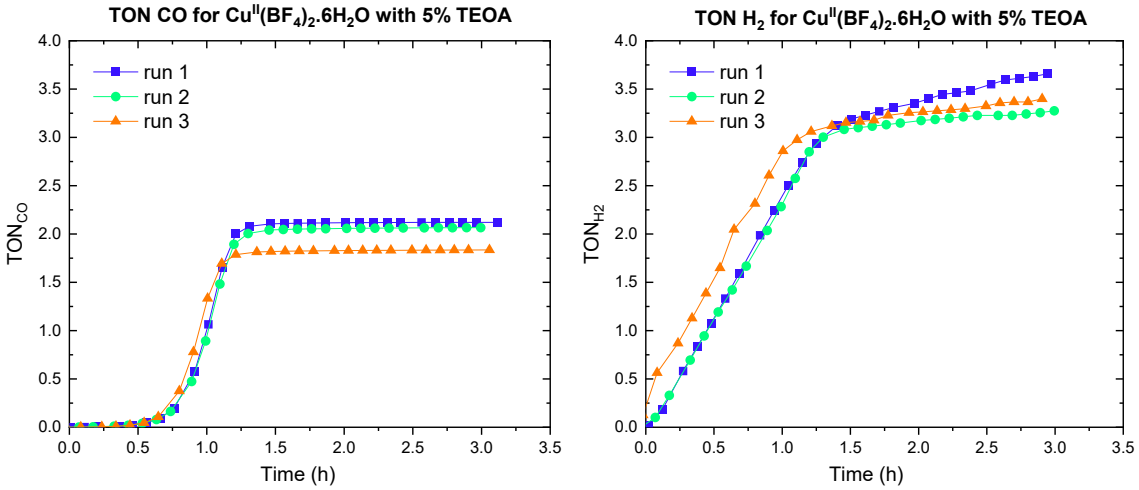


***Figure S34:*** Triplicate runs showing TON, $CO_2$ to CO (left) and $H_2$ (right) during $CO_2$RR for **$Cu^{II}(BF_4)_2.6H_2O$ (control)** in MeCN ($C_{cat}$ = 5 µM), on irradiation with a blue LED (($\lambda$ = 445 nm), with 0.38 M (5%) TEOA, 0.2 mM $[Ru(bpy)_3](PF_6)_2$ and 0.05 M BIH under $CO_2$ saturated atmosphere.

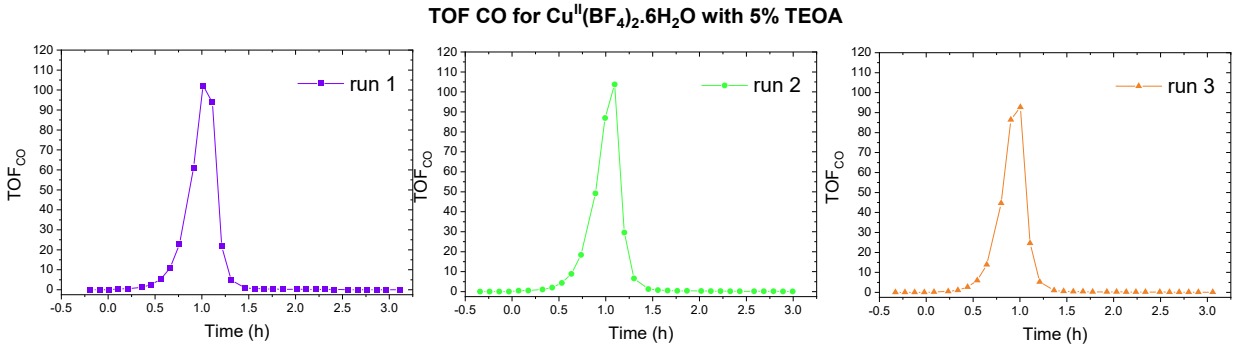


***Figure S35:*** Triplicate runs showing TOF, $CO_2$ to CO during $CO_2$RR for **$Cu^{II}(BF_4)_2.6H_2O$ (control)** in MeCN ($C_{cat}$ = 5 µM), on irradiation with a blue LED (($\lambda$ = 445 nm), with 0.38 M (5%) TEOA, 0.2 mM $[Ru(bpy)_3](PF_6)_2$ and 0.05 M BIH under $CO_2$ saturated atmosphere.

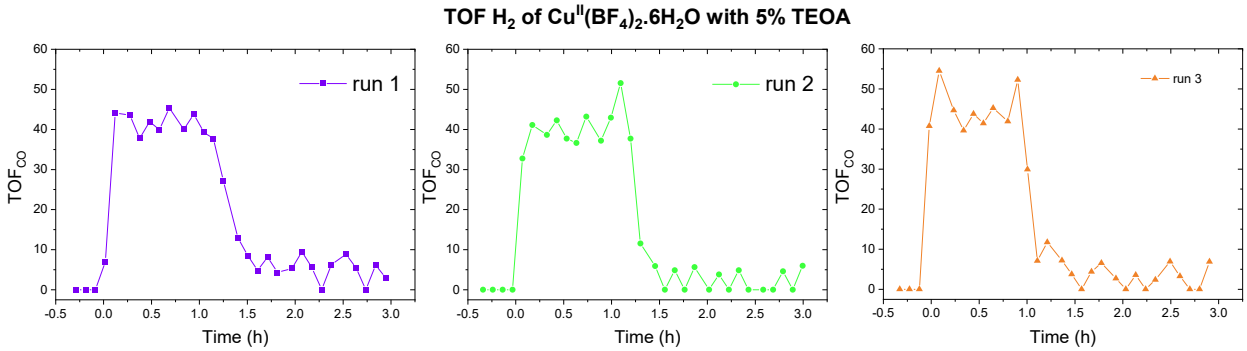


***Figure S36:*** Triplicate runs showing TOF, $CO_2$ to $H_2$ during $CO_2$RR for **$Cu^{II}(BF_4)_2.6H_2O$ (control)** in MeCN ($C_{cat}$ = 5 µM), on irradiation with a blue LED (($\lambda$ = 445 nm), with 0.38 M (5%) TEOA, 0.2 mM $[Ru(bpy)_3](PF_6)_2$ and 0.05 M BIH under $CO_2$ saturated atmosphere.

## 3.3. Control with complex 1 but without TEOA, BIH and PS

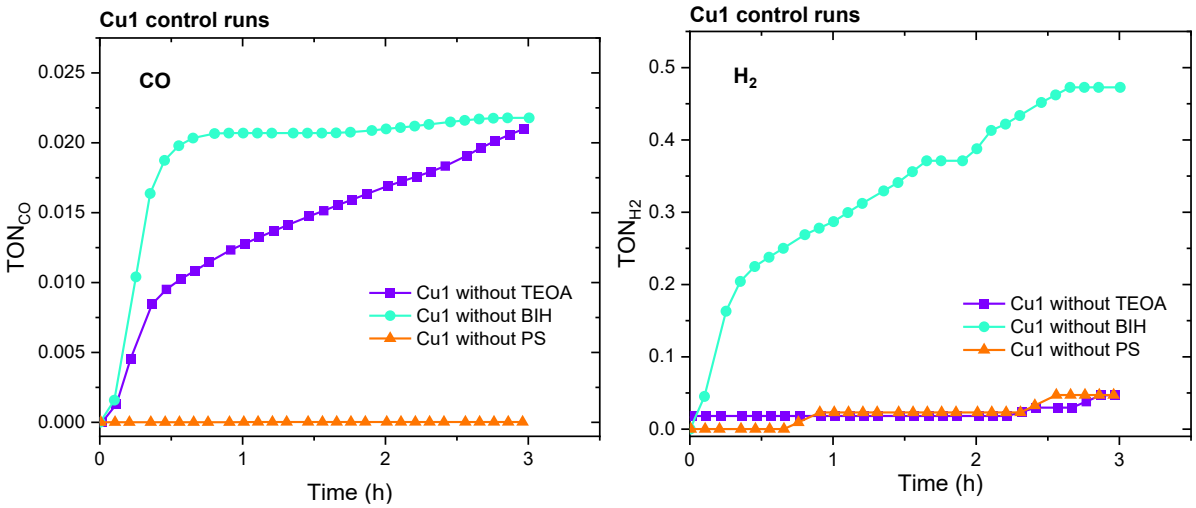


***Figure S37:*** **Complex 1 control** runs: without TEOA (purple), without BIH (teal), and without PS (orange) showing TON, $CO_2$ to CO (left) and $H_2$ (right) during $CO_2$RR in MeCN ($C_{cat}$ = 5 µM), on irradiation with a blue LED ((λ = 445 nm), under $CO_2$ saturated atmosphere.

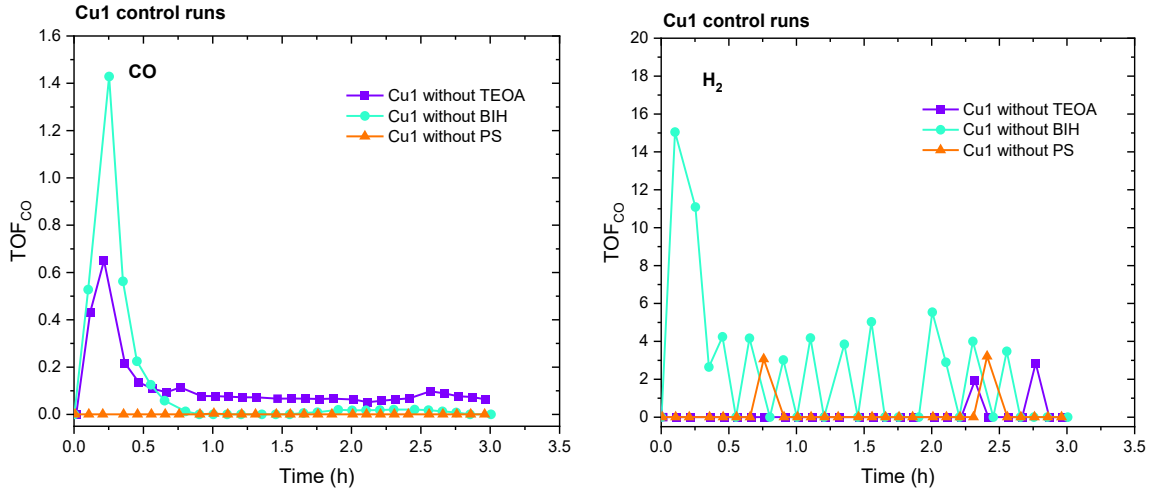


***Figure S38:*** **Complex 1 control** runs: without TEOA (purple), without BIH (teal), and without PS (orange) showing TOF, $CO_2$ to CO (left) and $H_2$ (right) during $CO_2$RR in MeCN ($C_{cat}$ = 5 µM), on irradiation with a blue LED ((λ = 445 nm), under $CO_2$ saturated atmosphere.

## 3.4. Photocatalytic $CO_2$RR for complexes 1-3 in MeCN

### 3.4.1 Complex 1, $CuL^{Et}BF_4$

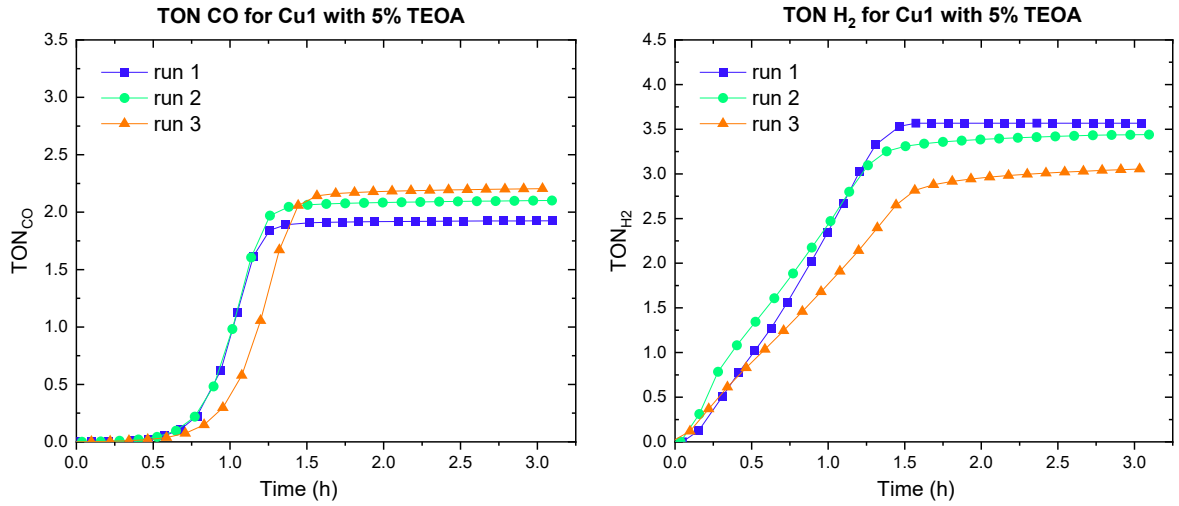


***Figure S39:*** Triplicate runs showing TON, $CO_2$ to CO (left) and $H_2$ (right) during $CO_2$RR for **complex 1** in MeCN ($C_{cat}$ = 5 µM), on irradiation with a blue LED ((λ = 445 nm), with 0.38 M (5%) TEOA, 0.2 mM $[Ru(bpy)_3](PF_6)_2$ and 0.05 M BIH under $CO_2$ saturated atmosphere.

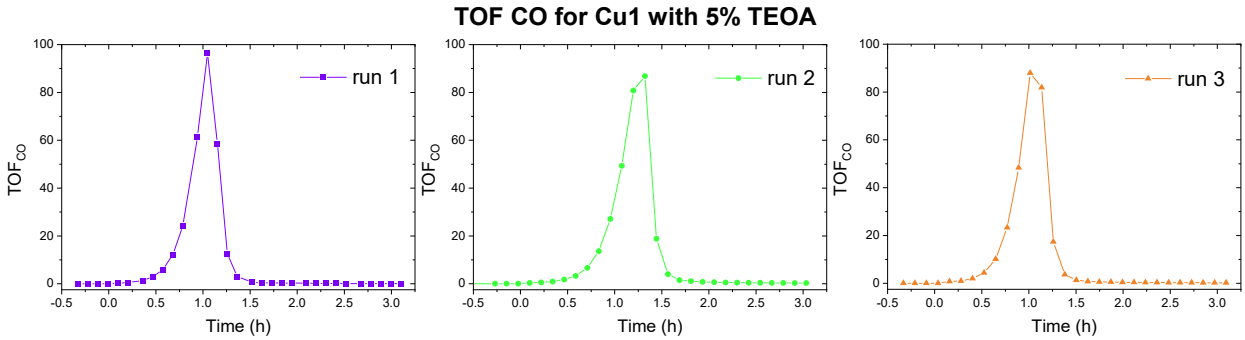


***Figure S40:*** Triplicate runs showing TOF, $CO_2$ to CO during $CO_2$RR for **complex 1** in MeCN ($C_{cat}$ = 5 µM), on irradiation with a blue LED ((λ = 445 nm), with 0.38 M (5%) TEOA, 0.2 mM $[Ru(bpy)_3](PF_6)_2$ and 0.05 M BIH under $CO_2$ saturated atmosphere.

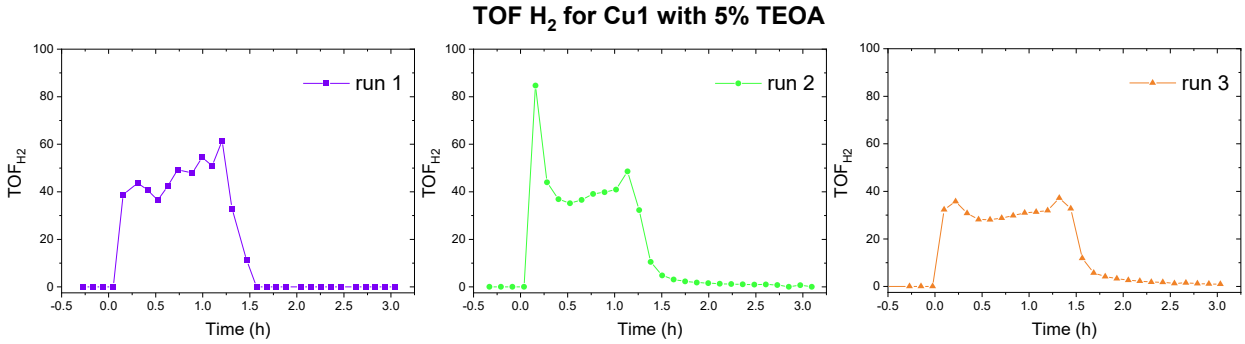


***Figure S41:*** Triplicate runs showing TOF, $CO_2$ to $H_2$ during $CO_2$RR for **complex 1** in MeCN ($C_{cat}$ = 5 µM), on irradiation with a blue LED ((λ = 445 nm), with 0.38 M (5%) TEOA, 0.2 mM $[Ru(bpy)_3](PF_6)_2$ and 0.05 M BIH under $CO_2$ saturated atmosphere.

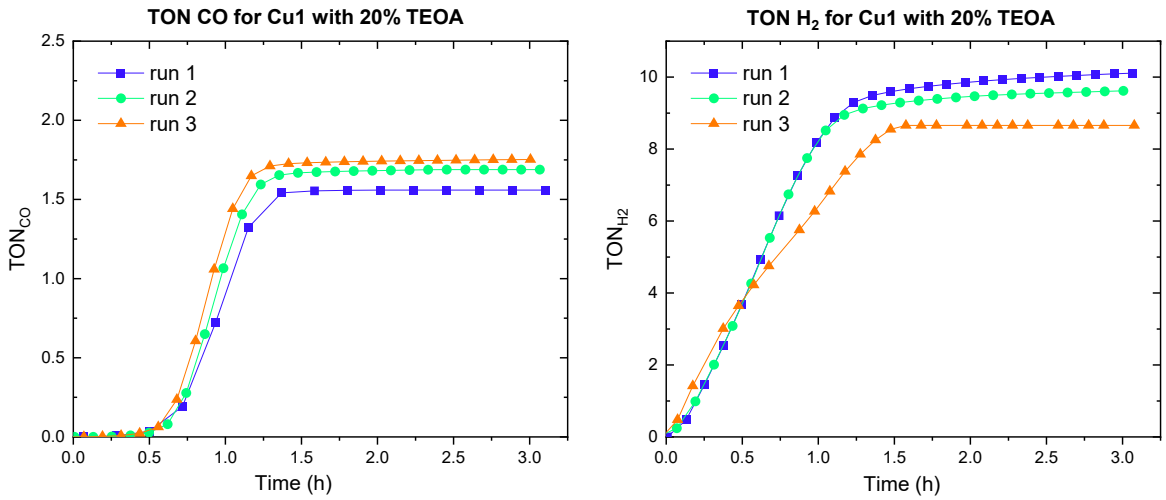


***Figure S42:*** Triplicate runs showing TON, $CO_2$ to CO (left) and $H_2$ (right) during $CO_2$RR for **complex 1** in MeCN ($C_{cat}$ = 5 µM), on irradiation with a blue LED ((λ = 445 nm), with 1.5 M (20%) TEOA, 0.2 mM $[Ru(bpy)_3](PF_6)_2$ and 0.05 M BIH under $CO_2$ saturated atmosphere.

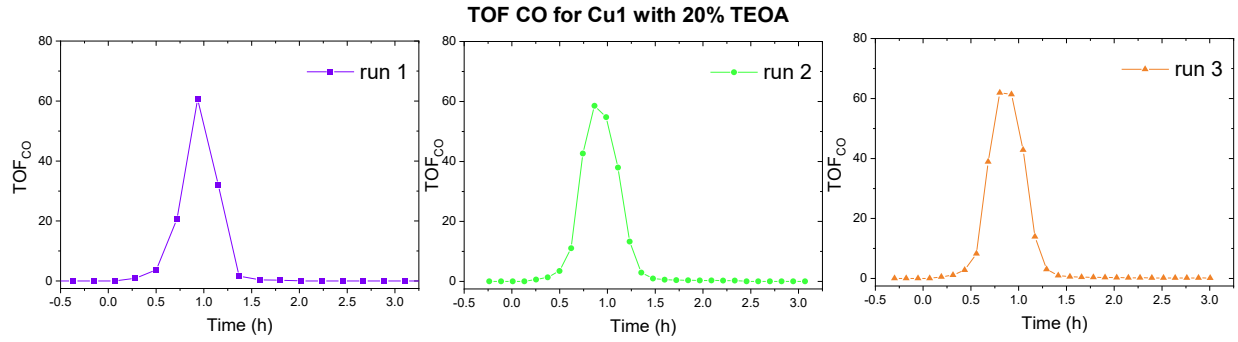


***Figure S43:*** Triplicate runs showing TOF, $CO_2$ to CO during $CO_2$RR for **complex 1** in MeCN ($C_{cat}$ = 5 µM), on irradiation with a blue LED ((λ = 445 nm), with 1.5 M (20%) TEOA, 0.2 mM $[Ru(bpy)_3](PF_6)_2$ and 0.05 M BIH under $CO_2$ saturated atmosphere.

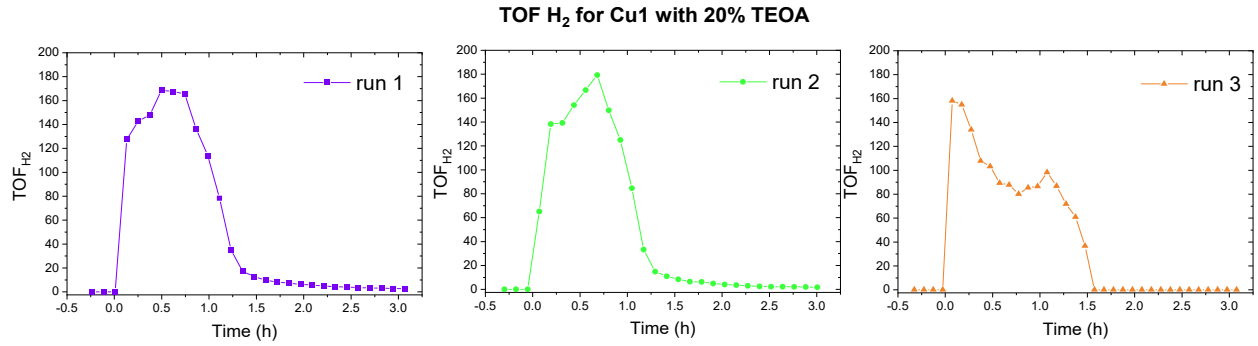


***Figure S44:*** Triplicate runs showing TOF, $CO_2$ to $H_2$ during $CO_2$RR for **complex 1** in MeCN ($C_{cat}$ = 5 µM), on irradiation with a blue LED ((λ = 445 nm), with 1.5 M (20%) TEOA, 0.2 mM $[Ru(bpy)_3](PF_6)_2$ and 0.05 M BIH under $CO_2$ saturated atmosphere.

## 3.4.2 Complex 2, $[Cu^{II}L^{Et\text{-}MePy}]BF_4$

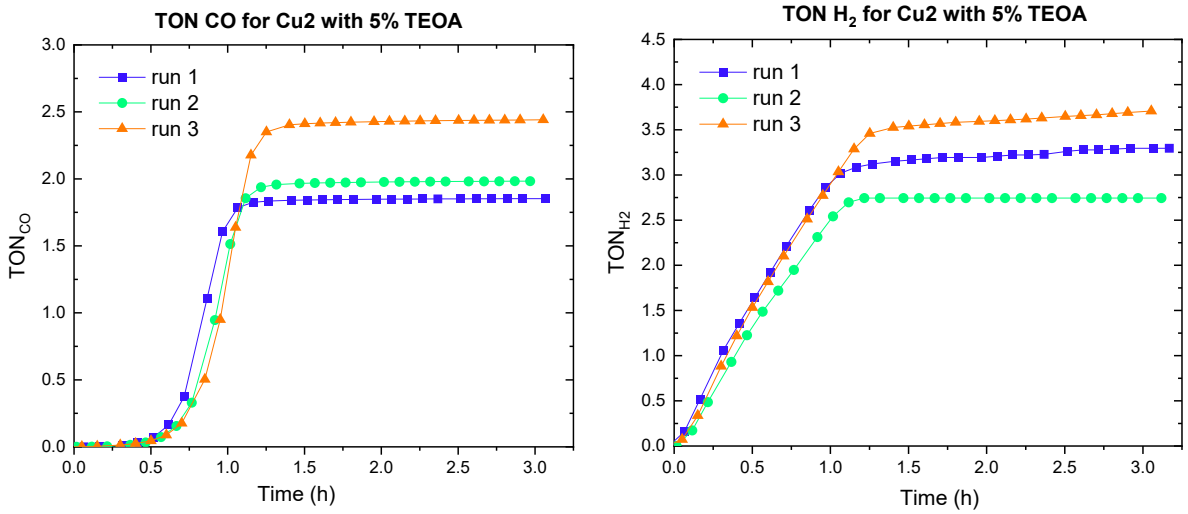


***Figure S45:*** Triplicate runs showing TON, $CO_2$ to CO (left) and $H_2$ (right) during $CO_2$RR for **complex 2** in MeCN ($C_{cat}$ = 5 µM), on irradiation with a blue LED (($\lambda$ = 445 nm), with 0.38 M (5%) TEOA, 0.2 mM $[Ru(bpy)_3](PF_6)_2$ and 0.05 M BIH under $CO_2$ saturated atmosphere.

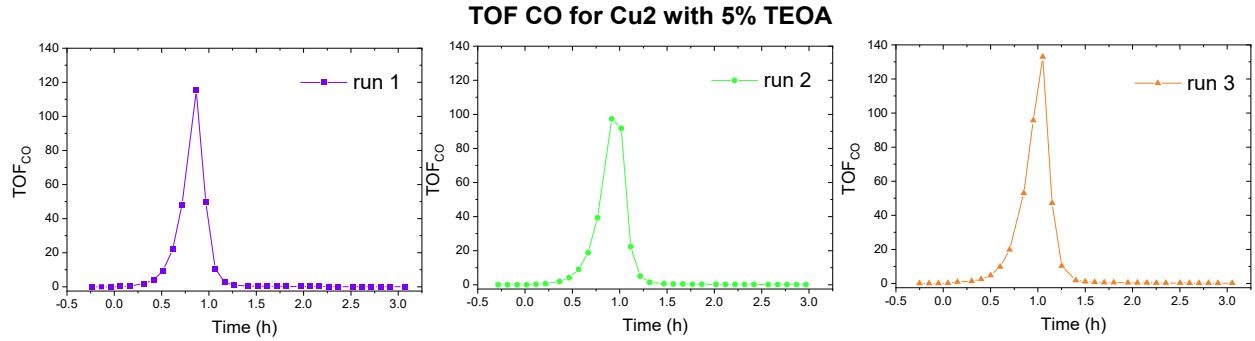


***Figure S46:*** Triplicate runs showing TOF, $CO_2$ to CO during $CO_2$RR for **complex 2** in MeCN ($C_{cat}$ = 5 µM), on irradiation with a blue LED (($\lambda$ = 445 nm), with 0.38 M (5%) TEOA, 0.2 mM $[Ru(bpy)_3](PF_6)_2$ and 0.05 M BIH under $CO_2$ saturated atmosphere.

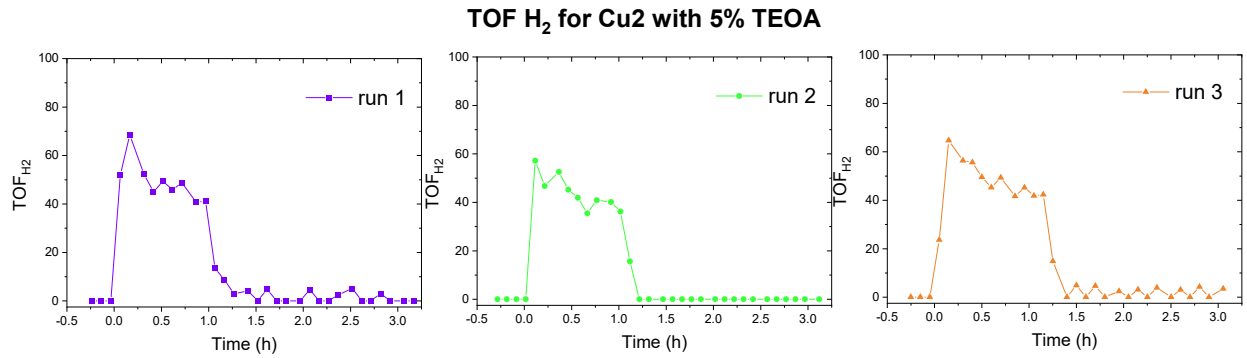


***Figure S47:*** Triplicate runs showing TOF, $CO_2$ to $H_2$ during $CO_2$RR for **complex 2** in MeCN ($C_{cat}$ = 5 µM), on irradiation with a blue LED (($\lambda$ = 445 nm), with 0.38 M (5%) TEOA, 0.2 mM $[Ru(bpy)_3](PF_6)_2$ and 0.05 M BIH under $CO_2$ saturated atmosphere.

## 3.4.3 Complex 3, $[Cu^{II}L^{EtPy2}]BF_4$

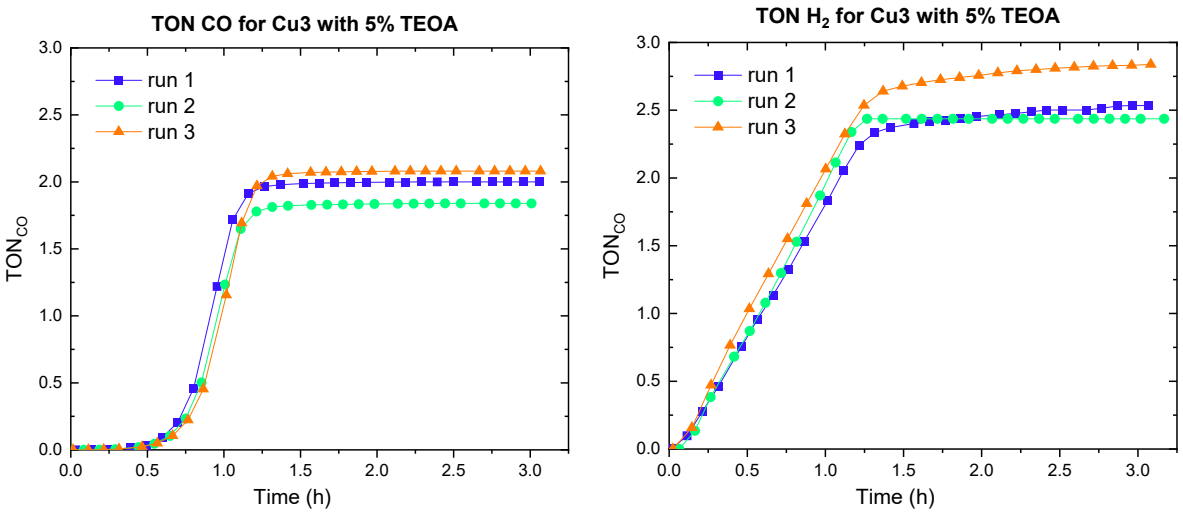


***Figure S48:*** Triplicate runs showing TON, $CO_2$ to CO (left) and $H_2$ (right) during $CO_2$RR for **complex 3** in MeCN ($C_{cat}$ = 5 µM), on irradiation with a blue LED ((λ = 445 nm), with 0.38 M (5%) TEOA, 0.2 mM $[Ru(bpy)_3](PF_6)_2$ and 0.05 M BIH under $CO_2$ saturated atmosphere.

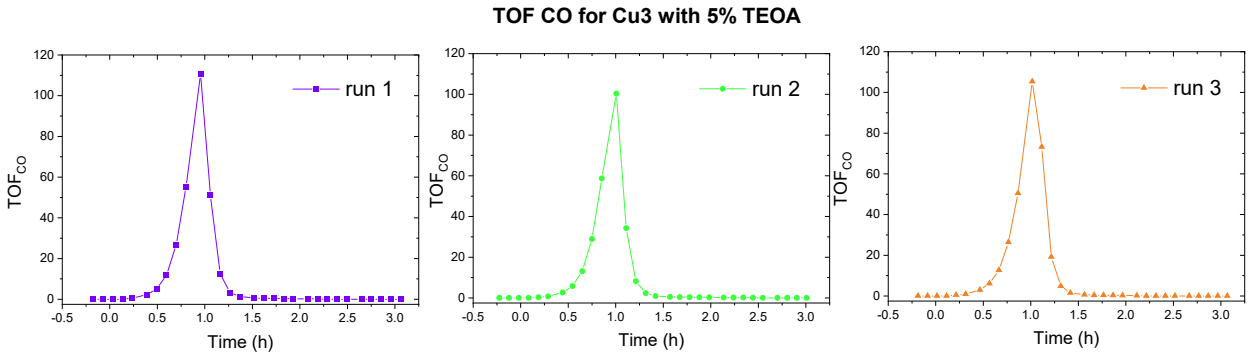


***Figure S49:*** Triplicate runs showing TOF, $CO_2$ to CO during $CO_2$RR for **complex 3** in MeCN ($C_{cat}$ = 5 µM), on irradiation with a blue LED ((λ = 445 nm), with 0.38 M (5%) TEOA, 0.2 mM $[Ru(bpy)_3](PF_6)_2$ and 0.05 M BIH under $CO_2$ saturated atmosphere.

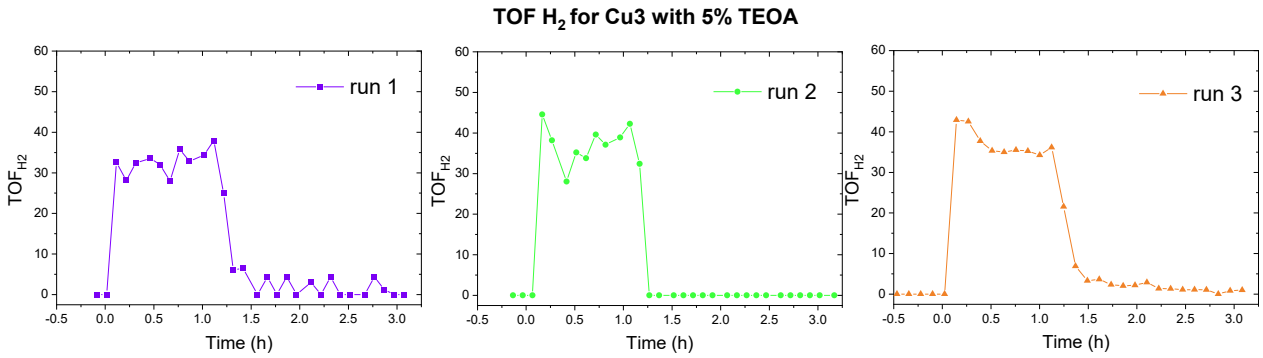


***Figure S50:*** Triplicate runs showing TOF, $CO_2$ to $H_2$ during $CO_2$RR for **complex 3** in MeCN ($C_{cat}$ = 5 µM), on irradiation with a blue LED ((λ = 445 nm), with 0.38 M (5%) TEOA, 0.2 mM $[Ru(bpy)_3](PF_6)_2$ and 0.05 M BIH under $CO_2$ saturated atmosphere.

# 4. Results for Photocatalytic $CO_2$RR in MeCN with 5% water

## 4.1. Blank (no complex present)

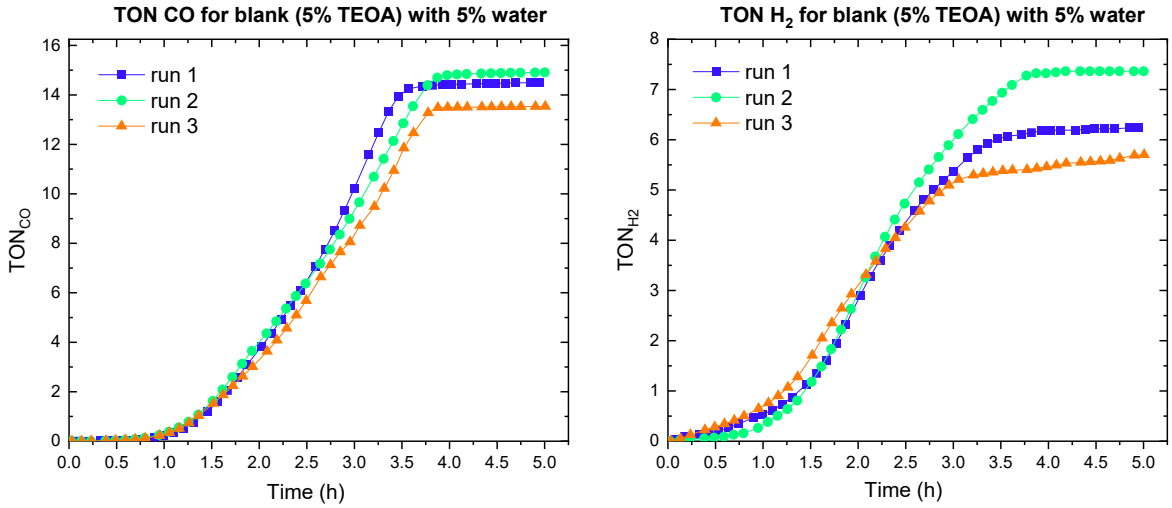


***Figure S51:*** Triplicate runs showing TON, $CO_2$ to CO (left) and $H_2$ (right) during $CO_2$RR for **blank** in MeCN, on irradiation with a blue LED ((λ = 445 nm), with 0.38 M (5%) TEOA, 0.2 mM $[Ru(bpy)_3](PF_6)_2$, 0.05 M BIH and 2.8 mM (5%) water under $CO_2$ saturated atmosphere.

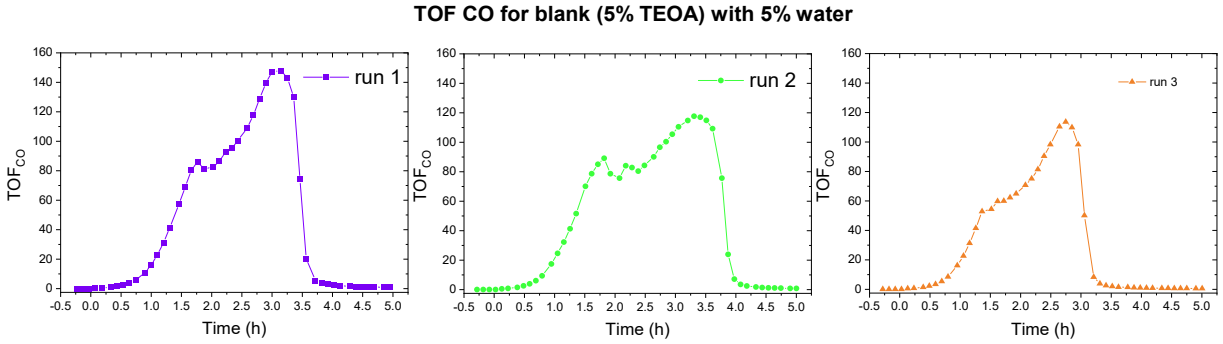


***Figure S52:*** Triplicate runs showing TOF, $CO_2$ to CO during $CO_2$RR for **blank** in MeCN, on irradiation with a blue LED ((λ = 445 nm), with 0.38 M (5%) TEOA, 0.2 mM $[Ru(bpy)_3](PF_6)_2$, 0.05 M BIH and 2.8 mM (5%) water under $CO_2$ saturated atmosphere.

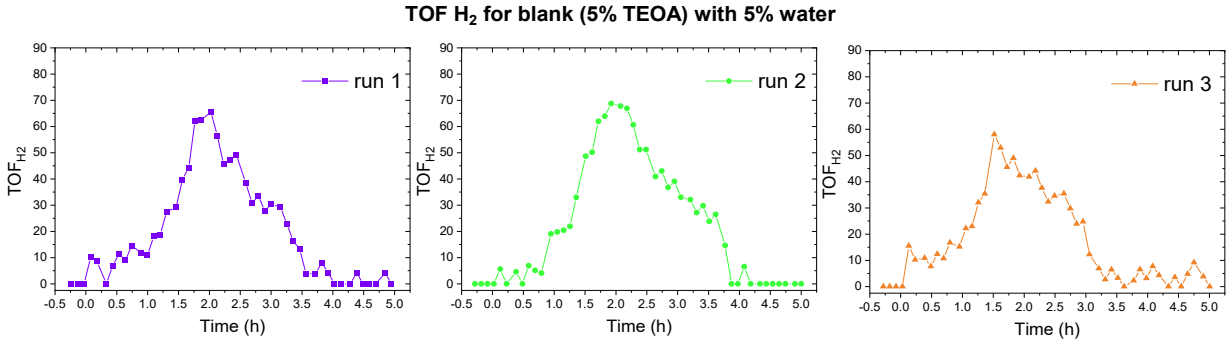


***Figure S53:*** Triplicate runs showing TOF, $CO_2$ to $H_2$ during $CO_2$RR for **blank** in MeCN, on irradiation with a blue LED ((λ = 445 nm), with 0.38 M (5%) TEOA, 0.2 mM $[Ru(bpy)_3](PF_6)_2$, 0.05 M BIH and 2.8 mM (5%) water under $CO_2$ saturated atmosphere.

## 4.2. Control with simple copper salt as catalyst

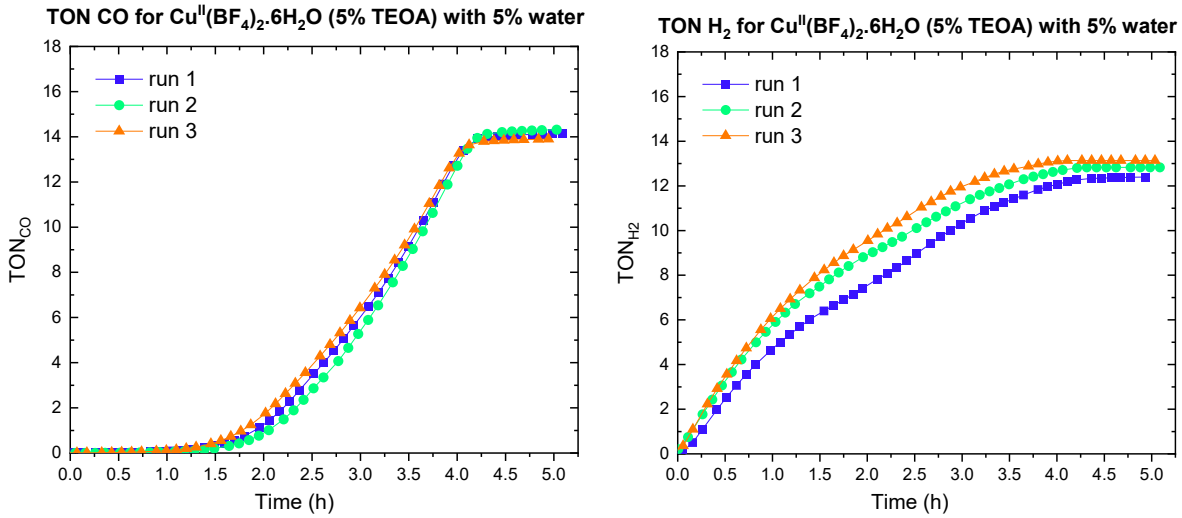


***Figure S54:*** Triplicate runs showing TON, $CO_2$ to CO (left) and $H_2$ (right) during $CO_2$RR for **$Cu^{II}(BF_4)_2.6H_2O$ (control)** in MeCN ($C_{cat}$ = 5 µM), on irradiation with a blue LED (($\lambda$ = 445 nm), with 0.38 M (5%) TEOA, 0.2 mM $[Ru(bpy)_3](PF_6)_2$, 0.05 M BIH and 2.8 mM (5%) water under $CO_2$ saturated atmosphere.

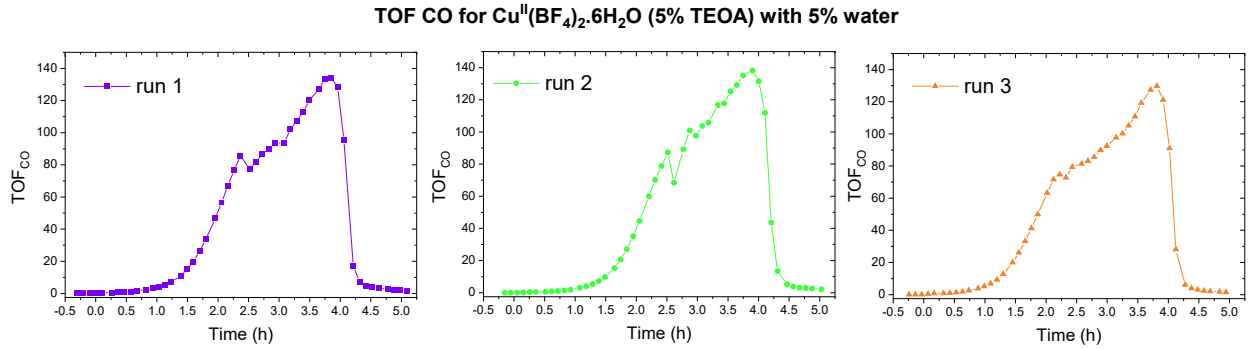


***Figure S55:*** Triplicate runs showing TOF, $CO_2$ to CO during $CO_2$RR for **$Cu^{II}(BF_4)_2.6H_2O$ (control)** in MeCN ($C_{cat}$ = 5 µM), on irradiation with a blue LED (($\lambda$ = 445 nm), with 0.38 M (5%) TEOA, 0.2 mM $[Ru(bpy)_3](PF_6)_2$, 0.05 M BIH and 2.8 mM (5%) water under $CO_2$ saturated atmosphere.

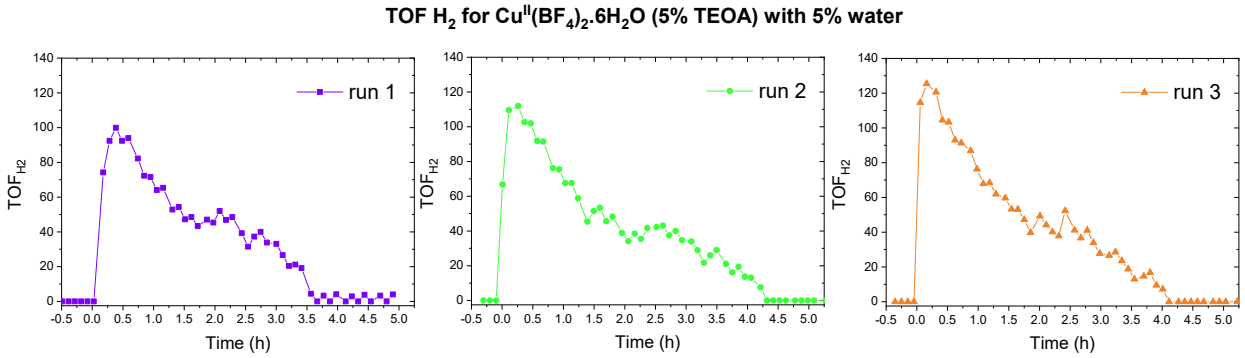


***Figure S56:*** Triplicate runs showing TOF, $CO_2$ to $H_2$ during $CO_2$RR for **$Cu^{II}(BF_4)_2.6H_2O$ (control)** in MeCN ($C_{cat}$ = 5 µM), on irradiation with a blue LED (($\lambda$ = 445 nm), with 0.38 M (5%) TEOA, 0.2 mM $[Ru(bpy)_3](PF_6)_2$, 0.05 M BIH and 2.8 mM (5%) water under $CO_2$ saturated atmosphere.

## 4.3. Photocatalytic $CO_2$RR for complexes 1-3 in MeCN with 5% water

### 4.3.1 Complex 1, $CuL^{Et}BF_4$

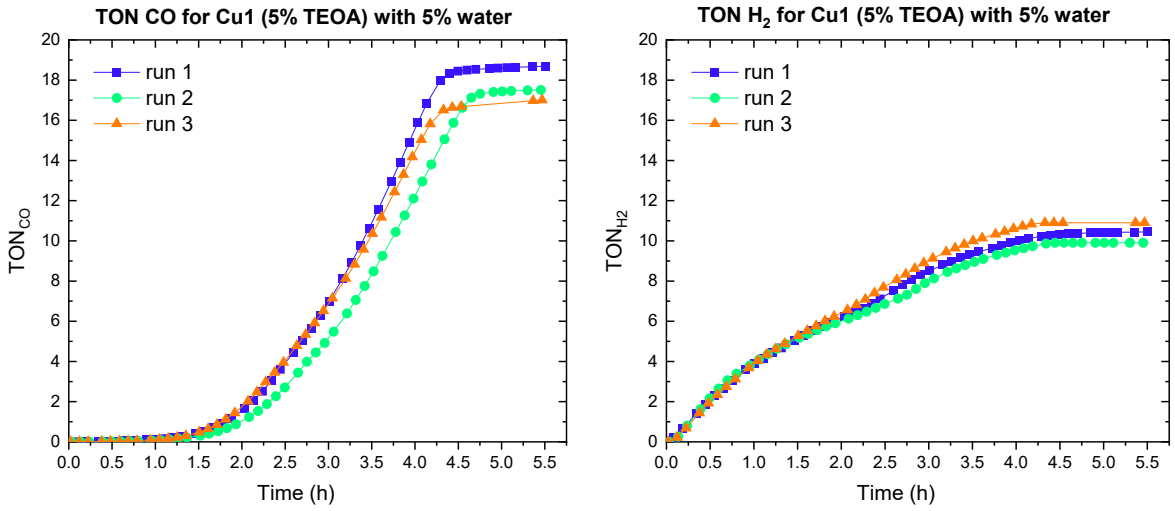


***Figure S57:*** Triplicate runs showing TON, $CO_2$ to CO (left) and $H_2$ (right) during $CO_2$RR for **complex 1** in MeCN ($C_{cat}$ = 5 µM), on irradiation with a blue LED ((λ = 445 nm), with 0.38 M (5%) TEOA, 0.2 mM $[Ru(bpy)_3](PF_6)_2$, 0.05 M BIH and 2.8 mM (5%) water under $CO_2$ saturated atmosphere.

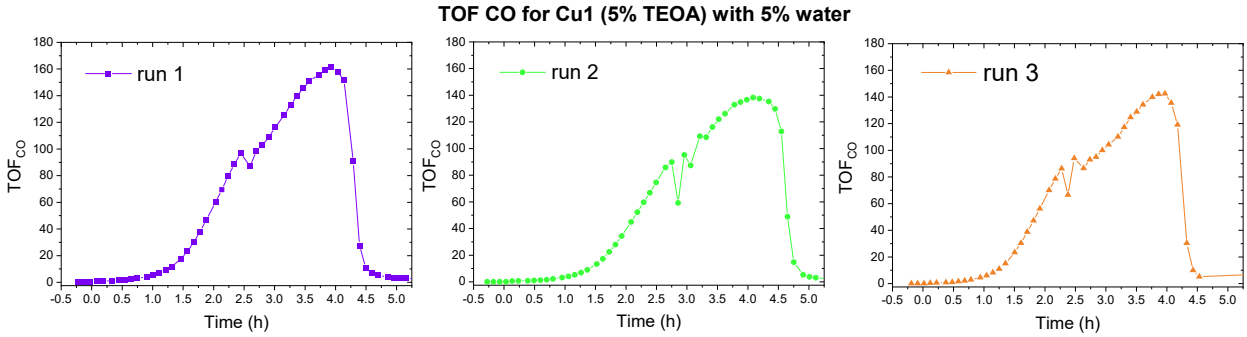


***Figure S58:*** Triplicate runs showing TOF, $CO_2$ to CO during $CO_2$RR for **complex 1** in MeCN ($C_{cat}$ = 5 µM), on irradiation with a blue LED ((λ = 445 nm), with 0.38 (5%) TEOA, 0.2 mM $[Ru(bpy)_3](PF_6)_2$, 0.05 M BIH and 2.8 mM (5%) water under $CO_2$ saturated atmosphere.

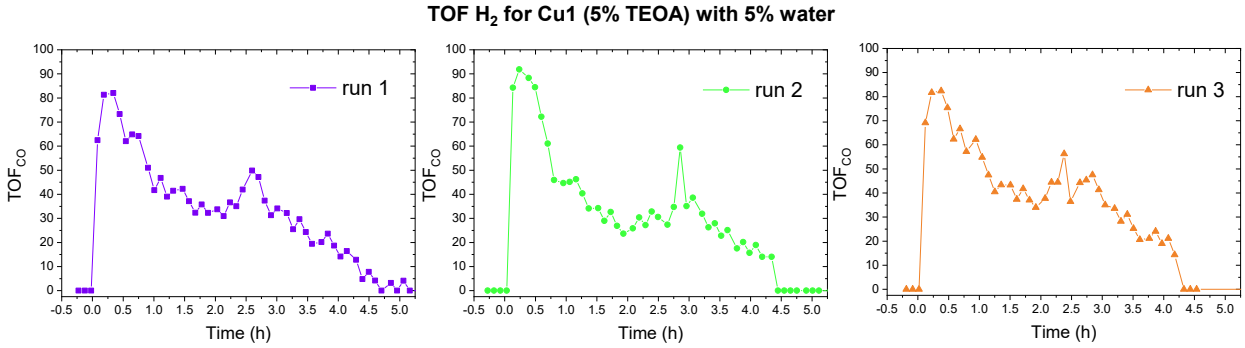


***Figure S59:*** Triplicate runs showing TOF, $CO_2$ to $H_2$ during $CO_2$RR for **complex 1** in MeCN ($C_{cat}$ = 5 µM), on irradiation with a blue LED ((λ = 445 nm), with 0.38 M (5%) TEOA, 0.2 mM $[Ru(bpy)_3](PF_6)_2$, 0.05 M BIH and 2.8 mM (5%) water under $CO_2$ saturated atmosphere.

## 4.3.2 Complex 2, $[Cu^{II}L^{Et\text{-}MePy}]BF_4$

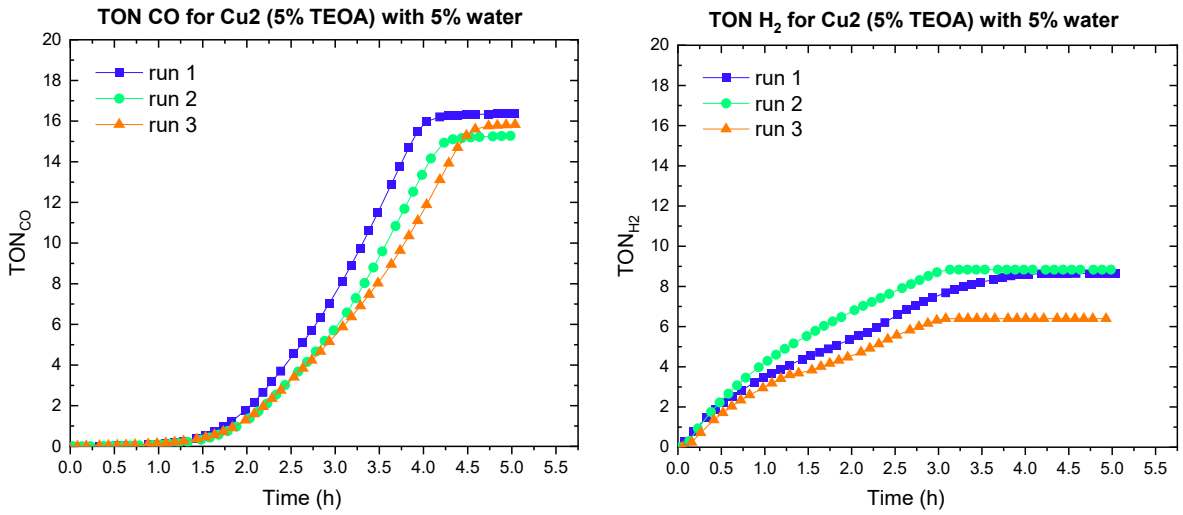


***Figure S60:*** Triplicate runs showing TON, $CO_2$ to CO (left) and $H_2$ (right) during $CO_2$RR for **complex 2** in MeCN ($C_{cat}$ = 5 µM), on irradiation with a blue LED ((λ = 445 nm), with 0.38 M (5%) TEOA, 0.2 mM $[Ru(bpy)_3](PF_6)_2$, 0.05 M BIH and 2.8 mM (5%) water under $CO_2$ saturated atmosphere.

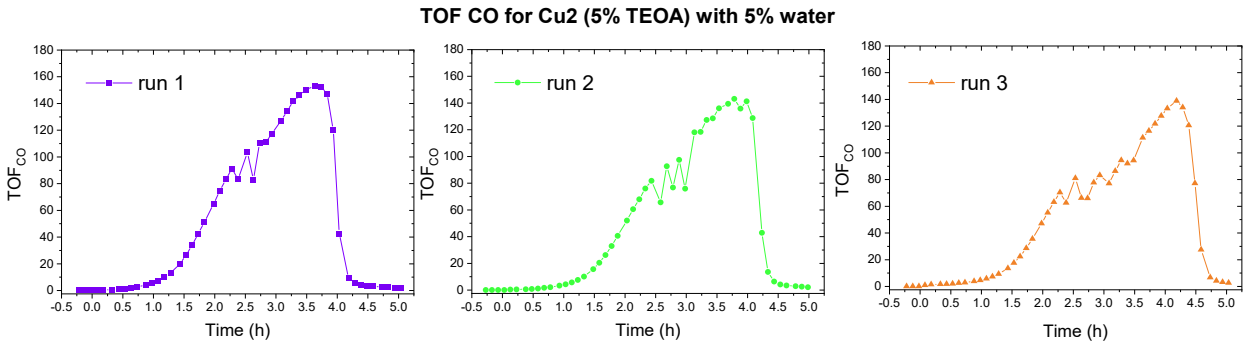


***Figure S61:*** Triplicate runs showing TOF, $CO_2$ to CO during $CO_2$RR for **complex 2** in MeCN ($C_{cat}$ = 5 µM), on irradiation with a blue LED ((λ = 445 nm), with 0.38 M (5%) TEOA, 0.2 mM $[Ru(bpy)_3](PF_6)_2$, 0.05 M BIH and 2.8 mM (5%) water under $CO_2$ saturated atmosphere.

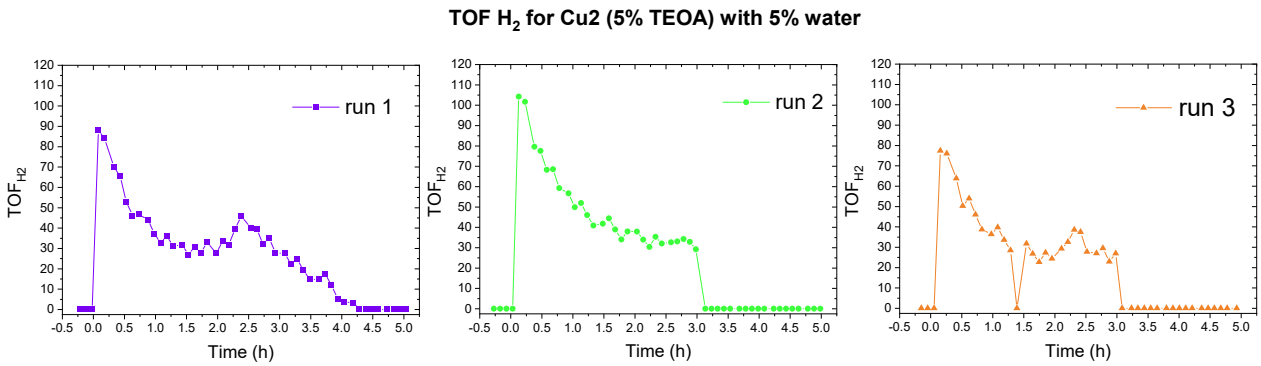


***Figure S62:*** Triplicate runs showing TOF, $CO_2$ to $H_2$ during $CO_2$RR for **complex 2** in MeCN ($C_{cat}$ = 5 µM), on irradiation with a blue LED ((λ = 445 nm), with 0.38 M (5%) TEOA, 0.2 mM $[Ru(bpy)_3](PF_6)_2$, 0.05 M BIH and 2.8 mM (5%) water under $CO_2$ saturated atmosphere.

## 4.3.3 Complex 3, $[Cu^{II}L^{EtPy2}]BF_4$

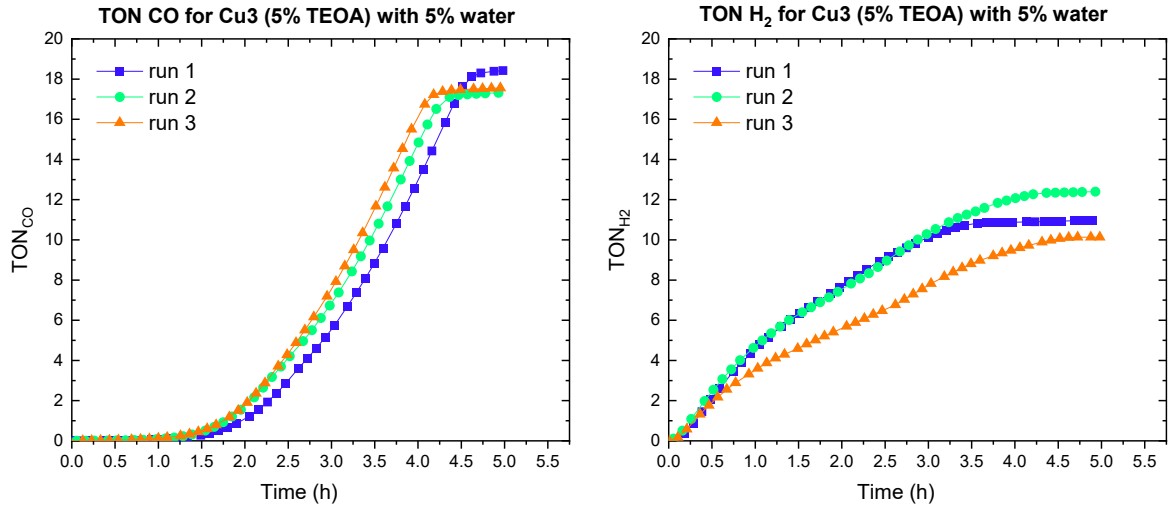


***Figure S63:*** Triplicate runs showing TON, $CO_2$ to CO (left) and $H_2$ (right) during $CO_2$RR for **complex 3** in MeCN ($C_{cat}$ = 5 µM), on irradiation with a blue LED (($\lambda$ = 445 nm), with 0.38 M (5%) TEOA, 0.2 mM $[Ru(bpy)_3](PF_6)_2$, 0.05 M BIH and 2.8 mM (5%) water under $CO_2$ saturated atmosphere.

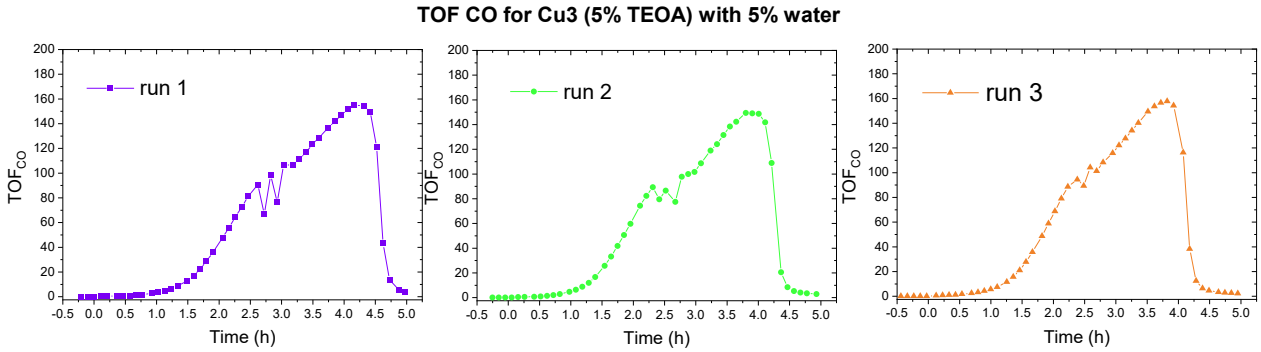


***Figure S64:*** Triplicate runs showing TOF, $CO_2$ to CO during $CO_2$RR for **complex 3** in MeCN ($C_{cat}$ = 5 µM), on irradiation with a blue LED (($\lambda$ = 445 nm), with 0.38 M (5%) TEOA, 0.2 mM $[Ru(bpy)_3](PF_6)_2$, 0.05 M BIH and 2.8 mM (5%) water under $CO_2$ saturated atmosphere.

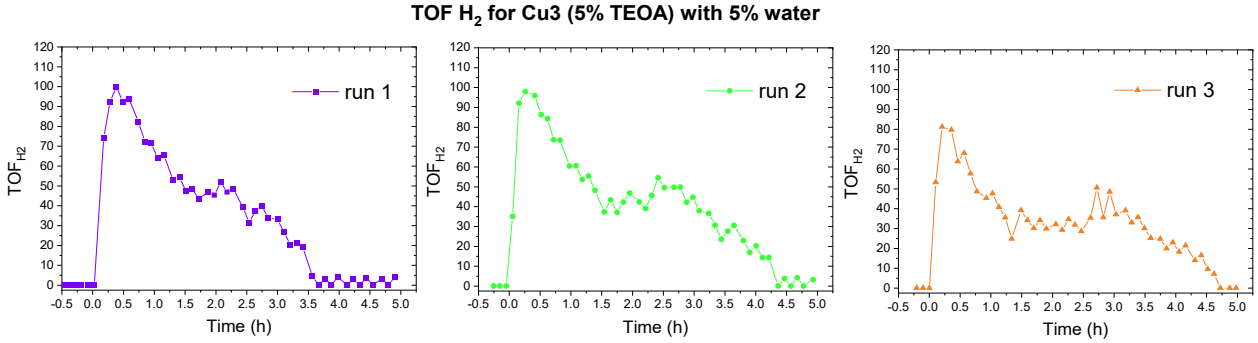


***Figure S65:*** Triplicate runs showing TOF, $CO_2$ to $H_2$ during $CO_2$RR for **complex 3** in MeCN ($C_{cat}$ = 5 µM), on irradiation with a blue LED (($\lambda$ = 445 nm), with 0.38 M (5%) TEOA, 0.2 mM $[Ru(bpy)_3](PF_6)_2$, 0.05 M BIH and 2.8 mM (5%) water under $CO_2$ saturated atmosphere.

## 4.4. Complex 3, with higher catalyst loading

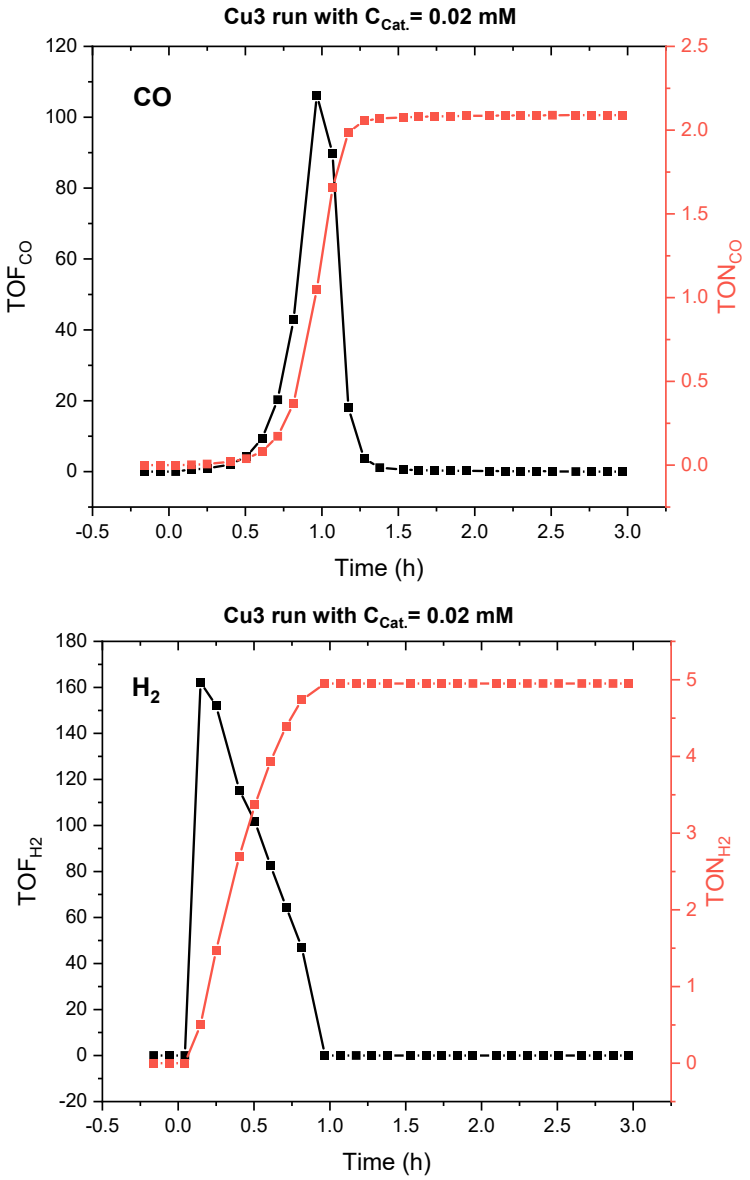


***Figure S66:*** Plots showing TON (red) and TOF (black), $CO_2$ to CO (top) and $H_2$ (bottom) during $CO_2$RR for **complex 3** in MeCN ($C_{cat}$ = 0.02 mM), on irradiation with a blue LED ((λ = 445 nm), with 0.38 M (5%) TEOA, 0.2 mM $[Ru(bpy)_3](PF_6)_2$ and 0.05 M BIH under $CO_2$ saturated atmosphere.

## 4.5. Blank and complex 1, with 5% and 20% TEOA loading

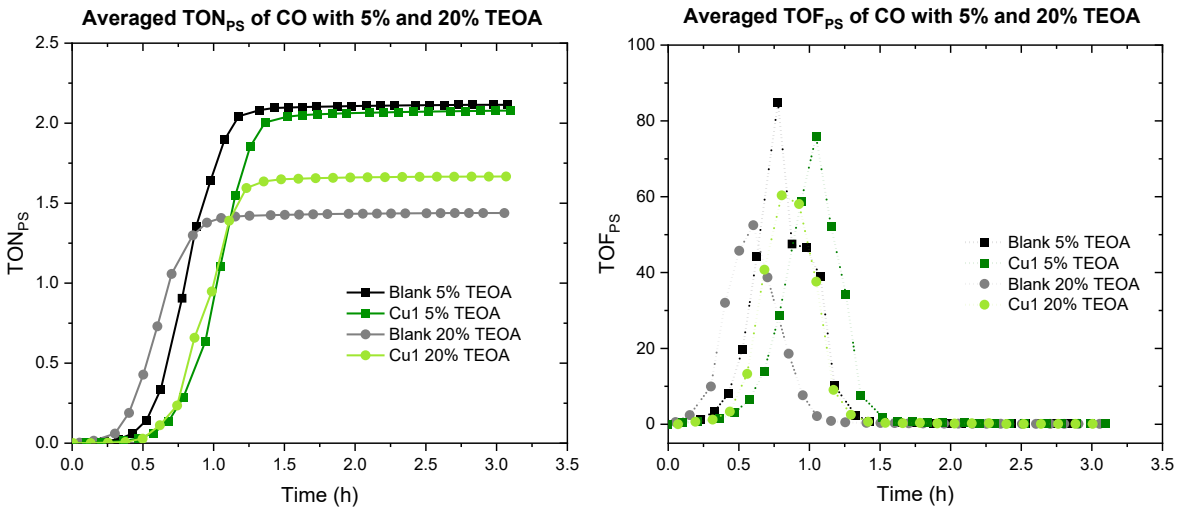


***Figure S67:*** *(Left) Average $TON_{PS}$ for CO during $CO_2RR$ over 3 hrs, for control **blank** in absence of catalyst (black) and **1** (dark green), with 0.25 M (5%) TEOA, and $TON_{PS}$ for control **blank** (grey) and **1** (light green) with 1.0 M (20%) TEOA. (Right) Average $TOF_{PS}$ for CO during $CO_2RR$ over 3 hrs, for control **blank** in absence of catalyst (black) and **1** (dark green), with 0.25 M (5%) TEOA, and $TOF_{PS}$ for control **blank** (grey) and **1** (light green) with 1.5 M (20%) TEOA, in MeCN ($C_{cat}$ = 5 µM) on irridation with a blue LED (λ = 445 nm), 0.2 mM $[Ru(bpy)_3](PF_6)_2$ and 0.05 M BIH under $CO_2$ saturated atmosphere.*

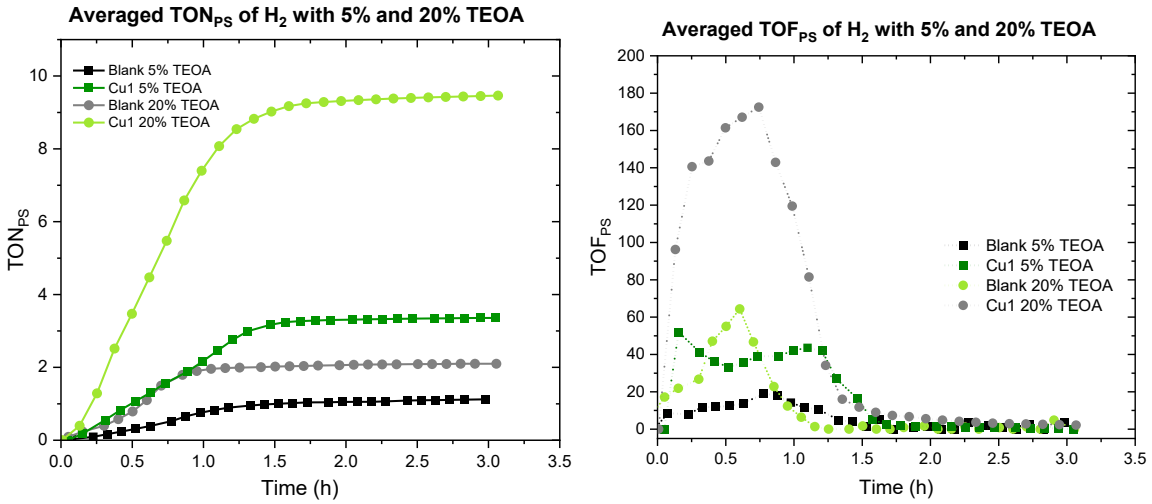


***Figure S68:*** (Left) Average $TON_{PS}$ for $H_2$ during $CO_2RR$ over 3 hrs, for control **blank** in absence of catalyst (black) and **1** (dark green), with 0.25 M (5%) TEOA, and $TON_{PS}$ for control **blank** (grey) and **1** (light green) with 1.0 M (20%) TEOA. (Right) Average $TOF_{PS}$ for $H_2$ during $CO_2RR$ over 3 hrs, for control **blank** in absence of catalyst (black) and **1** (dark green), with 0.25 M (5%) TEOA, and $TOF_{PS}$ for control **blank** (grey) and **1** (light green) with 1.5 M (20%) TEOA, in MeCN ($C_{cat}$ = 5 µM) on irridation with a blue LED (λ = 445 nm), 0.2 mM $[Ru(bpy)_3](PF_6)_2$ and 0.05 M BIH under $CO_2$ saturated atmosphere.

# 5. Formate quantification post-catalysis for complexes 1-3

Please see sections 2.5.3 and 2.5.4 for the details of the method used, and the calibration line employed, in analysing the raw data obtained to determining $[formate]_{photocat.\ soln}$ in these MeCN solutions post-photocatalysis. All the observed values, and those determined from them, are provided in Table S4 below.

***Table S4**: $^1$H NMR quantification of formate from reaction mixture post photoreaction using calibration determined earlier.*

| **Experiment** | benzyl benzoate $CH_2$ (2H) integration **set to 2H (1 mM)** | formate (1H) signal relative integration **RI(formate)** | **[formate]$_{nmr\ tube}$** obtained from previous column value using eq. 9 (correlation) | **[formate]$_{postcat\ soln}$** obtained from previous column using eq. 10 (dilution) | **$TON_{PS}$ using eq. 6** | **$TON_{CAT}$ using eq. 5** |
|---|---|---|---|---|---|---|
| **Blanks and Controls** | | | | | | |
| Blank with 20% TEOA | 2 | 0.10 | 0.10 | 0.14 | 0.7 | 27 |
| Blank with 5% TEOA | 2 | 0.04 | 0.04 | 0.06 | 0.3 | 11 |
| Blank without TEOA | | No formate peak observed | | | | |
| Cu salt control | 2 | 0.04 | 0.04 | 0.06 | 0.3 | 11 |
| **1** without TEOA | 2 | 0.016 | 0.02 | 0.02 | 0.1 | 4.4 |
| **1** without BIH | | No formate peak observed | | | | |
| **1** without PS | | No formate peak observed | | | | |
| **Complexes** | | | | | | |
| **1** with 20% TEOA | 2 | 0.12 | 0.12 | 0.16 | 0.8 | 33 |
| **1** with 5% TEOA | 2 | 0.03 | 0.03 | 0.04 | 0.2 | 8 |
| **2** with 5% TEOA | 2 | 0.04 | 0.04 | 0.05 | 0.3 | 11 |
| **3** with 5% TEOA | 2 | 0.04 | 0.04 | 0.05 | 0.3 | 11 |
| **Blank, control and complexes with addition of 5% water in MeCN** | | | | | | |
| Blank with 5% water | 2 | 1.45 | 1.39 | 1.99 | 9.9 | 397 |
| Cu salt with 5% water | 2 | 1.15 | 1.10 | 1.56 | 7.8 | 315 |
| **1** with 5% water | 2 | 1.32 | 1.27 | 1.81 | 9.0 | 362 |
| **2** with 5% water | 2 | 1.31 | 1.26 | 1.79 | 8.9 | 360 |
| **3** with 5% water | 2 | 1.35 | 1.29 | 1.85 | 9.2 | 370 |

# 6. Results for photocatalytic $CO_2$RR in DMF

## 6.1. Blank experiments

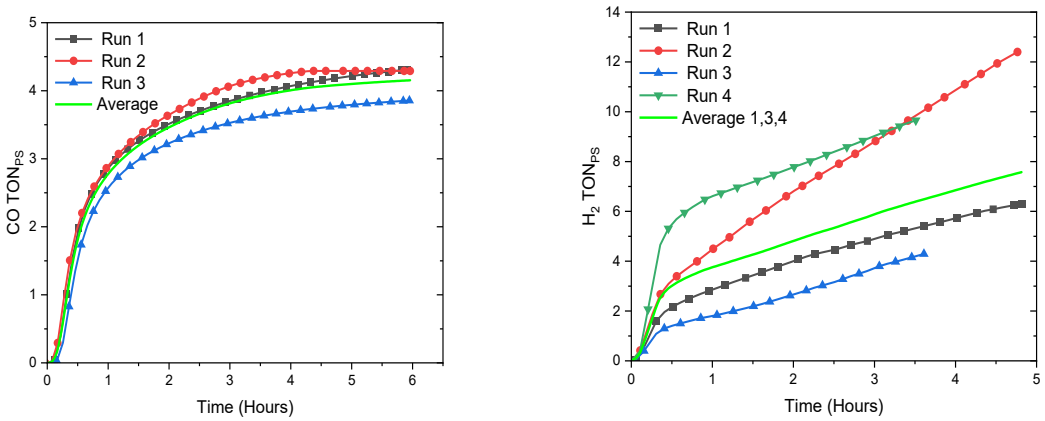


***Figure S69:*** Quadruplicate runs showing TON, $CO_2$ to CO (top) and $H_2$ (bottom) during $CO_2$RR for **Blank** in DMF, on irradiation with a blue LED ((λ = 445 nm), with 1.5 M (20%) TEOA, 0.2 mM $[Ru(bpy)_3](PF_6)_2$ and 0.05 M BIH under $CO_2$ saturated atmosphere.

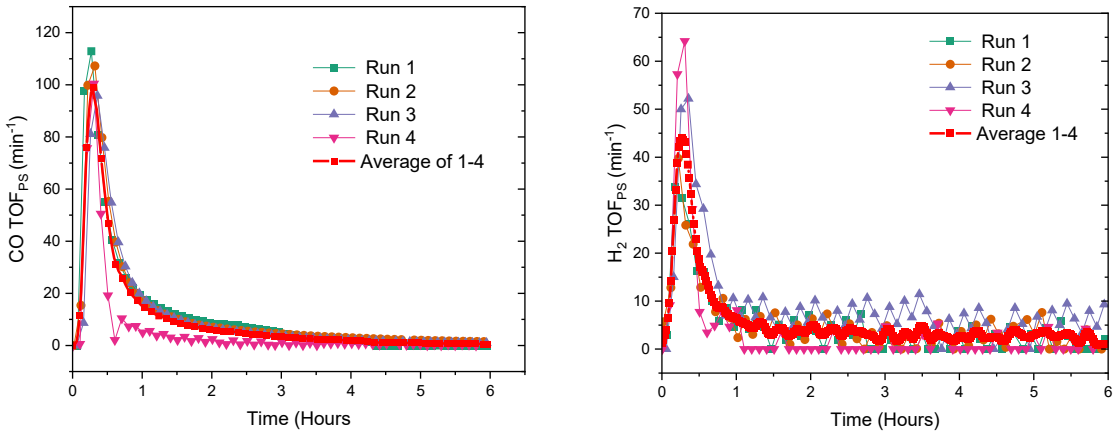


***Figure S70:*** Quadruplicate runs showing TOF, $CO_2$ to CO (left) and $H_2$ (right) during $CO_2$RR for **blank** in DMF, on irradiation with a blue LED ((λ = 445 nm), with 1.5 M (20%) TEOA, 0.2 mM $[Ru(bpy)_3](PF_6)_2$ and 0.05 M BIH under $CO_2$ saturated atmosphere.

## 6.2. Controls with simple Cu and Tb nitrate salts

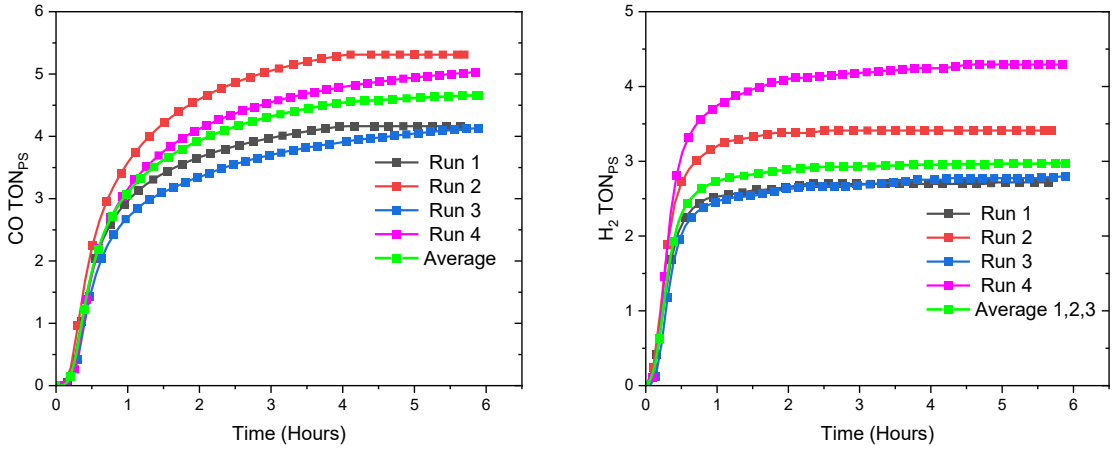


***Figure S71:*** Quadruplicate runs showing TON, $CO_2$ to CO (top) and $H_2$ (bottom) during $CO_2$RR for **$Cu^{II}(NO_3)_2.6H_2O$ (control)** in DMF ($C_{cat}$ = 15 µM), on irradiation with a blue LED (($\lambda$ = 445 nm), with 1.5 M (20%) TEOA, 0.2 mM $[Ru(bpy)_3](PF_6)_2$, 0.05 M BIH under $CO_2$ saturated atmosphere.

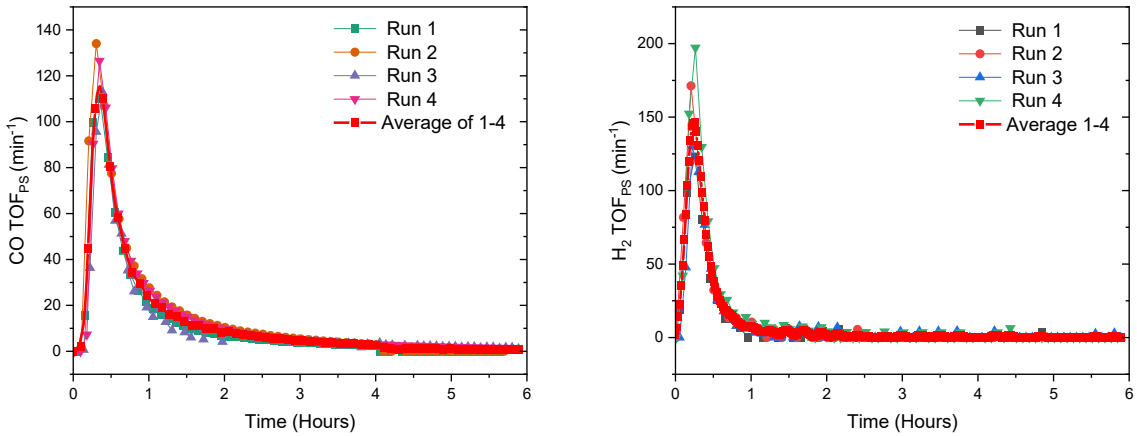


***Figure S72:*** Quadruplicate runs showing TOF, $CO_2$ to CO (left) and $H_2$ (right) during $CO_2$RR for **$Cu^{II}(NO_3)_2.6H_2O$ (control)** in DMF ($C_{cat}$ = 15 µM), on irradiation with a blue LED (($\lambda$ = 445 nm), with 1.5 M (20%) TEOA, 0.2 mM $[Ru(bpy)_3](PF_6)_2$ and 0.05 M BIH under $CO_2$ saturated atmosphere.

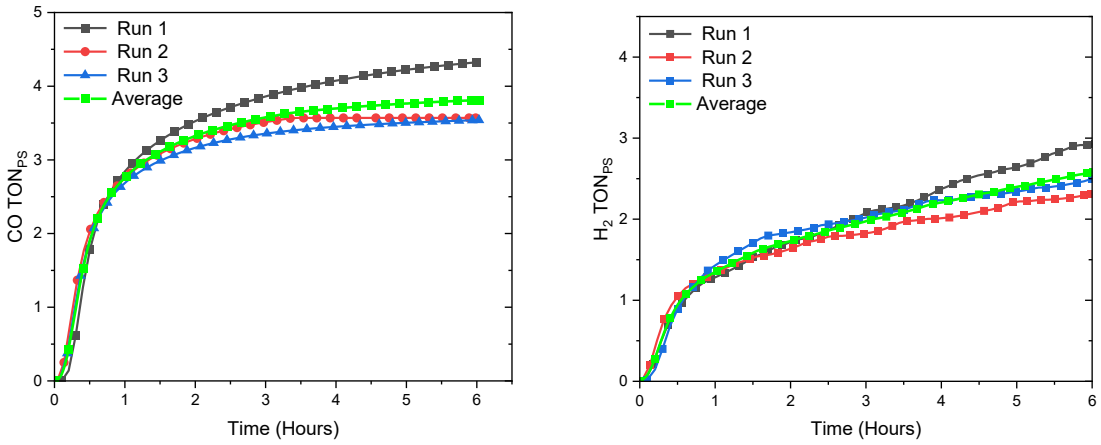


***Figure S73:*** Triplicate runs showing TON, $CO_2$ to CO (top) and $H_2$ (bottom) during $CO_2$RR for **$Tb^{III}(NO_3)_3.5H_2O$ (control)** in DMF ($C_{cat}$ = 5 µM), on irradiation with a blue LED (($\lambda$ = 445 nm), with 1.5 M (20%) TEOA, 0.2 mM $[Ru(bpy)_3](PF_6)_2$, 0.05 M BIH under $CO_2$ saturated atmosphere.

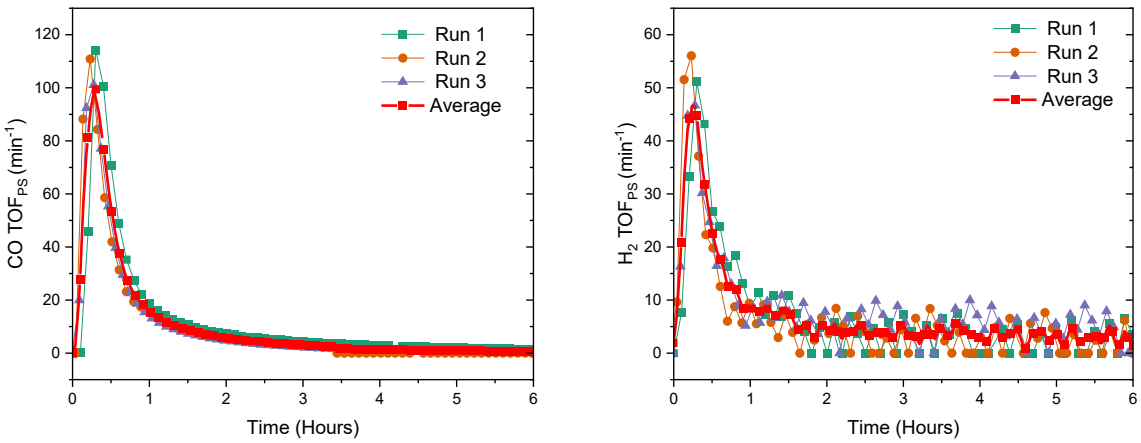


***Figure S74:*** Triplicate runs showing TOF, $CO_2$ to CO (left) and $H_2$ (right) during $CO_2$RR for **$Tb^{III}(NO_3)_3.5H_2O$ (control)** in DMF ($C_{cat}$ = 5 µM), on irradiation with a blue LED (($\lambda$ = 445 nm), with 1.5 M (20%) TEOA, 0.2 mM $[Ru(bpy)_3](PF_6)_2$ and 0.05 M BIH under $CO_2$ saturated atmosphere.

## 6.3. Photocatalytic $CO_2$RR for complexes 4-5 in DMF

### 6.3.1 Complex 4, $[Cu^{II}_3Tb^{III}(L^{Pr})(NO_3)_3]$

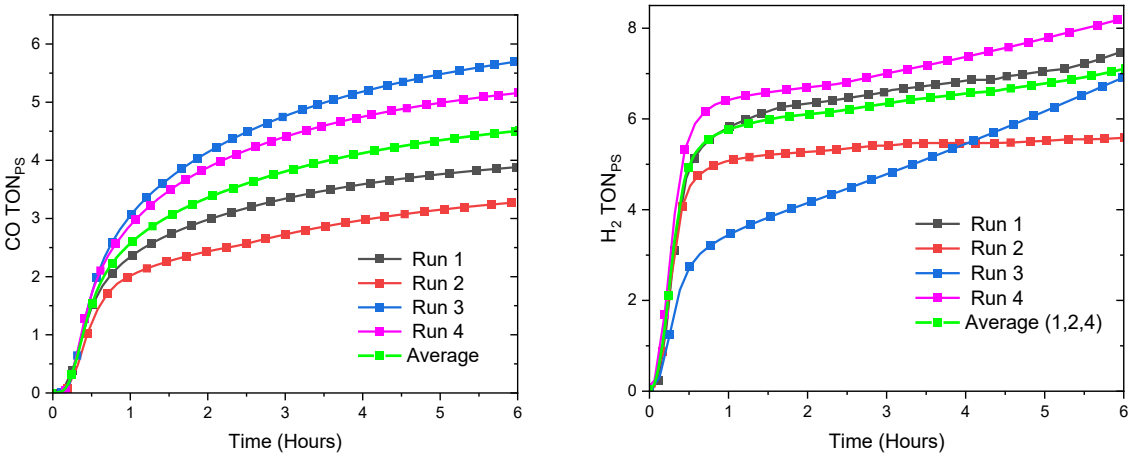


***Figure S75:*** Quadruplicate runs showing TON, $CO_2$ to CO (top) and $H_2$ (bottom) during $CO_2$RR for **$[Cu^{II}_3Tb^{III}(L^{Pr})(NO_3)_3]$ (Complex 4)** in DMF ($C_{cat}$ = 5 µM), on irradiation with a blue LED (($\lambda$ = 445 nm), with 1.5 M (20%) TEOA, 0.2 mM $[Ru(bpy)_3](PF_6)_2$, 0.05 M BIH under $CO_2$ saturated atmosphere.

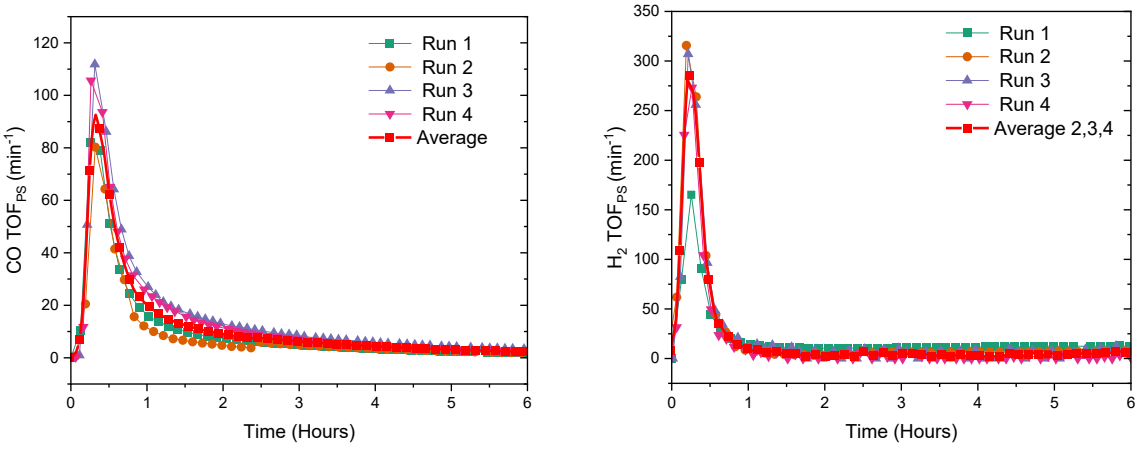


***Figure S76:*** Quadruplicate runs showing TOF, $CO_2$ to CO (left) and $H_2$ (right) during $CO_2$RR for **$[Cu^{II}_3Tb^{III}(L^{Pr})(NO_3)_3]$ (Complex 4)** in DMF ($C_{cat}$ = 5 µM), on irradiation with a blue LED (($\lambda$ = 445 nm), with 1.5 M (20%) TEOA, 0.2 mM $[Ru(bpy)_3](PF_6)_2$ and 0.05 M BIH under $CO_2$ saturated atmosphere.

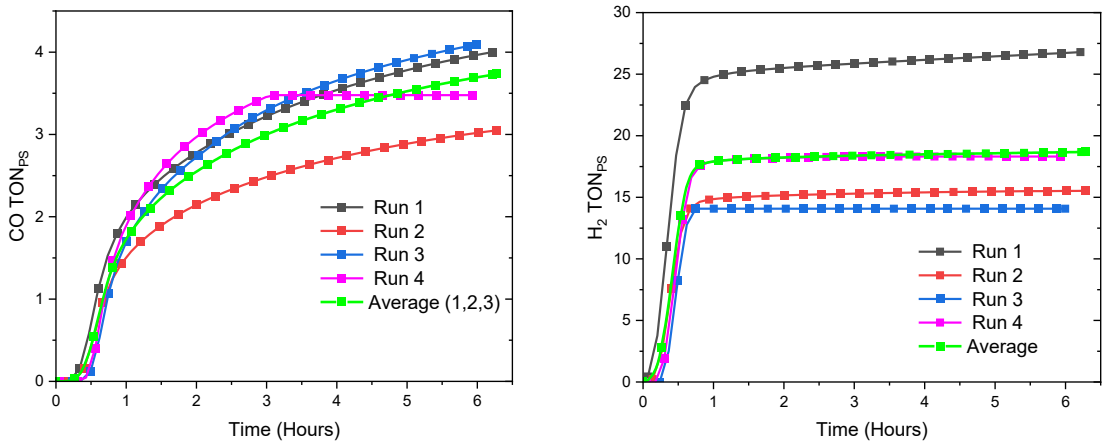


***Figure S77:*** Quadruplicate runs showing TON, $CO_2$ to CO (top) and $H_2$ (bottom) during $CO_2$RR for **[$Cu^{II}_3Tb^{III}(L^{Pr})(NO_3)_3$] (Complex 4)** in DMF ($C_{cat}$ = 20 µM), on irradiation with a blue LED (($\lambda$ = 445 nm), with 1.5 M (20%) TEOA, 0.2 mM $[Ru(bpy)_3](PF_6)_2$, 0.05 M BIH under $CO_2$ saturated atmosphere.

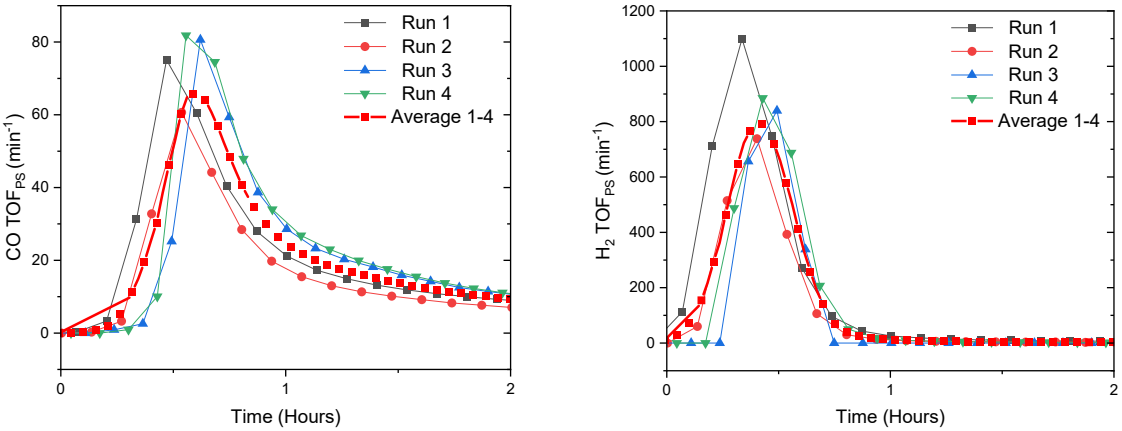


***Figure S78:*** Quadruplicate runs showing TOF, $CO_2$ to CO (left) and $H_2$ (right) during $CO_2$RR for **[$Cu^{II}_3Tb^{III}(L^{Pr})(NO_3)_3$] (Complex 4)** in DMF ($C_{cat}$ = 20 µM), on irradiation with a blue LED (($\lambda$ = 445 nm), with 1.5 M (20%) TEOA, 0.2 mM $[Ru(bpy)_3](PF_6)_2$ and 0.05 M BIH under $CO_2$ saturated atmosphere.

## 6.3.2 Complex 5, $[Cu^{II}_3Tb^{III}(L^{HU})_3(NO_3)_3]$

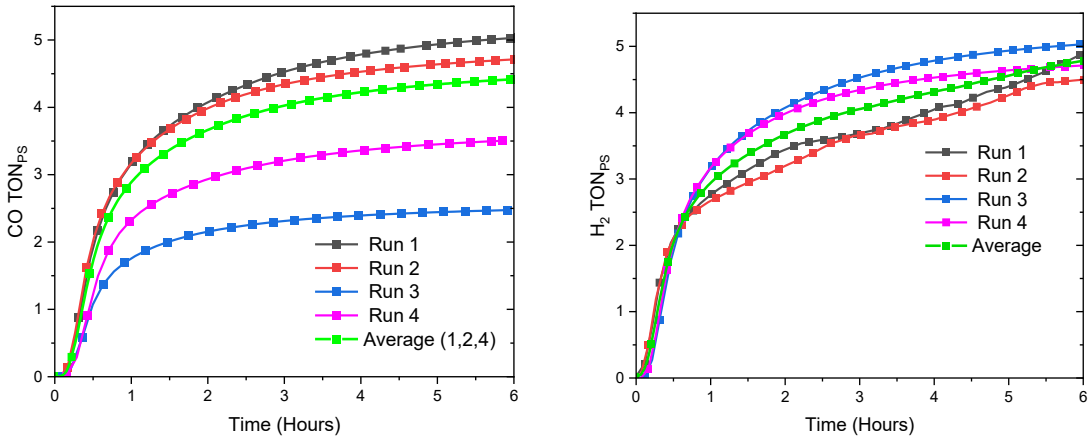


***Figure S79:*** Quadruplicate runs showing TON, $CO_2$ to CO (top) and $H_2$ (bottom) during $CO_2$RR for **$[Cu^{II}_3Tb^{III}(L^{HU})_3(NO_3)_3]$ (Complex 5)** in DMF ($C_{cat}$ = 5 µM), on irradiation with a blue LED ((λ = 445 nm), with 1.5 M (20%) TEOA, 0.2 mM $[Ru(bpy)_3](PF_6)_2$, 0.05 M BIH under $CO_2$ saturated atmosphere.

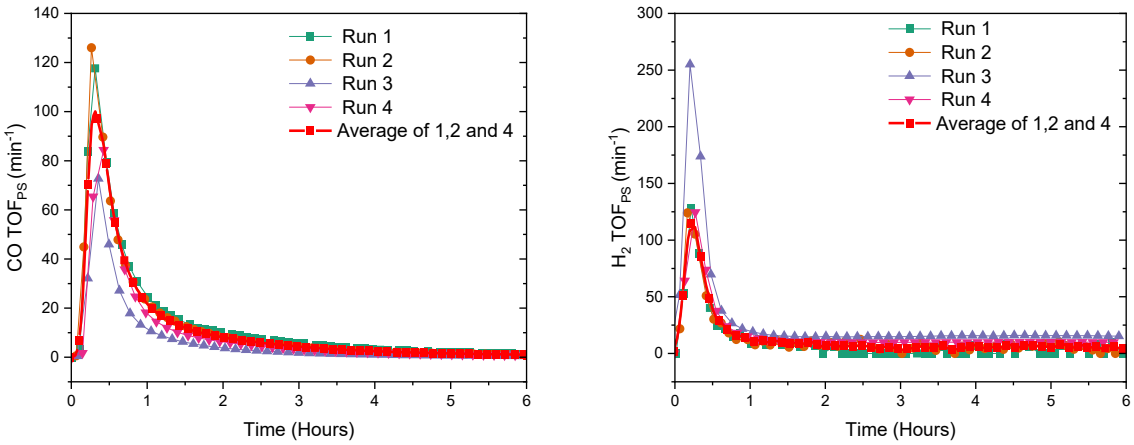


***Figure S80:*** Quadruplicate runs showing TOF, $CO_2$ to CO (left) and $H_2$ (right) during $CO_2$RR for **$[Cu^{II}_3Tb^{III}(L^{HU})_3(NO_3)_3]$ (Complex 5)** in DMF ($C_{cat}$ = 5 µM), on irradiation with a blue LED ((λ = 445 nm), with 1.5 M (20%) TEOA, 0.2 mM $[Ru(bpy)_3](PF_6)_2$ and 0.05 M BIH under $CO_2$ saturated atmosphere.

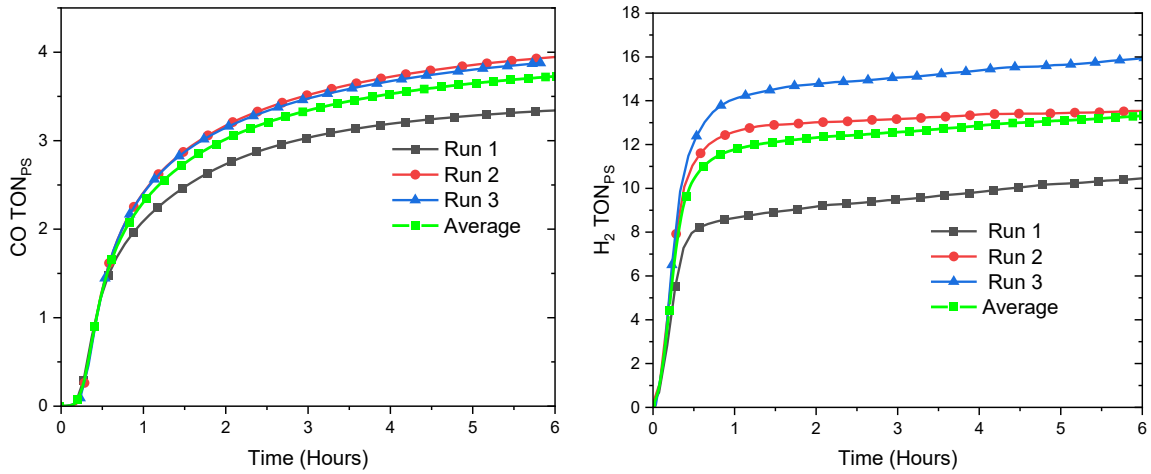


***Figure S81:*** Triplicate runs showing TON, $CO_2$ to CO (top) and $H_2$ (bottom) during $CO_2$RR for **[$Cu^{II}_3Tb^{III}(L^{HU})_3(NO_3)_3$] (Complex 5)** in DMF ($C_{cat}$ = 20 µM), on irradiation with a blue LED (($\lambda$ = 445 nm), with 1.5 M (20%) TEOA, 0.2 mM [Ru(bpy)$_3$](PF$_6$)$_2$, 0.05 M BIH under $CO_2$ saturated atmosphere.

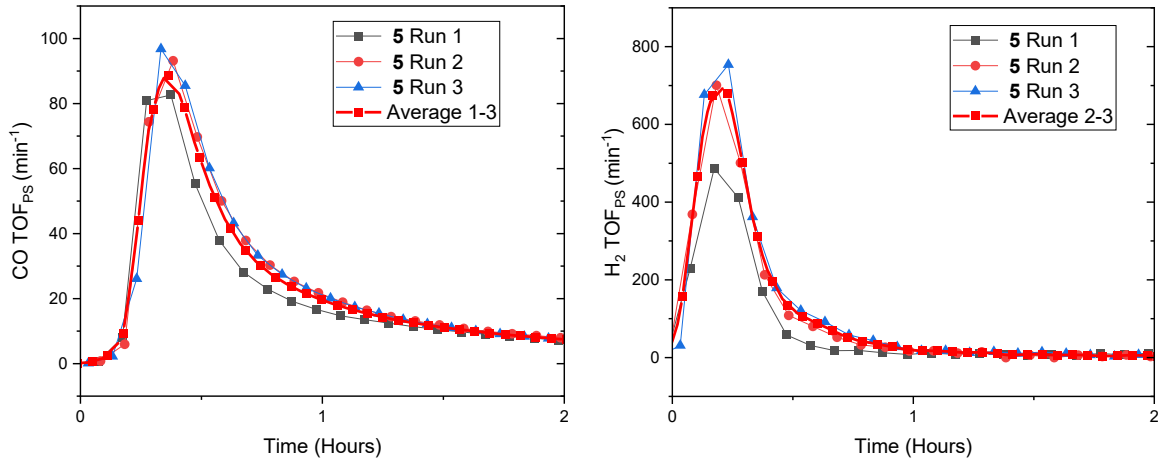


***Figure S82:*** Triplicate runs showing TOF, $CO_2$ to CO (left) and $H_2$ (right) during $CO_2$RR for **[$Cu^{II}_3Tb^{III}(L^{HU})_3(NO_3)_3$] (Complex 5)** in DMF ($C_{cat}$ = 20 µM), on irradiation with a blue LED (($\lambda$ = 445 nm), with 1.5 M (20%) TEOA, 0.2 mM [Ru(bpy)$_3$](PF$_6$)$_2$ and 0.05 M BIH under $CO_2$ saturated atmosphere.

# 7. Results for photocatalytic $CO_2$RR in DMF with 5% water

## 7.1. Blank experiments

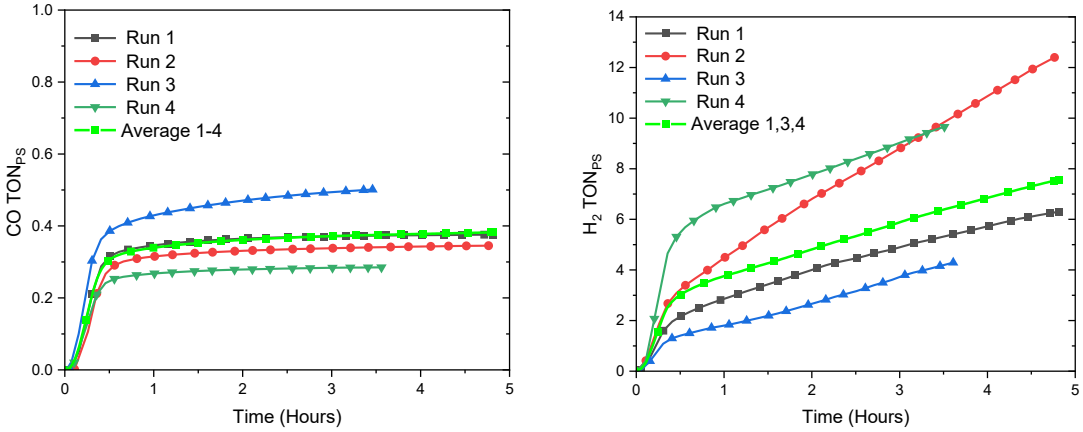


***Figure S83:*** Quadruplicate runs showing TON, $CO_2$ to CO (top) and $H_2$ (bottom) during $CO_2$RR for **Blank (Control)** in DMF ($C_{cat}$ = 5 µM), with 5% $H_2O$, on irradiation with a blue LED ((λ = 445 nm), with 1.5 M (20%) TEOA, 0.2 mM $[Ru(bpy)_3](PF_6)_2$, 0.05 M BIH under $CO_2$ saturated atmosphere.

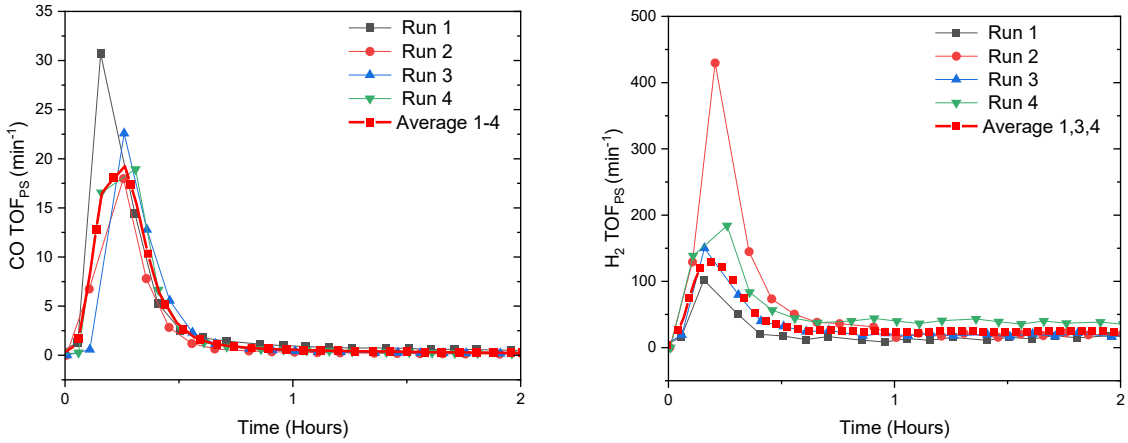


***Figure S84:*** Quadruplicate runs showing TOF, $CO_2$ to CO (left) and $H_2$ (right) during $CO_2$RR for **Blank (Control)** in DMF ($C_{cat}$ = 5 µM), with 5% $H_2O$, on irradiation with a blue LED ((λ = 445 nm), with 1.5 M (20%) TEOA, 0.2 mM $[Ru(bpy)_3](PF_6)_2$ and 0.05 M BIH under $CO_2$ saturated atmosphere.

## 7.2. Photocatalytic $CO_2$RR for complexes 4-5 in DMF with 5% water

### 7.2.1 Complex 4, $[Cu^{II}_3Tb^{III}(L^{Pr})(NO_3)_3]$

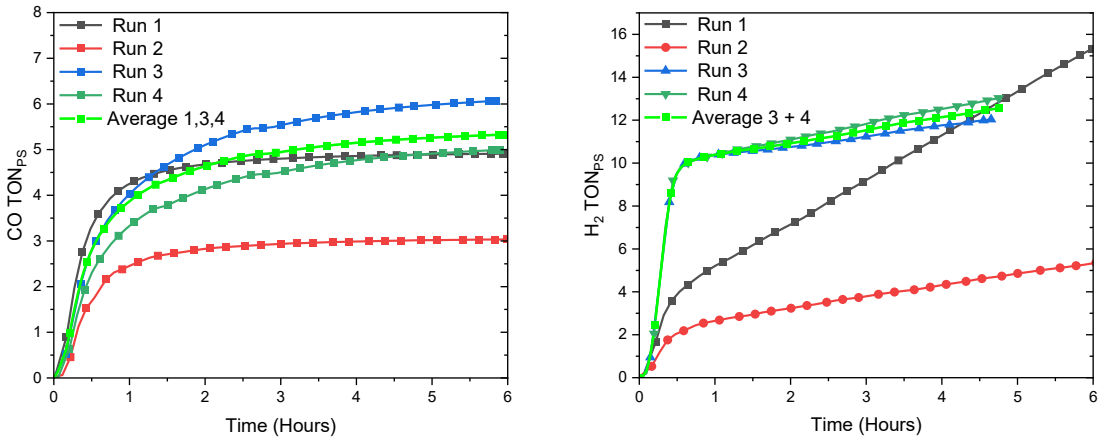


***Figure S85:*** Quadruplicate runs showing TON, $CO_2$ to CO (top) and $H_2$ (bottom) during $CO_2$RR for **$[Cu^{II}_3Tb^{III}(L^{Pr})(NO_3)_3]$ (Complex 4)** in DMF ($C_{cat}$ = 5 µM), with 5% $H_2O$, on irradiation with a blue LED (($\lambda$ = 445 nm), with 1.5 M (20%) TEOA, 0.2 mM $[Ru(bpy)_3](PF_6)_2$, 0.05 M BIH under $CO_2$ saturated atmosphere.

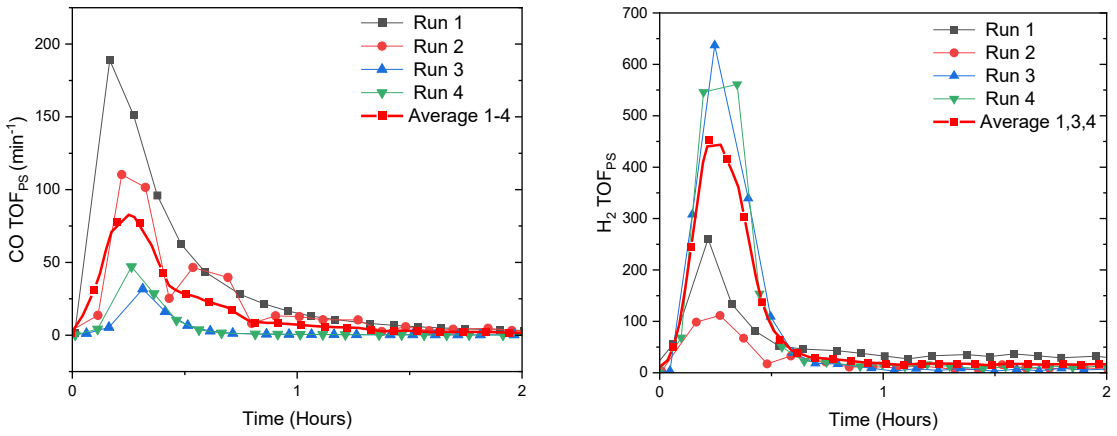


***Figure S86:*** Quadruplicate runs showing TOF, $CO_2$ to CO (left) and $H_2$ (right) during $CO_2$RR for **$[Cu^{II}_3Tb^{III}(L^{Pr})(NO_3)_3]$ (Complex 4)** in DMF ($C_{cat}$ = 5 µM), with 5% $H_2O$, on irradiation with a blue LED (($\lambda$ = 445 nm), with 1.5 M (20%) TEOA, 0.2 mM $[Ru(bpy)_3](PF_6)_2$ and 0.05 M BIH under $CO_2$ saturated atmosphere.

## 7.2.2 Complex 5, $[Cu^{II}_3Tb^{III}(L^{HU})_3(NO_3)_3]$

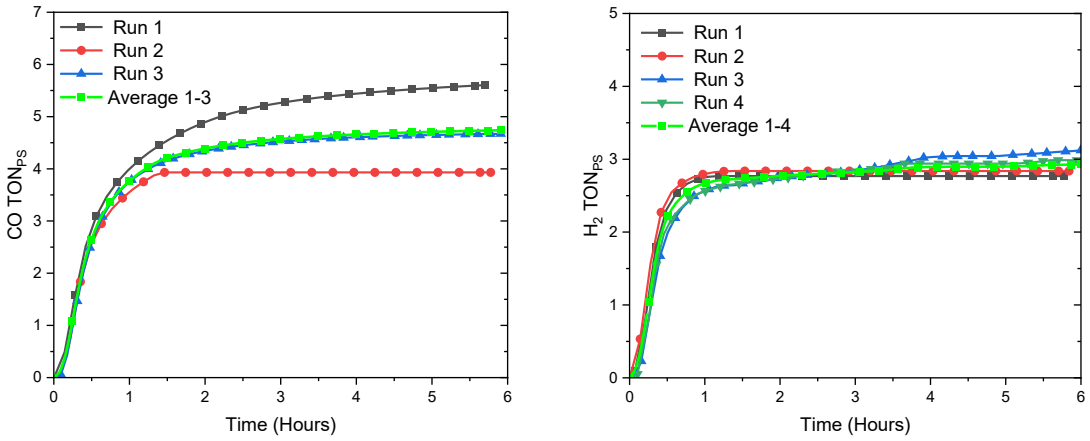


***Figure S87:*** Quadruplicate runs showing TON, $CO_2$ to CO (top) and $H_2$ (bottom) during $CO_2$RR for **$[Cu^{II}_3Tb^{III}(L^{HU})_3(NO_3)_3]$ (Complex 5)** in DMF ($C_{cat}$ = 5 µM), with 5% $H_2O$, on irradiation with a blue LED (($\lambda$ = 445 nm), with 1.5 M (20%) TEOA, 0.2 mM $[Ru(bpy)_3](PF_6)_2$, 0.05 M BIH under $CO_2$ saturated atmosphere.

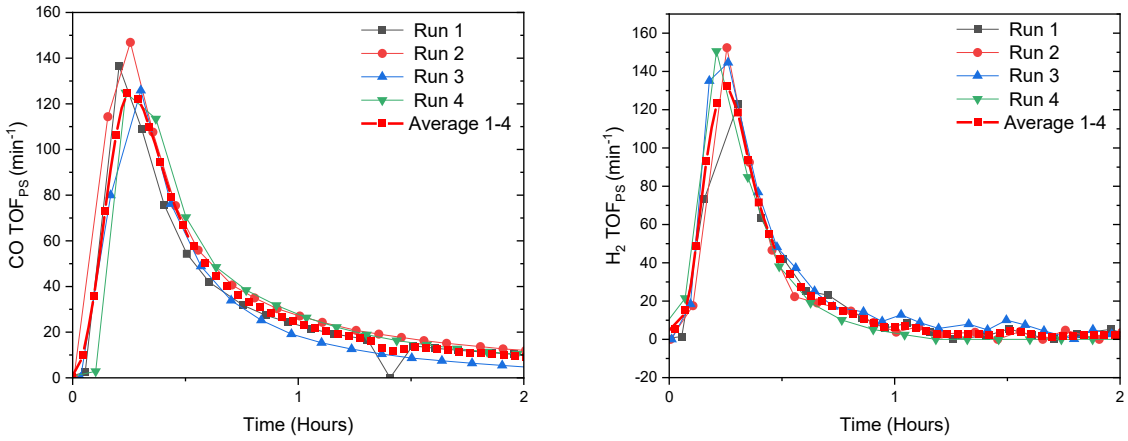


***Figure S88:*** Quadruplicate runs showing TOF, $CO_2$ to CO (left) and $H_2$ (right) during $CO_2$RR for **$[Cu^{II}_3Tb^{III}(L^{HU})_3(NO_3)_3]$ (Complex 5)** in DMF ($C_{cat}$ = 5 µM), with 5% $H_2O$, on irradiation with a blue LED (($\lambda$ = 445 nm), with 1.5 M (20%) TEOA, 0.2 mM $[Ru(bpy)_3](PF_6)_2$ and 0.05 M BIH under $CO_2$ saturated atmosphere.

# 8. Formate quantification post-photocatalysis for complexes 4-5

Please see sections 2.5.5 and 2.5.6 for the details of the method used, and the calibration line employed, in analysing the raw data obtained to determining **[formate]$_{photocat.\ soln}$** in these DMF solutions post-photocatalysis. All the observed values, and those determined from them, are provided in Table S5 below.

***Table S5:*** *$^1$H NMR quantification of formate from DMF reaction mixture post photoreaction for complexes **4-5** using calibration determined earlier.*

| **Experiment** | benzyl benzoate $CH_2$ (2H) integration **set to 2H (5 mM)** | formate (1H) signal relative integration **RI(formate)** | **[formate]$_{nmr\ tube}$** obtained from previous column value using **eq. 11** (correlation) | **[formate]$_{postcat\ soln}$** obtained from previous column using **eq. 10** | **TON$_{PS}$** obtained using **eq. 6** | **TON$_{CAT}$** obtained using **eq. 5** |
|---|---|---|---|---|---|---|
| Blank no TEOA | 2 | 0 | 0 | 0 | 0 | - |
| Blank with TEOA | 2 | 0.25 | 1.2 | 1.8 | 8.9 | - |
| Cu Nitrate salt | 2 | 0.77 | 3.9 | 5.5 | 27.5 | 1100.0 |
| Tb Nitrate salt | 2 | 0.69 | 3.4 | 4.9 | 24.6 | 985.8 |
| **4 (**5 µM) | 2 | 0.71 | 3.6 | 5.1 | 25.4 | 1014.4 |
| **5** (5 µM) | 2 | 0.85 | 4.3 | 6.1 | 30.4 | 1214.4 |
| **4** (20 µM) | 2 | 0.80 | 4.0 | 5.7 | 28.6 | 1142.9 |
| **5** (20 µM) | 2 | 0.15 | 0.8 | 1.1 | 5.4 | 214.3 |
| Blank + 5% $H_2O$ | 2 | 0.87 | 4.4 | 6.2 | 31.1 | - |
| **4** + 5% $H_2O$ | 2 | 1.27 | 6.4 | 9.1 | 45.4 | 1814.4 |
| **5** + 5% $H_2O$ | 2 | 1.46 | 7.3 | 10.4 | 52.1 | 2085.9 |

# 9. References


1. B. D. Naab, S. Guo, S. Olthof, E. G. B. Evans, P. Wei, G. L. Millhauser, A. Kahn, S. Barlow, S. R. Marder and Z. Bao, Mechanistic Study on the Solution-Phase n-Doping of 1,3-Dimethyl-2-aryl-2,3-dihydro-1H-benzoimidazole Derivatives, *J. Am. Chem.Soc.*, 2013, **135**, 15018-15025.

2. F. M. Wisser, M. Duguet, Q. Perrinet, A. C. Ghosh, M. Alves-Favaro, Y. Mohr, C. Lorentz, E. A. Quadrelli, R. Palkovits, D. Farrusseng, C. Mellot-Draznieks, V. de Waele and J. Canivet, Molecular Porous Photosystems Tailored for Long-Term Photocatalytic $CO_2$ Reduction, *Angew. Chem. Int. Ed.*, 2020, **59**, 5116-5122.

3. X.-Q. Zhu, M.-T. Zhang, A. Yu, C.-H. Wang and J.-P. Cheng, Hydride, Hydrogen Atom, Proton, and Electron Transfer Driving Forces of Various Five-Membered Heterocyclic Organic Hydrides and Their Reaction Intermediates in Acetonitrile, *J. Am. Chem. Soc.*, 2008, **130**, 2501-2516.

4. M. Biner, H. B. Buergi, A. Ludi and C. Roehr, Crystal and molecular structures of $[Ru(bpy)_3](PF_6)_3$ and $[Ru(bpy)_3](PF_6)_2$ at 105 K, *J. Am. Chem. Soc.*, 1992, **114**, 5197-5203.

5. C. Costentin, S. Drouet, M. Robert and J.-M. Savéant, Turnover Numbers, Turnover Frequencies, and Overpotential in Molecular Catalysis of Electrochemical Reactions. Cyclic Voltammetry and Preparative-Scale Electrolysis, *J. Am. Chem. Soc.*, 2012, **134**, 11235-11242.